CHEMICAL REVIEWS

pubs.acs.org/CR

Review

Membranes under the Magnetic Lens: A Dive into the Diverse World of Membrane Protein Structures Using Cryo-EM

Sarah J. Piper,* Rachel M. Johnson,* Denise Wootten,* and Patrick M. Sexton*

Cite This: *Chem. Rev.* 2022, 122, 13989−14017

Read Online

ACCESS | Metrics & More | Article Recommendations

ABSTRACT: Membrane proteins are highly diverse in both structure and function and can, therefore, present different challenges for structure determination. They are biologically important for cells and organisms as gatekeepers for information and molecule transfer across membranes, but each class of membrane proteins can present unique obstacles to structure determination. Historically, many membrane protein structures have been investigated using highly engineered constructs or using larger fusion proteins to improve solubility and/or increase particle size. Other strategies included the deconstruction of the full-length protein to target smaller soluble domains. These manipulations were often required for crystal formation to support X-ray crystallography or to circumvent lower resolution due to high noise and dynamic motions of protein subdomains. However, recent revolutions in membrane protein biochemistry and cryo-electron microscopy now provide an opportunity to solve high resolution structures of both large, >1 megadalton (MDa), and small, <100 kDa (kDa), drug targets in near-native conditions, routinely reaching resolutions around or below 3 Å. This review provides insights into how the recent advances in membrane biology and biochemistry, as well as technical advances in cryo-electron microscopy, help us to solve structures of a large variety of membrane protein groups, from small receptors to large transporters and more complex machineries.

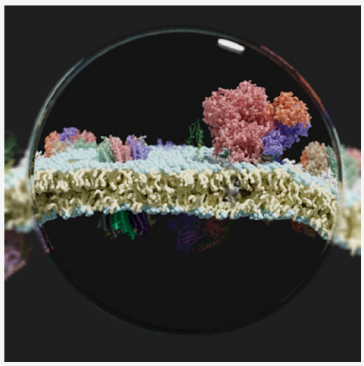

CONTENTS

Special Issue: Cryo-EM in Biology and Materials Research

Received: September 28, 2021
Published: July 18, 2022

https://doi.org/10.1021/acs.chemrev.1c00837
Chem. Rev. 2022, 122, 13989−14017

1. INTRODUCTION TO THE WORLD OF MEMBRANE PROTEINS

By the simplest of definitions, membrane proteins are proteins incorporated into cellular membranes. Classically, many biology textbooks group membrane proteins into two categories: integral and peripheral membrane proteins.[1,2] Due to the complexity of biological membranes, as well as their diverse roles within the cell, membrane proteins can be very variable in size and oligomeric state and can have vastly different chemical, physical, and biological properties, which can also depend on the organism from which these were derived.

In a chemical sense, biological membranes are made of phospholipid bilayers that are amphipathic: comprising lipid tails that consist of hydrophobic carbon chains and hydrophilic lipid headgroups with varying charge. The chemical complexity and variety of membrane lipids can change drastically between different tissues, organelles, or organisms. Given their incorporation into hydrophobic lipid bilayers, membrane proteins contain domains that are highly hydrophobic. Some software programs can predict membrane protein topologies and can even be used to discover new membrane proteins. Most recently, AlphaFold2, a computational method for protein structure prediction, has been at the forefront of the structural biology news due to its success in predictions of protein structures that had not been tractable to traditional homology model approaches. It has provided a novel resource to broadly predict structures of the human proteome,[3] with an important feature of output predictions being a robust scoring of the confidence of the structure prediction of subregions within the protein. Nonetheless, AlphaFold2 does not robustly predict distinct conformational states of proteins or the dynamics of proteins, and these will be discussed further in section 5. These properties are critical to protein function and are especially relevant for membrane proteins.

Advances in structural biology have proven pivotal to efficiently determining the structures of increasing numbers of membrane protein classes, and individual proteins within classes, which has shed light into their function within biological membranes. There have been many advances in understanding the biology of membranes and membrane proteins that, coupled with new tools to address the biochemical challenges associated with studying membrane proteins and with technical innovations in hardware and software around cryogenic electron microscopy (cryo-EM), have enabled the field to rapidly gain insights into membrane protein structures, including understanding the molecular mechanisms underlying the function of important drug targets.

Below, we discuss recent developments in membrane protein structural biology, with a focus on the biochemistry and cryo-EM techniques at the forefront of solving challenging membrane protein structures. We also review highlights of past and recent membrane protein structures solved using cryo-EM, made possible due to the aforementioned advances in method developments. Finally, we provide an outlook on how we envisage the future of membrane protein cryo-EM, overcoming current limitations through the development of faster, more accurate, and cheaper techniques that can be applied in a more biologically and medically relevant context.

2. MEMBRANE PROTEIN CRYO-EM STRUCTURES: OVERVIEW AND TYPICAL WORKFLOWS

2.1. Membrane Protein Molecular Biology and Biochemistry

2.1.1. Constructs and Expression Systems for Membrane Proteins. Extracting and purifying membrane proteins for structural characterization can often be a challenging process due to their low stability outside of the biological membrane. Therefore, being able to obtain material of sufficient purity, yield, and stability represents a major hurdle in the structural determination pipeline. To overcome these hurdles, decisions need to be made on the expression system and purification approaches that can be used to obtain the protein of interest. These have a common goal of extraction and stable reconstitution of target membrane proteins. Figure 1 offers an overview of some of the typical steps involved in the biochemistry of membrane proteins for cryo-EM.

One approach is to purify the protein from the native source organism or tissue, but this requires sufficiently high levels of expression to allow recovery of enough protein to support structural studies. An example of successful purification of native protein is the cytochrome bc_1 complex, purified from heart tissue that was used for the determination of structure by both X-ray crystallography and cryo-EM[4] and the bovine rhodopsin isolated from bovine rod outer segments and also used for structural characterization.[5] Nonetheless, most membrane proteins, in particular human proteins that are of high medical interest, are recombinantly expressed to achieve high yields of functional proteins for structural studies. In this context, the most appropriate expression system can vary for different protein classes and may need to be empirically explored. In one study of the human *ether-a-go-go*-related gene (hERG) ion channel, both an important drug target and a critical "off-target" for toxicology, a variety of expression systems and purification methods were compared to provide insight into the different advantages and disadvantages of individual approaches.[6] The key is to balance expression yields and downstream solubilization efficiencies while maintaining protein function; for the hERG channel, the authors tested bacterial *Escherichia coli*, insect *Spodoptera frugiperda* (Sf9), yeast *Pichia pastoris*, and human embryonic kidney (HEK) cell lines and concluded that expression in HEK cells and solubilization using dodecyl-maltoside (DDM) led to functional channels, albeit at lower yields. The protein of interest is typically tagged, using motifs on protein termini that are recognized in affinity chromatography, to assist in both purification and monitoring of the protein, and overexpressed in the system of choice. Moreover, the protein(s) may be further modified to stabilize interfaces within protein−protein complexes or subdomains within individual proteins, which can be beneficial for higher resolution cryo-EM reconstructions. However, while such modifications have been typically required to make crystallization feasible for X-ray crystallography, they may be unnecessary for structure determination by cryo-EM and should be critically assessed before being adopted in order to make the protein complexes more biologically relevant and to enable capture of native conformational dynamics. Nonetheless,

https://doi.org/10.1021/acs.chemrev.1c00837
Chem. Rev. 2022, 122, 13989−14017

biochemical manipulation of one or more components of membrane protein complexes is often still required to stabilize otherwise transient interactions. Further options for protein engineering and/or antibody-like additions to membrane proteins are discussed in the context of specific protein classes in section 3.

It is important to note that the nature of the expression system that is adopted must be able to support the transport to and stabilization in the correct membrane environment for the protein of interest, as shown in the hERG example above,[6] in addition to supporting functionally important posttranslational modification (e.g., the importance of which is highlighted in a review on posttranslational modification on G protein-coupled receptors (GPCRs)[7]).

2.1.2. Membrane Protein Solubilization and Purification. After cellular expression of membrane proteins and cell lysis, one typical bottleneck is the solubilization of membrane proteins. Classic detergents, often used in laboratories for denaturing and unfolding proteins, are used in membrane protein biochemistry to remove protein domains from their lipid environment, albeit with a lot of care and thorough troubleshooting and screening needed for each protein investigated to optimize the stability and recovery of functional protein.[8,9] Detergents consist of amphipathic units (hydrophilic and hydrophobic), similar to lipid molecules. Due to their chemical properties, detergents typically form micelles, which are small circular units of detergent molecules with hydrophobic tails facing inward and hydrophilic, charged groups facing outward (as displayed in Figure 1).

A disadvantage of the detergent solubilization strategy is that it can strip native lipids from the protein, which not only creates an artificial environment but also potentially reduces the stability of the protein of interest.[10] Many alternatives to detergents exist that can either maintain or create a lipid environment for the protein of interest. These approaches involve the formation of nanodisc particles that result in the membrane protein being surrounded by lipids and encapsulated by a stabilizing protein, thus making it soluble in aqueous solutions while maintaining a more native environment. Examples for these approaches for the solubilization/reconstitution of membrane proteins are discussed in section 3.

2.1.3. Quality Control of Membrane Protein Samples Prior to Cryo-EM Imaging. The protein expression and purification steps require thorough troubleshooting, and therefore, quality control steps are needed to ensure the best sample is obtained, as well as information on the steps where the protein is lost or enriched. While protein-specific affinity columns are often required for efficient enrichment of target proteins/complexes, running the sample through chromatography columns, such as size exclusion or ion exchange, can provide information on the heterogeneity of the sample while also purifying the sample further. One of the most common, and still most important, techniques for identifying and quantifying relative levels of proteins is Western blotting, which utilizes antibodies to recognize proteins within samples. Due to its high sensitivity and ease of use with affinity-tagged proteins, many laboratories routinely use Western blotting to determine the quality of the sample and the efficiency of the purification process. However, to ensure purity of samples, methods for nonspecific labeling of all proteins are essential, with Coomassie blue staining of sodium dodecyl sulfate polyacrylamide gel electrophoresis (SDS PAGE) gels remaining the most common method. Nonetheless, where access to lower cost transmission electron microscopes (TEMs) is readily available, negative staining of samples can provide enriched information that is oftentimes (i) more quickly obtained, (ii) more informative on sample quality and heterogeneity, and (iii) obtained with less protein (Figure 1). Negative staining protocols need to account for differences for optimization of soluble versus membrane proteins, due to the change of buffer properties in the presence of detergents. Approaches for general optimization of negative staining protocols for membrane proteins,[11] and for specific classes of membrane proteins such as GPCRs,[12] have been developed. It should be noted that negative staining protocols (e.g., sample concentration and grid type) cannot be translated to cryo-EM grid preparation due to the inherent differences of the two techniques. More details on cryo-EM grid preparation are discussed in section 3.3.1.

As well as checking the purity and homogeneity of the sample prior to imaging, it is also important to check that the protein is functional to ensure that the resulting structure is biologically relevant.[13] Before starting the purification experiments, one can make sure that the introduction of affinity tags, introduced to aid the purification process, has not in fact disrupted the function of the protein. This can be assessed in cell-based assays where the activity of the construct used for purification is compared to the wild-type construct. It would also be ideal to check that the purified protein remains functional once it has been solubilized and removed from the membrane. In the absence of a functional assay, other quality control steps could be undertaken. One such example is multiple angle light scattering (MALS), which determines the molecular weight of proteins within solution and when coupled to size exclusion chromatography (SEC-MALS) is a powerful technique at providing information about the oligomeric state and/or heterogeneity of samples eluting from the purification column.[14] Other examples include the following: dynamic light scattering to check for aggregates and provide information on the size of the molecules;[15] circular dichroism to evaluate the secondary structure of the protein, ensuring that it is correctly folded;[16] and mass spectrometry to check that the sample is of the desired molecular weight and/or contains the expected stoichiometry of a protein complex.[17] The information yielded from these techniques will provide confidence in the quality of the sample subsequently being imaged.

2.2. Cryo-EM Advances for Membrane Protein Structure Determination

Over the past ∼10 years, cryo-EM has become an incredibly powerful tool in determining the structures of biological macromolecules to high resolution. This was facilitated by the cryo-EM "resolution revolution" that was underpinned by developments in microscope stability, the introduction of direct electron detectors, and advances in image processing algorithms, which have collectively led to a wide range of diverse structures being determined.[18] These include viruses,[19−21] ribosomes,[22] proteasomes,[23,24] and even filament structures;[25,26] the latter are isolated from brain tissue and are associated with various neurological diseases such as Alzheimer's.

As cryo-EM developments continue to advance, so does the resolution of the structures being deposited. For instance, in late 2020 a 1.2 Å map of apoferritin was determined that allowed the density for hydrogen atoms to be visualized within a map for the first time.[27,28] Moreover, the number of structures being deposited with resolutions <4 Å continues to increase each year, with parallel improvement in the average resolution of the

https://doi.org/10.1021/acs.chemrev.1c00837
Chem. Rev. 2022, 122, 13989−14017

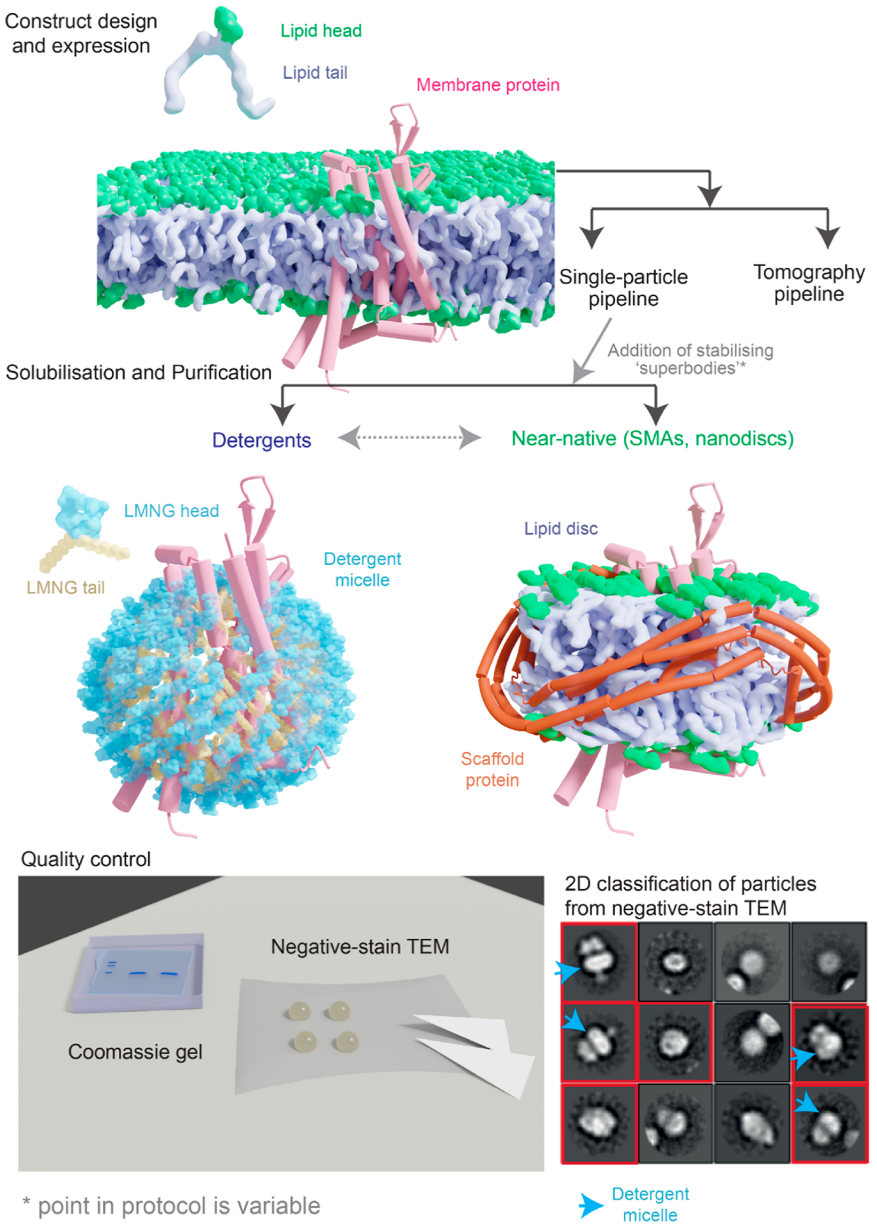

Figure 1. Overview of the protein biochemistry pipeline for cryo-EM on membrane proteins. Examples are shown for a typical single-particle cryo-EM pipeline with the expression of the protein in a membrane (lipid bilayer), common solubilization/reconstitution options (in detergents and nanodiscs), and using quality control steps such as Coomassie staining of protein samples and negative-stain TEM using uranyl acetate or uranyl formate as a stain. An example of a typical 2D classification of a membrane protein particle (GPCR in LMNG micelle) is shown for assessment of sample quality, highlighting different orientations of the particles' 2D classes (red boxes). Optional is the addition of stabilizing superbodies (such as fab fragments). SMA, styrene-maleic acid; LMNG, lauryl maltose neopentyl glycol; TEM, Transmission electron microscope.

structures being deposited (Figure 2). This highlights the major contribution that cryo-EM is making to the structural biology field, as protein targets that were previously poorly tractable to structural characterization are now routinely being determined.

Membrane protein structural biology has benefited enormously from improvements within the cryo-EM field. By removing the need to form well-diffracting crystals, cryo-EM has eliminated a major bottleneck for determining the structure of membrane proteins. This has led to a rise in the number of membrane protein structures being released each year,[29] enabling critical new structural information to be obtained. Detailed examples of the variety of membrane protein structures determined will be discussed in section 4. This section of the review will instead give a brief overview of cryo-EM and will highlight some of the key developments within the field that have enabled the structures of membrane proteins to be determined. Beyond the scope of this review are the theoretical aspects of cryo-EM; if this is of interest, then the reader is directed to refs 30−32.

2.2.1. Cryo-EM Overview. Cryo-EM can be split into two main branches: single-particle analysis (SPA) and cryoelectron tomography (cryo-ET). The before mentioned "resolution revolution" was particularly focused on the SPA "branch", thus yielding high resolution structures. However, cryo-ET also plays a major role in looking at how proteins behave within a cell, when they are in their native environment.[33] For cryo-ET studies, biological organisms, tissues, or cells are applied to cryo-EM grids, flash frozen, and then thinned to an appropriate

https://doi.org/10.1021/acs.chemrev.1c00837
Chem. Rev. 2022, 122, 13989−14017

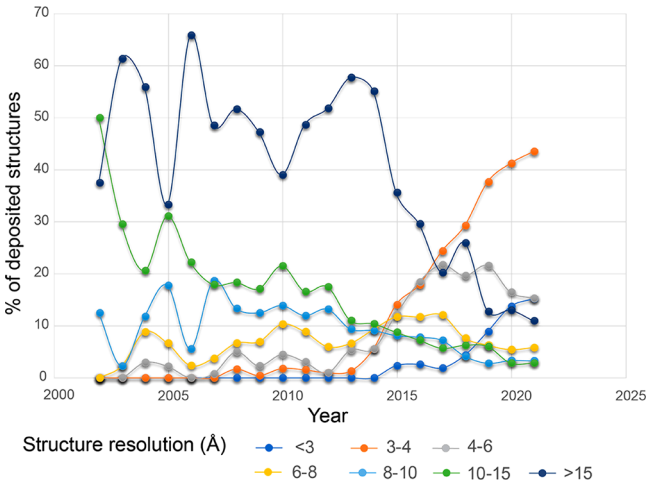

Figure 2. EMDB entry resolution in shells per year (date: 09-23-2021). The *X*-axis represents the year the structures were deposited. The *Y*-axis is the percentage of structures at the resolution shell deposited each year. The lines are colored according to the resolution range as described in the figure.

thickness (milled) before being inserted into the electron microscope. The images collected are often obtained as a tilt series, with images typically taken between ±65°, allowing for the specimen to be imaged from different angles. Using subtomogram averaging methodologies, these tilted images are then computationally recombined to generate a 3D map allowing for visualization of the target protein(s) *in situ*.[34]

The cells for imaging can be deposited or grown onto cryo-EM grids. However, cryo-ET is effectively limited to samples that are less than 500 nm in thickness; otherwise, the electron beam would not be able to pass though the sample.[35] As cells are often greater than this thickness, different approaches can be used to ensure the samples are electron transparent. One such approach is FIB-milling, which uses a focused ion beam (FIB) to carve out a region from the frozen cells (called lamella) with the desired thickness, usually 100−250 nm, for cryo-ET studies.[36] If the protein or tissue of interest is fluorescently tagged, then FIB-milling can be combined with fluorescence microscopy, in particular correlated light and electron microscopy (cryo-CLEM), to ensure that the correct region of the cell is being prepared.[37]

Traditionally, the resolutions achieved are on the nanometer scale, which allows cryo-ET to bridge the gap between high resolution SPA cryo-EM imaging and light microscopy. However, improvements in cryo-ET methodologies have enabled some recent high resolution structures to be obtained, including the 3.9 Å structure of the HIV capsid.[38] Another, highly impressive, example is the 3.5 Å antibiotic-bound 70S ribosome structure from inside of the cell.[39] To our knowledge, cryo-ET has not yet yielded high resolution structures of membrane proteins but has still provided useful insights into how proteins behave within cells (discussed in section 4).

The rest of the review will predominantly focus on the SPA "branch" of cryo-EM, as this has been the predominant technique for obtaining membrane protein structures. The process of determining a cryo-EM structure can be broadly split into three main sections: sample preparation, data collection, and image processing. These three sections will be discussed below.

2.2.2. Sample Preparation and Freezing Conditions. In order to visualize the sample within the electron microscope, the protein needs to be protected from the high vacuum of the microscope to prevent dehydration of the sample. To achieve high resolution structures, samples are protected within a thin layer of ice. Typically, 3−5 μL of purified protein is applied to a cryo-EM grid that contains a metal mesh (gold or copper) and is overlaid with a thin layer of amorphous carbon or gold.[40] Either this support layer can contain irregular holes (lacey grids), or the holes can be even in size and spacing (Quantifoils).[41] After the sample has been applied to the grid, it is plunged into a cryogen (typically liquid ethane), so the protein molecules become suspended in a thin layer of vitreous ice. Ideally the vitrified protein will reside in multiple orientations within the ice and away from the often-denaturing air−water interface. Unfortunately, obtaining the ideal grid can be a challenging and time-consuming process. Common problems encountered are (1) preferred orientation (particles adopt one conformation within the ice), (2) denaturation at the air−water interface, (3) an uneven distribution of protein in the holes, particularly in the thinnest ice, and (4) the protein having high affinity to the support film and subsequently not going into the holes (Figure 3), which is discussed in more detail in ref 42.

For membrane proteins in particular, it can be common for detergent-solubilized proteins to have high affinity for the carbon or gold support layer, resulting in a poor distribution of protein within the ice.[43] Moreover, in areas of the grid where the ice is thin, and ideal for obtaining high resolution structures, a "halo effect" is sometimes observed.[42] This is where the protein is clumped toward the edge of the hole and is absent in the center. These problems can potentially be overcome by having a high concentration of sample. By saturating the support layer, the protein is forced into the holes for imaging. Moreover, if using a high concentration is not successful, then imaging in areas of the ice that are slightly thicker can also visualize proteins with suitable distribution and sometimes overcome the preferred orientation.[44]

A key component to grid preparation for SPA is providing a very thin layer of ice that both provides minimal electron beam distortion during imaging and ensures that only a single particle is present in the beam path.[44] Conventionally, this is achieved by blotting of the samples applied to the grid prior to rapid immersion into the cryogen. This blotting approach to grid preparation is largely the same as that first developed by Jacques Dubochet in the 1980s and which led to the award of the 2017 Nobel Prize in Chemistry.[45,46] Vitrification can be performed manually or by using commercial devices such as the Leica or Thermo Fisher Scientific Vitrobots. However, a disadvantage of the blotting approach is that it can be difficult for users to apply reproducibly, while it is also wasteful, with ∼99% of the sample being blotted away.[47] The way in which cryo-EM grids are prepared is an active area of research within the community and has led to the development of several nonblotting devices, including both commercial and homemade instruments. Example devices include Spotiton,[48,49] VitroJet,[50] and cryoWriter.[51]

These devices make use of novel technologies for applying the sample to the grid. For instance, Spotiton uses a piezo inkjet dispensing system to apply the sample to the grid and utilizes self-wicking grids to create a thin layer of ice,[52] whereas VitroJet uses pin-printing technology to apply sub-nanoliter amounts of sample to the grid. In comparison, cryoWriter uses a microfluidic approach and capillary action to "write" the sample onto the

https://doi.org/10.1021/acs.chemrev.1c00837
Chem. Rev. 2022, 122, 13989−14017

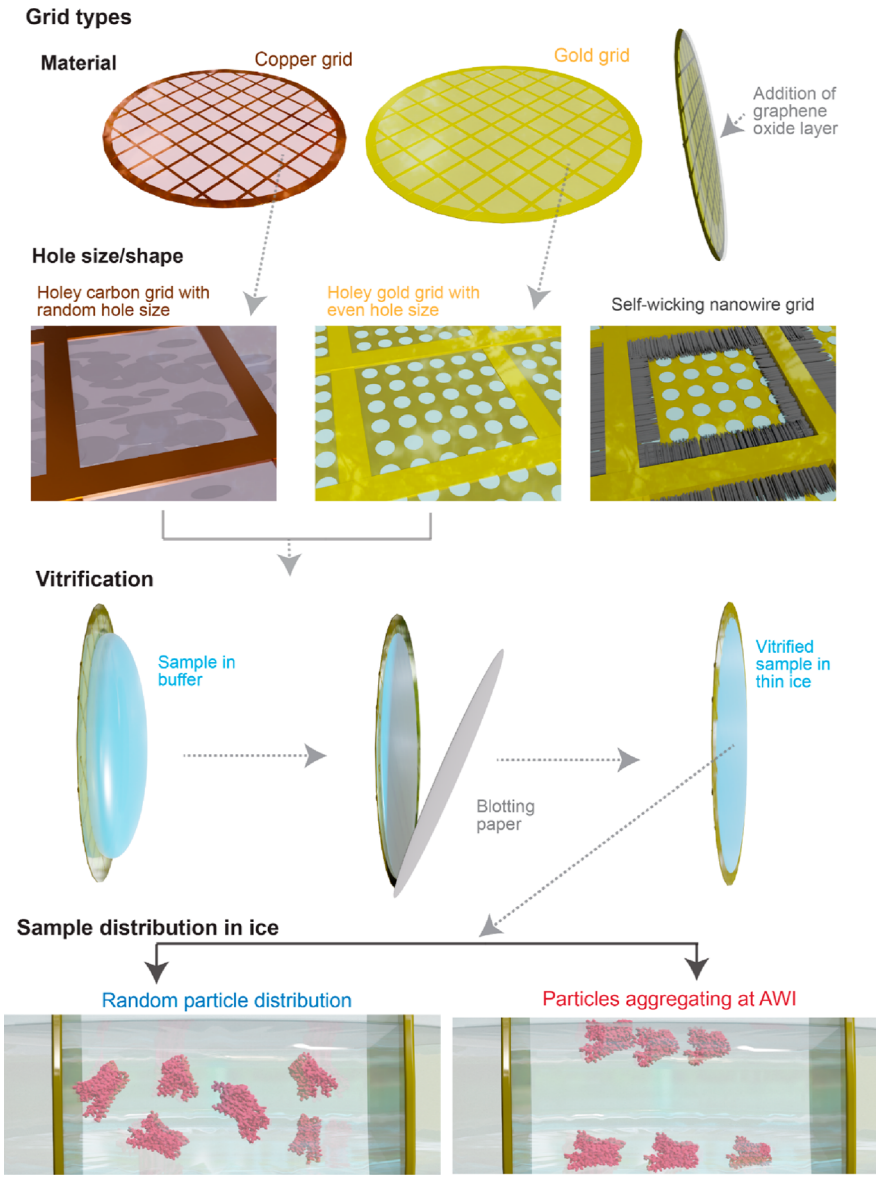

Figure 3. Overview of the steps involved in single-particle cryo-EM on membrane proteins. Illustrated are typical single-particle cryo-EM preparation processes such as decision on grid types (including gold grids, copper grids, or other layers, such as graphene oxide) or self-wicking nanowire grids that do not rely on blotting away excess sample using blotting paper. Hole sizes and shapes for grids range from random distributions that offer a variety of ice thicknesses to even hole sizes suitable for automated data collection. Vitrification (standard Vitrobot technology) starts with deposition of the sample, in a buffer solution, onto the grid of choice, blotting of excess liquid, and rapid vitrification of the sample in a thin ice layer. The sample distribution in ice can differ significantly for individual particles. Commonly, particles form preferred orientations and aggregates at the air−water interface (AWI). Random particle distribution across the thin ice layer is ideal for successful data processing.

grid. Recently, this technology was used to determine a 3.2 Å structure of the 20S proteasome where the protein was isolated from just 1 μL of cell lysate before being applied to the grid.[53] An advantage of all three instruments is that much smaller sample volumes are required to make grids, thus preventing precious samples from being wasted. Moreover, all three devices have supported grid preparation used to solve ∼2.5−3 Å structures, proving that nonblotting approaches are successful in the determination of high resolution structures.[48−51]

Moreover, several "homemade" devices have also been developed for cryo-EM grid preparation. One such device uses a voltage assisted sprayer to apply droplets of samples onto the grid.[54] This device was primarily designed for time-resolved experiments and allows for samples to be mixed together just before freezing. An advantage of this system is the speed at which the grids are prepared, as it can occur on the millisecond time scale, which can reduce issues of preferred orientation in some samples.[55] Another homemade device is the "Shake-it-off" system that was assembled using "easy to obtain" materials or by utilizing 3D printing to manufacture parts.[56] This technology uses an ultrasonic humidifier to apply sample to self-wicking grids and enables the determination of a 2.6 Å apoferritin structure in benchmark testing.[56] Although some of the newer devices are not yet available to the wider cryo-EM community, their developments remain exciting. By using less sample, improving the reproducibility, and significantly reducing the time scales needed to prepare grids, these devices may address some of the limitations of the conventional blotting method for sample vitrification, hopefully leading to the determination of more high resolution structures.

https://doi.org/10.1021/acs.chemrev.1c00837
Chem. Rev. 2022, 122, 13989−14017

2.2.3. Data Acquisition Hardware. A key factor in the "resolution revolution" was the introduction of direct electron detectors that greatly enhance the signal-to-noise ratio within the cryo-EM images, thus improving the contrast and making protein particles easier to "see".[57,58] Moreover, the images collected are actually movies consisting of a series of frames that can be computationally aligned to produce a single image (often termed micrograph). By taking movies, the movement which can occur during the image acquisition, due to beam-induced motion and/or stage drift, can be corrected for, resulting in high quality unblurred images.[59,60]

One of the main limitations to achieving high resolution structures by cryo-EM is that the sample becomes damaged by prolonged exposure to the electron beam, termed radiation damage.[61,62] One of the advantages of recording the images as movies, rather than single images, is that the total dose that the sample is exposed to can be split between the different frames. This means that the later frames, which have been exposed to the electron beam for the longest time and have subsequently suffered the most damage, can be removed, thereby enabling the high resolution features to be restored.

The detectors that are most commonly used are the Thermo Fisher Falcon III/IV and the GATAN K2/K3. Both detector brands are usually operated in electron counting mode, which means that the individual electrons that hit the detector are recorded. Unique to the Falcon IV is the electron event representation mode (EER), which allows movies to be captured at the raw frame rate of the detector.[63] This means that the user does not need to specify the number of frames into which to split the movie before the data is collected (required for conventional imaging modes) but instead after it has finished. This allows the motion-correction to be performed at the physical frame rate of the camera. The EER also allows the data to be collected in "super-resolution" mode, which theoretically means that resolutions beyond the Nyquist limit can be achieved.

To further enhance contrast within the cryo-EM images, an energy filter can be used. These work by filtering out inelastically scattered electrons based upon their wavelengths.[64,65] These electrons would normally contribute noise to the final images; by removing them, the contrast within the micrographs is increased. Example energy filters include the GATAN Bioquantum and the Thermo Fisher Selectris. The Thermo Fisher combination of a Falcon IV detector in combination with the newly developed Selectris energy filter resulted in a 1.2 Å structure of apoferritin and 1.7 Å structure of the $\beta 3$ γ-aminobutyric acid type A (GABA-A) receptor being recently solved.[27] Such results highlight the value that improvements to microscope hardware can deliver in gains in map quality and resolution.[27]

Until a few years ago, it was thought that routine high resolution structure determination via cryo-EM was likely to be limited to samples with molecular weights >200 kDa due to the low contrast of small proteins. This led to the development of the Volta Phase Plate (VPP).[66,67] The phase plate is inserted into the back-focal plane of the objective lens and boosts the contrast in the cryo-EM images, allowing structures of small proteins to be resolved. However, within the past 2−3 years it has become clear that the phase plate is no longer required for single-particle analysis. If the sample quality is high, data collection settings are optimized, and the ice is thin enough, small proteins can now be resolved without the need for a phase plate (examples discussed in section 3). Nonetheless, the phase plate is still likely to be advantageous for tomography studies, as the contrast within the cell will be enhanced. Moreover, a laser phase plate is currently being developed that could allow even smaller proteins to be studied via cryo-EM.[68]

2.2.4. Data Processing. A typical data set can consist of thousands of raw images that need to be processed in order to reconstruct a high resolution cryo-EM map suitable for structure determination. Fundamentally, the process relies upon the protein being frozen in multiple orientations within the ice. Briefly, protein particles are picked to generate a particle stack consisting of hundreds of thousands to millions of particles. These particles are then classified based upon their different orientations, resulting in the signal within the individual particles being averaged together to increase the signal-to-noise ratio. The classes are 2D projections of the sample which can be combined together to generate a 3D reconstruction of the protein using the Fourier projection theorem.[69] The map quality can be further enhanced using a variety of techniques before a model can be fit into the density. These include particle polishing (to correct for individual particle movement during the data collection),[70] focused refinements (to improve the map quality in certain regions),[71] local and global contrast transfer function (CTF) refinements (to account for misalignment or microscope aberrations)[72] and postprocessing (applies a B factor to the map that enhances the high resolution features).[73,74] For in-depth details about typical image processing pipelines, the reader is directed to the following review articles.[75,76]

There are a variety of software packages available that can be used to analyze cryo-EM data to obtain high resolution structures, including RELION,[72,77] cryoSPARC,[78] EMAN,[79] cisTEM,[80] and SIMPLE,[81] among others. Each program has its own algorithms and workflow that can be advantageous for different samples, so it is advised that multiple software approaches are trialed to obtain the best result. Particle picking is also a key step in the processing pipeline; the development of software packages that use neural networks to recognize particles from contaminants or noise such as crYOLO[82] and TOPAZ[83] has enhanced the ability to accurately pick low contrast particles in recent years.

Once the data processing is complete, a model can be built or fitted into the map. This is often the final step in the process and allows for the intricate structural details of the protein to be visualized. The approach taken to model fitting depends on the resolution of the map and whether there are any existing, related, structures that have been solved. The release of the AlphaFold2 database of predicted protein structures[84,85] has recently become a valued tool where limited pre-existing structural information on protein classes is available. For high resolution maps where side chain densities are visible, the model can be built and refined into the density using programs that were developed to support modeling by X-ray crystallographers including COOT,[86] PHENIX,[87] and Refmac.[88] A newer tool, which has only recently become available, is ISOLDE, which uses a molecular dynamics-based flexible fitting approach, guided by the cryo-EM map, and can oversee modeling statistics in real time.[89] This can particularly benefit regions of low resolution density or when only the backbone model is being fitted into the map. At more moderate resolutions, where only secondary structural information is available, an initial model should be flexibly fit into the map using programs such as MDFF/NAMD.[90] If there is no prior structural information, then one should consider generating a homology model or using

https://doi.org/10.1021/acs.chemrev.1c00837
Chem. Rev. 2022, 122, 13989−14017

AlphaFold2 to generate an initial template that can be fit into the density.[84,85] Furthermore, for low resolution maps, large protein domains or existing crystal structures could be rigidly positioned into the cryo-EM density to determine the approximate location within a complex.

Cryo-EM maps and models can be visualized using programs such as UCSF Chimera,[91] ChimeraX,[92,93] and PYMOL.[94] All three programs are commonly used to prepare figures for manuscripts/presentations as well as analyzing the structures and/or making comparisons to existing structures. ChimeraX can also be useful for building/refining models, as ISOLDE and AlphaFold are integrated into the software. After the modeling is complete, care needs to be taken not to overfit or overinterpret the data. For instance, commenting on side chain positions when there is no side chain density present in the map would be an example of overinterpreting the data.

In the data processing pipeline, different software packages utilize gold-standard Fourier shell correlation (FSC) to determine the resolution of 3D maps using independent half-sets of data. Most publications cite the resolution at the fixed 0.143 FSC cutoff,[95] whereas others report the 1/2-bit threshold.[96] To determine how well the model fits a cryo-EM map, one can calculate a model-map FSC, which is a useful validation tool and is implemented in software packages such as PHENIX.[87,97] In any case, uploading the half-maps, as well as masks and all unfiltered and final filtered maps, to the Electron Microscopy database (EMDB) or the Protein database (PDB) for map and model deposition through the OneDep system[98] (prior to publication) is, in most cases, a requirement (journal-dependent). This gives the reviewers and readers access to unmanipulated map/model and validation files to assess reported global and local resolution versus perceived resolution, e.g. by high resolution features, such as water molecules or aromatic rings, present in the map. At this stage it is the author's and/or reviewer's responsibility to provide/request map and model files prior to deposition; however, we propose this to be made mandatory for the reviewing process to ensure high data quality and correct data interpretation.

Making all raw data (e.g., raw movie files) available at public databases such as EMPIAR (https://www.ebi.ac.uk/empiar/), and providing the opportunity for everyone to process this data, is another suitable option for data transparency. Past examples report issues with overinterpretation of data and biased data processing, in the community known as the "Einstein-from-noise" phenomenon.[99,100] To avoid these issues in the future, the aforementioned quality controls at the data deposition step have been made available, in addition to publications that demonstrate examples of overfitting and/or overinterpretation of data.[101]

3. TECHNICAL ADVANCES SUPPORTING HIGH RESOLUTION OF MEMBRANE PROTEIN STRUCTURE DETERMINATION

3.1. *In Situ* Membrane Protein Biology

Despite advances in a variety of cryo-EM and cryo-ET methods, capturing the actions of membrane proteins *in vivo* is still difficult. Characterizing *in situ* protein structures within membranes at high resolution using microscopy methods is limited by factors such as small size, low contrast, and low abundance of single homogeneous proteins in membranes. Alternative methods using hydrogen and deuterium labels observed through neutron scattering make it possible to characterize bacterial membranes *in situ*, for example determining the membrane thickness and lateral lipid organization through small-angle neutron scattering (SANS).[102] Within the past few years, particularly due to the technical advances in cryoelectron tomography hardware and software, combined with correlative-light imaging (CLEM), these powerful tools have enabled ultrastructure biology *in situ*, with increasing automation.[103] Cryo-CLEM and cryo-ET have also allowed dynamic processes that occur within the membrane to be visualized, for example shedding events in response to damaged HeLa cell membranes.[104] Currently, only particularly large membrane protein structures are suitable for *in situ* cryo-EM, for example secretion systems;[105] further examples will be described in section 4. Smaller integral membrane proteins such as receptors or channels, which are typical drug targets in cells, are not yet amenable *in situ* to high resolution, but considering the rate of progress in this area, it is only a matter of time before smaller, lower abundance, proteins will also be resolved.

3.2. Optimizing Biochemistry and Stability of Membrane Proteins in Single-Particle Experiments

While substantial advances in *in situ* cryo-ET are evident, the majority of integral membrane proteins, in particular important drug targets such as GPCRs, transporters, and ion channels, are primarily being determined using recombinant expression and purification approaches that allow for single-particle cryo-EM analysis. Considerable effort has been directed toward establishing protocols for extraction and reconstitution of membrane proteins in near-native environments due to their importance for structural integrity and function, with a focus on using disclike lipid particles held together by stabilizing proteins, often termed nanodiscs (Figure 1). Using these mimics, membrane proteins are investigated outside of their original membrane environment but still within a lipid bilayer or in the presence of natively associated lipids, which can be used for high resolution single-particle structure determination methods.

Proteins that support stable nanodiscs include saposin A and membrane scaffold proteins, such as apolipoprotein A1 (apoA1), which are α-helical proteins that wrap around the protein and associated lipids like a belt[106,107] (Figure 1). However, in most cases, before the formation of nanodiscs, the proteins are still solubilized in detergent and reconstituted either during the purification protocol or after purified protein is obtained.[106,108,109] In these approaches, synthetic or purified lipids are included during reconstitution to mimic prototypical membrane environments. Another approach to extraction of membrane proteins uses styrene maleic acid polymers to create styrene maleic acid lipid particles (SMALPs). These directly remove the protein from the membrane and can retain lipids from the local membrane environment of the target protein.[110] One advantage to this approach for cryo-EM is that, once the protein is extracted within the SMALP, no other detergents need to be added to the buffer, thereby potentially improving contrast within the cryo-EM images.[111] Another example of a membrane mimetic system is the "peptidisc", which uses a peptide to surround the transmembrane region of the membrane protein and stabilize it following extraction from the membrane.[112] As the peptide molecules bind around the transmembrane helices, this approach can work on all sizes of membrane protein. The reconstitution to form the peptidisc follows a quick and easy protocol that mitigates the need to optimize the correct protein-to-lipid ratios.[112] For more technical information on these different solubilization and reconstitution systems, the inter-

https://doi.org/10.1021/acs.chemrev.1c00837
Chem. Rev. 2022, 122, 13989−14017

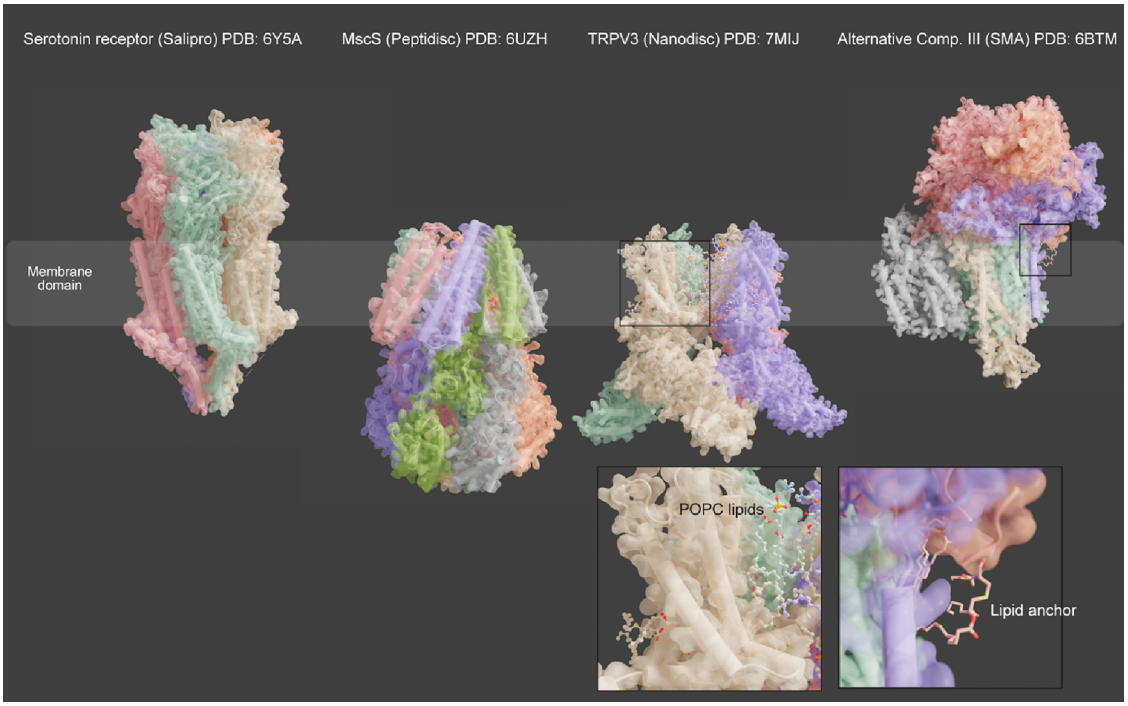

Figure 4. Examples of membrane protein structures solved using different solubilization/reconstitution methods. A variety of membrane protein structures have recently been solved using near-native membrane encapsulation methods, such as saposin A discs (Salipro), peptidisc, lipid nanodisc (membrane scaffold protein such as apolipoprotein A1), and styrene-maleic acid (SMA), with the latter two showing resolved lipids. The illustrated examples are colored by molecule chains, with surface representations of the models and secondary structures shown as cylinders and stubs through ChimeraX and rendered in Blender.

ested reader can choose from a variety of publications, which cover development, detailed protocols, and advantages for use of near-native or lipid-associated, detergent-free methods for single-particle cryo-EM: for example, SMA copolymers for membrane solubilization[113] and SMA polymers and variations,[114] comparison of novel detergent-free solubilization methods, including SMALPs, diisobuytl maleic acid lipid particles (DIBMA), cyclohexane-modified amphiphile polymer (CyclAPol), and native cell membrane nanoparticles (NCMN),[115] the latest applications and developments of nanodisc tools,[116] and statistical analyses of detergents and lipidic environment mimetics used for deposited membrane protein structures since 2010.[29] The more recent, nondetergent, solubilization techniques that focus on solving membrane protein structures in more native, biologically relevant contexts have also made it possible to resolve more details on lipids or lipid components in the transmembrane regions of membrane proteins,[117−119] as highlighted in Figures 4 and 5.

In terms of examples of cryo-EM membrane protein structures in near-native environments, Yao et al. have established a pipeline to investigate membrane protein structures using liposomes with the prototypical *E. coli* AcrB, a 350 kDa bacterial transporter.[120] A combination of biochemical and grid optimization enabled a 3.9 Å resolution reconstruction of AcrB. However, the authors note that their strategy is most suitable for membrane proteins that contain a large enough soluble domain to provide a sufficient signal to help align particles in 2D classifications. Liposomes were also used in structure determination of large pore-forming proteins, such as MPEG1.[121]

In contrast to liposomes, polymers such as SMALPs drastically reduce the size of single particles, which renders them more suitable for distribution into thin ice for encapsulated smaller membrane proteins.[122,123] Acriflavine resistance B (AcrB) has also been an exemplar in cryo-EM experiments demonstrating the use of SMALPs in providing benefits for resolving lipids in a detergent-free contex,[124] or the combination of SMALP solubilization with subsequent exchange to detergents or amphipols for compatibility with mass spectroscopy methods.[125] SMALPs and other near-native solubilization methods have also been successfully used in high resolution cryo-EM structure determination experiments. Examples include the alternative complex III[119] as well as therapeutically relevant targets, such as an acid-sensing ion channel[126] and glycine receptor[127] where the use of SMALPs and capture of native lipids were essential to allow resolution of different states that were important for understanding protein function. G protein-coupled receptor (GPCR) structure and function have also been investigated using SMALPs or similar polymers, e.g. in functional assays using lipodisqs (dopamine receptors[128]) or SMALPs (adenosine 2A receptor (A2A)[129]), as well as study of conformational dynamics using hydrogen−deuterium exchange mass spectrometry (HDX-MS) (PTH1 receptor[130]). A side-by-side analysis of DIBMA and SMALPs has been published to examine protein yields and stability (e.g., on A2A and calcitonin gene-related peptide (CGRP) receptor[131]). However, these polymers have not yet been successfully used for high resolution cryo-EM studies of GPCRs, and therefore, the potential utility of this approach for GPCR structures remains to be established.

Nanodiscs that are formed using membrane scaffold proteins (MSPs) are commonly used for determining high resolution membrane protein structures. Different forms of MSPs can enable generation of nanodiscs of varying size, and consequently, nanodiscs can be used for reconstitution of a broad range of membrane proteins/protein complexes.[109] Indeed, numerous membrane protein structures in nanodiscs have been

https://doi.org/10.1021/acs.chemrev.1c00837
Chem. Rev. 2022, 122, 13989−14017

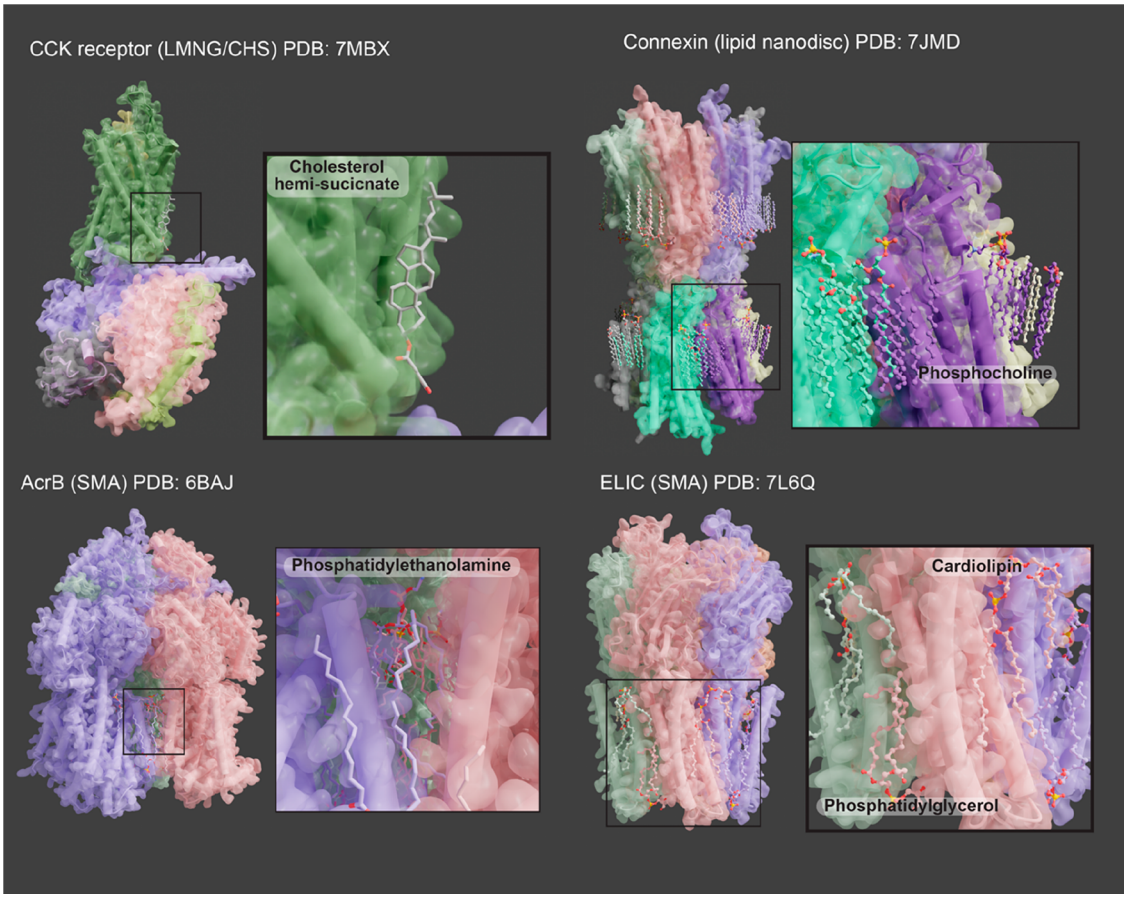

Figure 5. Examples of membrane protein structures with resolved lipids and lipid components. Membrane protein structures were resolved in detergents, lipid nanodisc, and SMA. The illustrated examples are colored by molecule chains, with surface representations of the models and secondary structures shown as cylinders and stubs through ChimeraX and rendered in Blender. Specific lipids are displayed in stick representation, colored by heteroatom. LMNG/CHS, lauryl maltose neopentyl glycol/cholesterol hemisuccinate; SMA, styrene-maleic acid.

published. One such example is Complex I, a protein involved in the mitochondrial electron transport chain where three different conformational states were identified.[132] The importance of ordered lipids was also revealed in the lipid nanodisc reconstituted Connexin structure, solved at 1.9 Å resolution (channel and lipids shown in Figure 5).[118] Other membrane protein structures solved in nanodiscs include the TASK2 potassium channel,[133] the β-barrell containing SAM complex,[134] a 120 kDa potassium chloride cotransporter KCC4,[135] and the SARS-CoV-2-ORF3a ion channel,[136] highlighting the diverse range of proteins nanodiscs can be used for. While high resolution GPCR structures have primarily been determined following detergent solubilization and purification, there are recent examples of structures solved using nanodisc technology, including complexes of the neurotensin receptor 1 with G protein,[137] the M2 muscarinic receptor in complex with β-arrestin,[138] and native rhodopsin dimers.[139] It is likely that retention or reconstitution of membrane lipids will play an important role for understanding of the conformational dynamics of GPCRs and to enable determination of complexes where lipid interactions are functionally important. The routine application of nanodiscs for study of GPCR structures is currently limited by the efficiency of GPCR reconstitution into nanodiscs and by structure resolution relative to well established pipelines for detergent-solubilized receptors. However, given the likely benefits of more native membrane-like environments in understanding the complexity of GPCR structure−function, the use of nanodiscs is expected to rise in parallel with improved methods for reconstitution and with the optimization of vitrification, cryo-EM imaging, and 3D reconstruction to achieve higher resolution.

Peptidiscs are a relatively new method for the stabile extraction of membrane proteins, where the scaffold peptides form a tight boundary around the target protein.[140] They have been successfully applied to the determination of a 3.3 Å structure of a mechanosensitive channel (MscS);[112] nonetheless, the extent to which these discs can support normal protein function is not well studied. Another relatively recent technology that is attracting attention is the use of the saposin A scaffold that has been commercialized by Salipro,[141] with recent examples of structures solved using the saposin-lipid nanoparticles to stabilize the protein. These include AcrB/DARPin at 3.1 Å and the serotonin bound 5-HT3A receptor at 2.8 Å.[142,143] These newer technologies have expanded the repertoire of approaches available for membrane structure determination and may open up new opportunities for currently poorly tractable proteins or improving structural pipelines.

Historically, most membrane protein structures deposited have been determined in detergents or amphipols. Amphipathic polymers such as amphipols do not form micelles and, therefore, offer advantages over classic detergents due to possible amphipol usage at very low concentrations.[144] Membrane protein structures solved in amphipols include TRPV1,[145] HCN4,[146] and the STRA6 receptor.[147] In the specific case of

https://doi.org/10.1021/acs.chemrev.1c00837
Chem. Rev. 2022, 122, 13989−14017

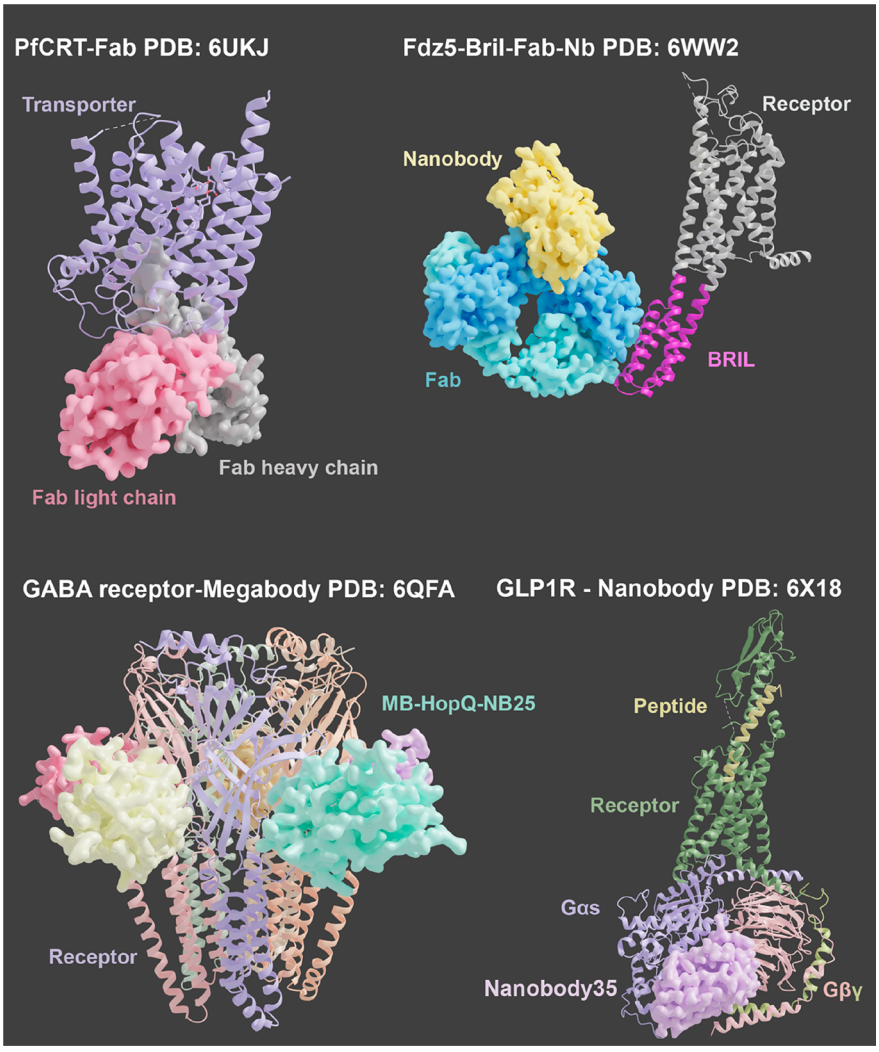

Figure 6. Membrane protein structures solved using "superbodies". Superbodies can be used to stabilize or increase the size of membrane proteins. The first example shown is the *Plasmodium falciparum* chloroquine resistance transporter (PfCRT) where the added Fabs increased the size of the protein making it amenable to cryo-EM. The other examples are the Frizzled-5 receptor (a GPCR), the gamma aminobutyruc acid (GABA) receptor (a ligand gated ion channel (LGIC)), and the glucagon-like peptide-1 receptor (GLP-1R; a GPCR) in complex with G proteins and nanobody-35. The Fabs were used to increase the size, orientation preference, and/or stability of the samples. The illustrated examples are colored by molecule chains with the surface representation of the superbodies and the secondary structure of the membrane proteins shown as ribbons and slabs through ChimeraX and rendered in Blender.

GPCRs, higher resolution (<3 Å) structures that have been determined to date predominantly use LMNG detergent, often supplemented with cholesterol hemisuccinate (CHS). CHS can be resolved in many of the cryo-EM structures and, therefore, infers a tight binding to the transmembrane helices, likely mimicking cholesterol (which is an important component of plasma membranes), and, in some cases for GPCRs, plays a critical functional role.[148]

To decide on the ideal solubilization and reconstitution method for the individual membrane protein, structural biologists need to consider different variables, including the intended use/interpretation of the solved structure. The retention of native membrane lipids or the incorporation of membrane proteins into reconstituted membranes or membrane mimetics is not straightforward, can be highly protein dependent, and often needs an additional step prior to detergent solubilization. Interestingly, a recent study points to the fact that, despite the use of different nanodisc MSPs, amphipol, or detergent agents, the amphipathic belts surrounding the extracted proteins are often of similar size when studied using cryo-EM,[149] indicating that the use of different methods reveals similarly ordered belts around transmembrane regions after 3D reconstructions, independent of the solubilization method or protein used.

Despite the rise in motivation to solve membrane protein structures in more native/lipid-like environments, many solubilization problems still need to be overcome for these to be routinely used for a variety of membrane proteins, and consequently, the "peak" of detergent use for cryo-EM studies is far from over. Novel detergents are continuingly in development as a means of broadening their application to proteins that are not well served by current detergents, for example via modifications that can confer higher stability.[150] If detergents/micelle size is an issue, technologies such as "GraDer" may help with the stability of membrane proteins and removal of excess micelles for subsequent cryo-EM studies.[151] No matter what choice of solubilization methods is taken, troubleshooting for

https://doi.org/10.1021/acs.chemrev.1c00837
Chem. Rev. 2022, 122, 13989−14017

each protein and quality control is key in optimizing samples for high resolution imaging.

Most membrane proteins function by undergoing conformational changes to alter their intrinsic properties (e.g., gating of ions) or by engaging with other proteins to form larger protein complexes. Stabilization of important states or otherwise transiently formed complexes and the ability to separate these, particularly for small or dynamic systems, are key for achieving high resolution cryo-EM structures. Thus, many of the recent developments that have enabled high resolution structural information to be resolved have not only focused on the ideal solubilization methods but also on the addition of binding partners to help with stabilizing flexible domains, increasing particle size and/or the alignment of particles outside the micelle/lipid belt for 2D and 3D reconstructions.[152] These stabilizing partners are often antibody-derived "superbodies", a term coined herein that covers and condenses all recent advances in development of additional antibody-like particles under the umbrella of a common terminology. "Superbodies" natively do not bind to the membrane protein of interest but are instead engineered to assist in membrane protein stability or resolvability. Figure 6 shows relevant membrane protein structures solved together with their superbodies.

Included in this terminology are nanobodies and single-chain fragments, often used in GPCR-G protein-complex structures. Examples include nanobody 35[153] and the short chain Fab scFv16,[154] as well as recently developed megabodies[155] and legobodies[156] that both contain stable scaffolds to enlarge particles, and nanobody-short chain Fab fusions—NabFabs.[157] In the case of nanobody 35, this nanobody binds across the interface of G protein subunits to stabilize their binding to activated GPCRs,[153] rather than being requisite for enlarging particle size. In other cases, the addition of the "superbodies" was the only approach to enable high resolution cryo-EM structure determination. An important drug target structure, the serotonin transporter, is an example of a small membrane protein with limited features outside of the membrane/micelle. Structure determination for this protein required the use of a Fab fragment targeting the protein to provide a fiducial marker to help particle alignment for single-particle cryo-EM. Binding of the Fab fragment did not influence the binding of the modulator or function of the receptor, with the determined high resolution structure enabling the identification of a unique binding site of an allosteric modulator.[158] Nonetheless, such fiducial markers need to have limited flexibility relative to the target protein to support alignment and reconstruction of the target.

For GPCRs that comprise the largest class of drug targets, cryo-EM structure determination has been primarily limited to active structures in complex with transducer proteins that increase particle size and provide distinctive features outside of the membrane/micelle. These structures are enabling understanding of the mode of agonist drug binding and the application of structure assisted design to the class of pharmacological agents. However, cryo-EM determination of inhibitor-bound, inactive GPCR structures is still extremely challenging due to the small size of individual receptor proteins (~40−50 kDa) that are mostly encased in the solubilization medium and their intrinsic conformational dynamics.[159] Consequently, methods for routine determination of inactive (transducer-free) structures by cryo-EM would significantly enhance the application of cryo-EM to drug discovery and development campaigns. Traditionally, obtaining inactive G protein structures has been the domain of X-ray crystallography. However, obtaining large amounts of purified receptor that is stable enough to form crystals has been a hurdle too large to overcome for many receptor systems. The ability to apply cryo-EM to small amounts of purified protein could, thus, greatly expand the spectrum of structures solved.

The binding of antibodies or "superbodies" could theoretically both increase the molecular weight of the small GPCR particles and provide a feature outside of the micelle to aid particle alignment. One example of successful adoption of this approach is the structure of the human Frizzled-class receptor-5 (Fzd5) bound to Wnt, where a thermostabilized apocytochrome (bRIL) fusion protein was inserted into intracellular loop 3 (ICL3) of the receptor, which allowed for an anti-bRIL Fab and an anti-Fab nanobody to bind to the complex. The bRIL-Fab-Nb acted as a fiducial marker outside of the membrane and enabled reconstruction of a 3.7 Å structure.[160] This approach could be applied to other membrane protein systems, not just GPCRs, which could enhance drug discovery campaigns against smaller membrane protein targets. However, it is important to note that a contributor to the success of the bRIL insertion for the Fzd5 receptor was that it formed a stable extension from the receptor with only limited conformational flexibility of the bRIL relative to the transmembrane core of the receptor. It is likely that robust alignment based on a marker that is dynamic relative to the target protein component would be very difficult and, thus, optimization of the choice and location of the inset protein is likely to be critical to the potential success of this approach.

Outside of the GPCR field, Fabs or "superbodies" have been used to determine a variety of membrane protein structures. These include ABC transporters[161] and the *Plasmodium falciparum* chloriquine resistant transporter (PfCRT).[162] PfCRT is an example of Fabs being used to rigidly increase the molecular weight of the complex (from 49 kDa to ~100 kDa) and provide a feature to align on the outside of the detergent micelle. Moreover, the visualization of how Fab fragments bind to proteins can also have implications for development of antibody-based therapeutics.[163,164] One example is the 3 Å structure of the STEAP1 protein that is upregulated in certain cancers. By determining the structure of the protein bound to three Fabs developed from a clinically used monoclonal antibody, molecular insights into the mechanism of STEAP1 inactivation could be made, which could lead to the development of new treatment options for certain cancers.[165]

In this section, we have described some of the crucial steps in the expression and purification protocols of membrane proteins and approaches that have been successfully applied for many different membrane proteins and complexes. It should be noted though that many of these steps have been optimized for each individual case of protein expression and purification and might need further optimization for future or broader applications.

3.3. New Developments within the Cryo-EM Field That Have Benefitted Membrane Protein Structural Determination

The following section will discuss how the developments in the cryo-EM field have enabled membrane protein structures to be solved, and it will once again be split into the three main stages: sample preparation, data collection, and image processing.

3.3.1. Sample Preparation. For the majority of membrane protein structures deposited into the EMDB, data were collected using Quantifoil grids following sample vitrification using traditional blotting devices (Leica or Thermo Fisher Vitrobot). The advantage of using Quantifoil grids is that the regular array of holes makes the data collection easier to set up; the stage or

https://doi.org/10.1021/acs.chemrev.1c00837
Chem. Rev. 2022, 122, 13989−14017

beam can move to fixed positions to acquire the images. Systematic evaluation of different parameters in vitrification and imaging can aid in the optimization and robustness of sample preparation for individual classes of membrane proteins, as was recently demonstrated for detergent-solubilized GPCRs,[166] where an optimized grid preparation strategy was identified. This involved the use of high concentrations of purified sample (4−6 mg/mL) applied to AuUltraFoil 1.2/1.3 grids in a Vitrobot chamber. Before the sample was applied to the grid, they had been rendered hydrophilic by using a long glow discharging setting (10 mA for 90 s), which was vital for achieving a good distribution of protein within the ice. High blot forces and blot times were used to create a thin layer of ice where the protein molecules were very tightly packed next to one another, which yielded high resolution structures (<2.5 Å). In this work, the most important factors for high resolution were switching from carbon to gold coated grids (~0.3 Å) and the use of a high sample concentration to enable robust partitioning into thin ice.[166] We have found that optimization of vitrification conditions is, not surprisingly, perhaps the most important factor in the final resolution of determined structures, accounting for as much as 1 Å difference in the obtained resolution of GPCR complexes. Things to try when optimizing the vitrification conditions include the following: using different types of grid to change the hole size or support material; altering the glow discharge parameters, which can also impact the particle distribution within the ice; optimizing the blotting conditions, specifically the blot force and blot time; and/or using a different vitrification device.

For samples where high yields of protein cannot be obtained, the newer generation of devices may prove useful, as less sample is required to prepare grids. This is illustrated in the example of the arabinofuranosyltransferase (AftD) protein.[167] Despite purifying from a 9.6 L culture, only 100 μg of protein could be obtained by the authors. Due to the low yield, the Spotiton system was used to prepare cryo-EM grids, as it applies picoliters of sample onto the grid, significantly less than traditional blotting approaches. Ultimately, a 2.9 Å structure of the mycobacterial AftD was obtained, which allowed for the identification of the ACP binding site and provided novel insights into the function of the enzyme.[167]

In cases where the protein distribution within the holes is poor, or there is considerable denaturation at the air−water interface, a thin layer of graphene oxide can be applied to the grid.[168,169] This can enable the protein to adhere to the carbon layer and move the protein away from the air−water interface. Moreover, if the protein has a high affinity for the carbon support layer, applying graphene oxide can artificially increase the concentration of protein within the holes. This is exemplified in a study using the NaChBac protein where the protein appeared to be at least 4 times more concentrated in grids coated with graphene oxide compared to normal carbon quantifoil grids.[168] Graphene oxide has also been used in the determination of the structures of the ryanodine receptor[170] and Lysenin pore,[171] emphasizing that graphene oxide coated grids may be useful for membrane protein structure determination.

Another technique for improving the particle distribution and orientation within the ice is the use of polyethylene glycol (PEG)ylated gold grids.[172] This was applied successfully for the determination of the structure of Complex I where the PEGylated gold not only reduced the aggregation of the sample but it also improved the orientation distribution of particles within the ice, leading to a 4.1 Å structure being resolved.[173] With the development of alternate grid supports and new generations of grid preparation devices becoming available, there are increasing options for structural biologists to trial when preparing membrane protein samples.

3.3.2. Data Collection. The predominant data collection strategy for obtaining high resolution membrane protein structures is to image the sample of interest at 300 kV on a Thermo Fisher Scientific Titan Krios or JEOL CRYO ARM microscope, particularly with either a K3 or Falcon IV detector. While this approach has been very successful and has been utilized for the majority of deposited membrane protein structures, there are drawbacks associated with the high financial expense of imaging and with the ability of researchers to access microscope time. With the ability to integrate the latest generation K3 or Falcon IV detectors, a viable alternative approach is to image at 200 kV on a microscope such as the Glacios (Thermo Fisher Scientific). These are generally more affordable and, thus, could become more commonplace in laboratories worldwide. Work by Lander et al. demonstrated it is possible to obtain high resolution structures at 200 kV, including smaller protein systems with molecular weights sub-100 kDa.[174,175] More recently, examples of membrane protein structures determined on a Glacios 200 kV microscope have been published, including the glucagon-like peptide-1 (GLP-1) receptor[176] and chemokine receptor 5 (CCR5).[177] These studies highlight that structural resolutions for membrane proteins within ~0.3 Å of those achieved with 300 kV microscopes are possible with 200 kV imaging.[176] Moreover, in the GLP-1R example, the authors were able to visualize not only well resolved small molecule binding to the receptor but also the coordinating water molecules, which yielded almost equivalent information to the same sample imaged at 300 kV.[176]

Some of the first GPCR structures were primarily determined with the aid of a Volta phase plate,[178,179] where the higher contrast enabled by the phase plate improved particle selection and alignment. GPCRs are now routinely solved to high resolution (often sub-2.5 Å) using the optimized approaches described above using conventional cryo-TEM.[166] Nevertheless, solving cryo-EM structures of apo GPCRs, without ligands or other modifying proteins, remains challenging. Improvements to software supporting particle picking and EM data processing rapidly overcame the prior limitations associated with low sample contrast, obviating the need for the phase plate; this is exemplified by the plethora of GPCR structures solved by conventional cryo-TEM that have been published since 2018, which the interested reader can easily access through the GPCR database (GPCRdb).[180] Similarly, there are numerous examples of other classes of sub-100 kDa membrane protein structures that have been resolved to high resolution, without the need for the phase plate. Examples of small membrane proteins now being solved by conventional TEM include the transporter class of membrane proteins, with structures of the blood brain lipid transporter MFSD2A,[181] human monocarboxylate transporter 1,[182] and DASS dicarboxylate transporter all being solved.[183]

3.3.3. Image Processing. RELION, cryoSPARC, cisTEM, and EMAN are among a number of different software packages that have successfully been used to determine high resolution structures of membrane proteins from cryo-EM data, including small <200 kDa proteins such as γ-secretase[184] and large >1 MDa complexes such as phycobiliosome.[185] Moreover, there are several examples of RELION being used to identify the protein residing in different conformations. One such example is highlighted by the RagAB and SusCD transporters that were

https://doi.org/10.1021/acs.chemrev.1c00837
Chem. Rev. 2022, 122, 13989−14017

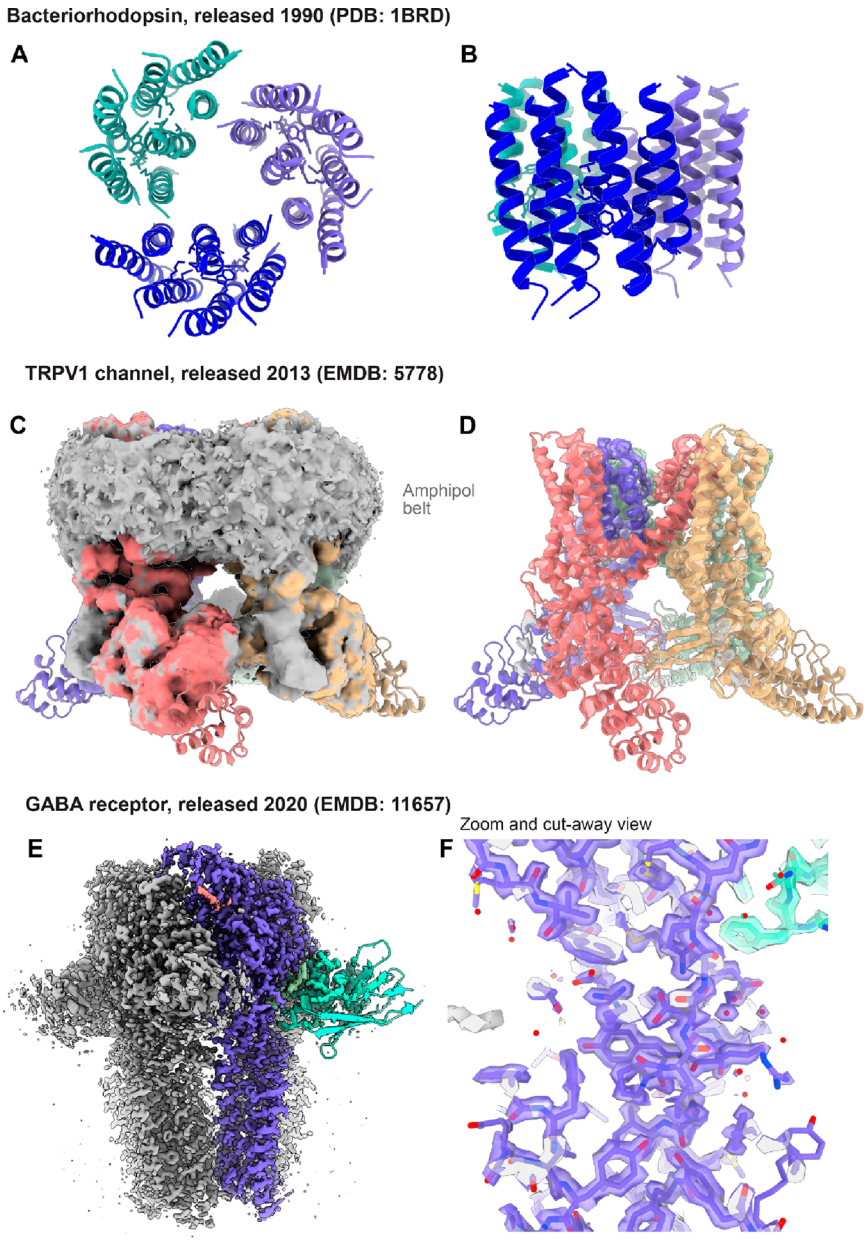

Figure 7. Historically important milestones in cryo-EM membrane protein structure determination. Illustrated are bacteriorhodopsin (originally solved in 1975; here represented by the PDB released in 1990) solved using electron crystallography (ribbon format; (A) top view, looking down the transmembrane helical bundle from the cytoplasmic side of the receptor, (B) side view with the extracellular side at the bottom of the figure), the TRPV1 channel reconstituted in amphipols, solved using single-particle cryo-EM ((C) cryo-EM map and model at lower map threshold, (D) cryo-EM map and model at higher map threshold), and the recent high resolution structure of the $GABA_A$ receptor published in 2020 ((E) cryo-EM map, (F) zoom-in illustrating near-atomic level features). Segments are colored by molecule chains. Figures were prepared using ChimeraX.

shown to exist in both open and closed conformations, allowing for insights into a "pedal bin" mechanism of action to be gleaned.[186,187]

Using cisTEM, the structures of CD20 bound to a monoclonal antibody,[188] NaV1.7 bound to a spider toxin,[189] and TRPA1 bound to a small molecule ligand[190] have all have been solved. For these three examples, the resulting structures have provided useful insights into how therapeutic agents bind to their target protein, thus aiding drug discovery and development programs.

Moreover, cryoSPARC is becoming a popular choice for membrane protein data processing. Built into the cryoSPARC package is a nonuniform refinement that particularly helps to improve the resolution and subsequent map quality of membrane proteins.[191] It works by systematically removing the noise from disordered regions, such as detergent micelles, while maintaining the signal in regions that are useful for particle alignment, such as the transmembrane helices, thus enhancing map quality. Another feature of the cryoSPARC package is the 3D variability analysis (3DVA), which allows the dynamics of the protein to be studied.[192] 3DVA has been extremely useful for probing the dynamics of GPCRs, especially with respect to peptide binding,[193−195] and has proven powerful in combination with other dynamics analyses, such as HDX-MS.[196] 3DVA can also be used to identify different conformational states within a data set via classification and clustering of the particles and was

https://doi.org/10.1021/acs.chemrev.1c00837
Chem. Rev. 2022, 122, 13989−14017

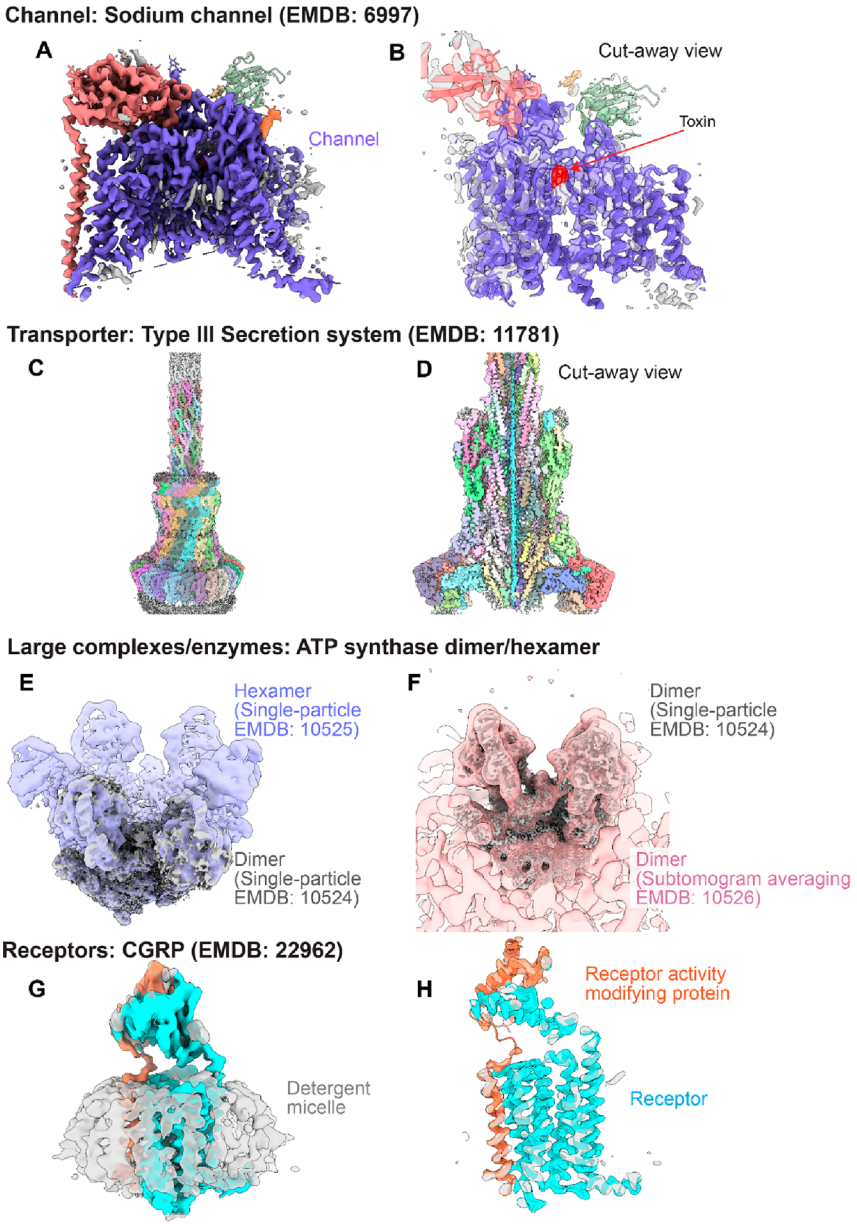

Figure 8. Examples of membrane proteins of differing size and complexity solved by single-particle cryo-EM or cryo-ET. The examples shown include a sodium channel (A, B), secretion system (C, D), ATP synthase (E, F), as well as a G protein-coupled receptor (G, H). The illustrated examples display the respective cryo-EM maps and are colored according to the molecule chains. Maps and models were visualized using ChimeraX.

used for AdeB, where six classes were identified that had open or closed periplasmic clefts.[197] Moreover, a new feature that will soon be implemented in the cryoSPARC package is 3DFlex, which is reported to improve the map quality and resolution of flexible proteins and has been applied the TRPV1 ion channel, suggesting that it may provide useful insights for membrane proteins.[198]

It is now becoming common for researchers to process the data using multiple software packages, utilizing the best algorithms implemented within each package, to obtain the best quality map. For instance, RELION was used to process the mitochondrial ATP synthase data set, which identified that the protein existed in 13 different conformations.[199] The particles from the different states were then imported into cryoSPARC, and nonuniform refinement was used to produce the final maps. Moreover, the Hedgehog receptor, Patched1, was predominantly processed in cryoSPARC, but the final particle stack was imported into cisTEM, where it underwent a local refinement using a mask that excluded the detergent micelle, to improve the final map,[200] and for the Type 1 IP_3R channel data processing with cryoSPARC, RELION, and EMAN were all used.[201] This shows that the different algorithms and features that the software packages offer are complementary to one another and a combination of programs should be considered for the data processing pipeline.

4. NOTABLE EXAMPLES IN MEMBRANE PROTEIN CRYO-EM: LEARNING FROM HISTORICAL SUCCESS AND THE LATEST MILESTONES

One cannot write a review about membrane protein cryo-EM without including the ground-breaking work from Richard Henderson and Nigel Unwin in 1975, who solved one of the very first examples of a membrane protein structure. In this study, the

https://doi.org/10.1021/acs.chemrev.1c00837
Chem. Rev. 2022, 122, 13989−14017

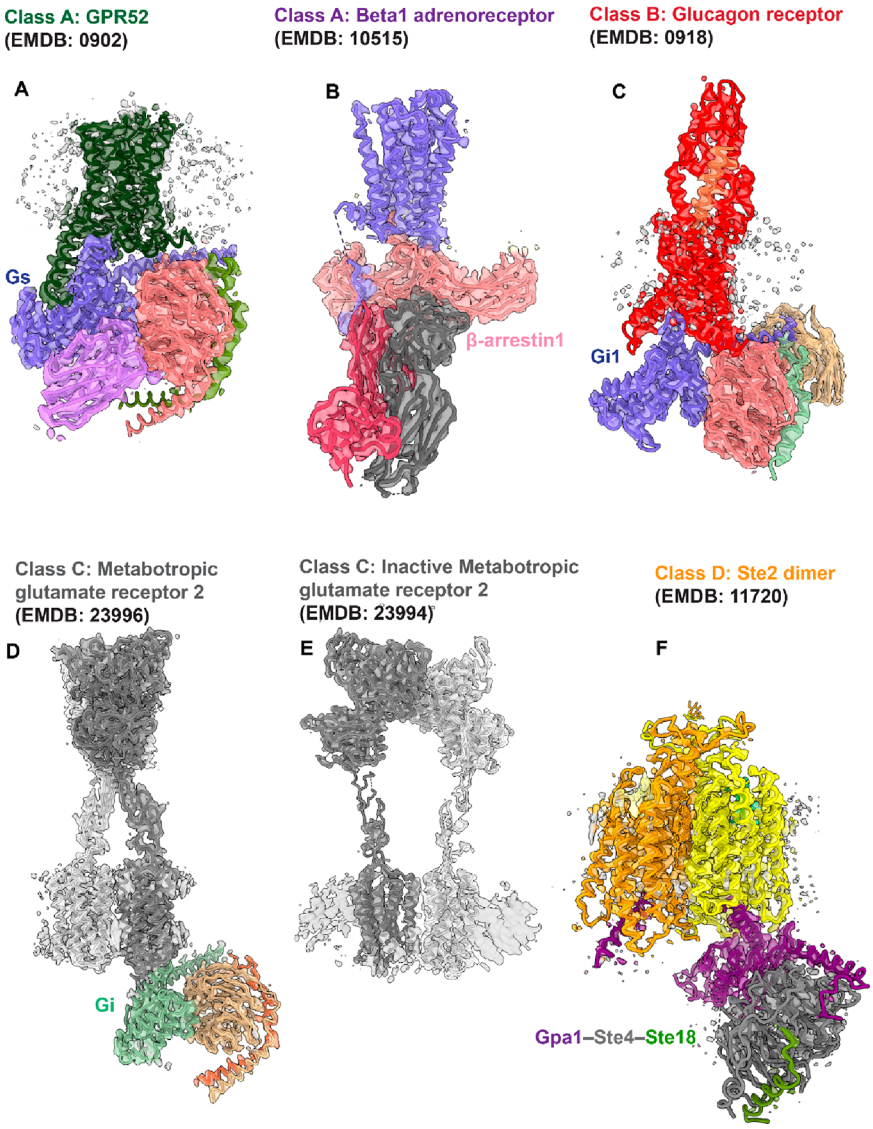

Figure 9. Cryo-EM structures of different G protein-coupled receptors, illustrating the structural diversity across representative examples of different major subclasses A, B, C, and D. The examples display the diversity of captured states; in complex with different G proteins, arrestins, or in the absence of transducer proteins. The class A subfamily is represented with the orphan receptor, GPR52, coupled to Gs (A) and the Beta1 adrenoreceptor with *β*-arrestin1 bound (B). The architecture of class B GPCRs is shown by the glucagon receptor coupled to Gi1 (C). The conformational change which occurs upon activation for the class C metabotropic glutamate receptor 2 is shown in parts D and E. Part F illustrates the dimeric nature of the class D Ste2 GPCR. The illustrated examples display respective cryo-EM maps (transparent surface) and modeled proteins (ribbon format), colored by molecule chains. Maps and models were visualized using ChimeraX.

structure of bacterial purple membrane protein was determined at 7 Å resolution using electron microscopy,[202] work that, in part, was the reason for the 2017 Nobel Prize in Chemistry awarded to Henderson, Frank, and Dubochet. Their sample, bacteriorhodopsin, is a predominant protein of purple membrane, with seven transmembrane helices, an ideal sample for 2D electron diffraction. Electron diffraction had a revival in the 2010s with the development of microED (micro-electron diffraction), which uses microscopic 3D crystals of proteins or chemical compounds, classically smaller than the crystals used for X-ray crystallography. Tamir Gonen's lab has been on the forefront to establish protocols to use these microcrystals on TEM grids and solve these using electron diffraction. While most novel structures solved by this method are soluble proteins or chemical compounds, researchers have also been successful in resolving membrane proteins such as a NaK ion channel solubilized in detergent,[203] as well as a voltage-dependent ion channel in lipid bicelles[204] and the adenosine A_{2A} GPCR in lipidic cubic phase,[205] with the latter two examples using FIB-milling to obtain suitable crystal sizes small enough for ED.

For many years, membrane protein structural biology was dominated by techniques other than cryo-EM, in particular X-ray crystallography following the advent of lipid cubic phase (LCP) methods.[206,207] The developments in cryo-EM, and also in membrane protein purification and solubilization strategies, led to the first cryo-TEM membrane protein structure being solved in 2013. This pioneering work, led by Yifan Cheng, resulted in determination of the 3.4 Å structure of TRPV1 in amphipol A8-35.[145] This marked the beginning of an incredible era for membrane protein structural biology. Quite remarkably, the developments mentioned above have now led to <2 Å structures being solved, with the 1.7 Å $GABA_A$ receptor the

https://doi.org/10.1021/acs.chemrev.1c00837
Chem. Rev. 2022, 122, 13989−14017

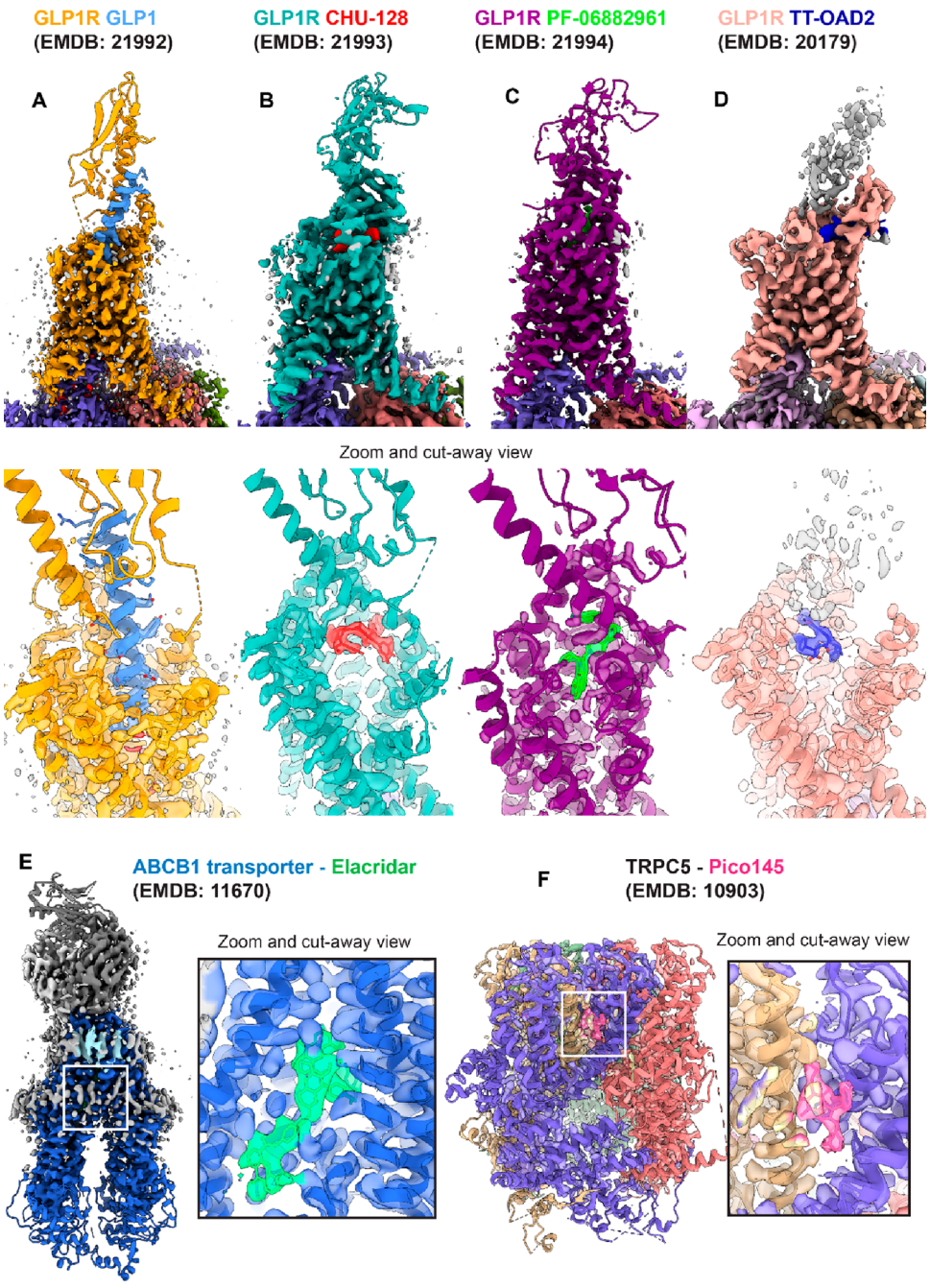

Figure 10. Cryo-EM structures of drug targets bound to different ligands. G protein-coupled receptors (GPCRs), ABC transporters, and TRP channels are important drug targets and are of high interest for structure-based drug development. (A–D) The glucagon-like peptide 1 receptor (GLP-1R) is shown here with the native peptide GLP-1, as well as with different small molecule agonist compounds; these examples highlight the different modes of drug binding and distinct receptor conformations when bound to different ligands. The ABCB1 transporter is shown bound to the small molecule elacridar (E), and the TRP channel, TRPC5, is shown with the small molecule, pico145 (F). The cryo-EM maps (surface representation) and protein models (ribbon format) are shown, together with enlargement of the drug binding site (transparent surface representation with compounds displayed in stick representation) colored by molecule chains. Maps and models were visualized using ChimeraX.

highest resolution membrane protein solved to date.[27] Figure 7 illustrates these famous historical structures.

Cryo-EM has now been used worldwide to determine a huge variety of membrane protein structures from many different protein classes; from large megadalton supercomplexes to small transporters with molecular weights lower than 100 kDa, cryo-EM can be used to provide fascinating insights into the function of these crucial proteins. This section will take a look at a few key examples from the following areas: large complexes and enzymes, ion channels, receptors, pore-forming proteins, and transporters, before moving on to give examples of how cryo-EM can benefit structure-based drug design programs. Example highlights are illustrated in Figures 8, 9, and 10.

4.1. Large Complexes and Enzymes

Cryo-EM has become an ideal technique to determine the structures of large and complex membrane protein assemblies in different states and, in particular, to understand their dynamics (further discussed in section 3.3.3). There are many examples of

https://doi.org/10.1021/acs.chemrev.1c00837
Chem. Rev. 2022, 122, 13989–14017

structures of individual components of the mitochondrial electron transport chain (ETC) being solved, including Complex I[208,209] and Complex III.[4,210] The structural insights gained have been immensely important in driving knowledge of fundamental biological processes. High resolution structures have also revealed that the components of the ETC can interact to form supercomplexes that contain different architectures and component stoichiometries in a variety of different species.[211,212]

For the larger systems, cryo-ET can also provide novel structural insights and can be used as a complementary technique to the high resolution structures solved by single-particle cryo-EM. For instance, cryo-ET first revealed that ATP synthases exist in a dimeric form, showing that these form rows and have the ability to bend the membrane within mitochondrial cristae.[213] The ATP synthase dimer was then subsequently solved to high resolution, which allowed for atomic level details to be gleaned and for three different catalytic rotational states to be observed.[214] The mode of action of this rotary enzyme was later enhanced by the identification of 13 different catalytic conformations.[199]

As cryo-EM uses less protein than traditional X-ray crystallography approaches, it can be used to provide unique structural insights for different organisms where limited sample is available. This is exemplified by the study of the *Toxoplasma gondii* ATP synthase that once again combined insights from both cryo-EM and cryo-ET.[215] First, high resolution structures of the dimeric ATP synthase were solved, which revealed that the parasitic enzyme had a novel overall architecture, containing 17 apicomplexan specific subunits. Tomography further showed that the dimers form a hexameric circular arrangement, consisting of a trimer of dimers, which contributes to the unique shape of parasitic mitochondrial cristae.[215]

An advantage of using a cryo-EM approach for structural determination is that different conformational states of a protein can be identified, providing unique insights into how proteins carry out their functional cycle. One such example is by Kolbe et al., who determined five cryo-EM structures of cytochrome c oxidase in key intermediate states (E, R, P, F, and O states), and allowed the authors to propose a mechanism for how the enzyme reduces oxygen to water.[216] Additionally, Sobti et al. were able to determine six structures of the F1-ATPase, including an elusive "binding dwell" conformational state that allowed a full mechanism to be proposed for how the F1-ATPase hydrolyses ATP.[217]

Other large protein systems, >1 MDa in size, outside of the mitochondrial electron transport chain, have also been resolved. These include the light harvesting complexes and photosystems that have yielded fascinating insights into the process of photosynthesis.[218−220]

4.2. Ion Channels

This review would not be complete without mentioning how cryo-EM has revolutionized transient receptor potential (TRP) channel structural biology.[221] Since the first structure was released, an avalanche of cryo-EM TRP channel structures have been solved, including at least one example for each of the six family members. This includes TRPA1,[222] TRPV2,[223] TRPC5,[224] TRPM8,[225] TRPML3,[226] and TRPP.[227] Moreover, the structures have been determined using a wide variety of reconstitution systems, including detergents, amphipols, nanodiscs, and SMALPs, and they have provided fascinating insights into how these important ion channels carry out their function. For instance, one recent paper by Nadezhdin et al. determined the structures of TRPV3 in nanodiscs at different temperatures, which revealed how the channel alters conformation in response to temperature changes.[117]

Sodium and potassium channels have also benefited from the cryo-EM resolution revolution. One particular noteworthy example is the 3.8 Å structure of the human hERG channel.[228] This channel plays an important role as an unwanted target for cardiac toxicity in drug discovery biology. If drug molecules bind to the hERG channel, it can result in fatal toxicity. Understanding of the mechanism of compound inhibition for this channel was advanced with solution of the astemizole-bound cryo-EM structure; astemizole is a small molecule known to inhibit the channel.[229] Such structures could prove valuable to many structure-based drug discovery campaigns as an early virtual screening countertarget for compound interactions that could have toxic liabilities. Many interesting structures of other ion channels have now been solved in the presence of pore blockers and gating modifying protein from animal toxin sources, giving insights on how animal toxins act on membrane proteins at a molecular level.[230,231]

4.3. G Protein-Coupled Receptors

Another major beneficiary of the cryo-EM revolution is the GPCR field. GPCRs are the most prevalent cell surface receptor proteins, and they are crucial drug targets that account for over a third of Food and Drug Administration (FDA) approved drugs. GPCRs contain seven transmembrane helices and are divided into six main classes based upon their structure and function (classes A−F). They are low abundance, intrinsically dynamic, allosteric, membrane proteins that convey extracellular signals to changes in intracellular function. These properties have made them extremely challenging to work with in their native states, while the transient nature of transducer engagement has required the development of methods for the stabilization of complexes with activated GPCRs. A major milestone in cryo-EM membrane protein structural biology was the publication of the first full-length activated class B1 GPCR-G protein complex structures. The first two GPCR structures solved by cryo-EM in 2017 were the active, Gs protein bound, calcitonin and GLP-1 receptors that are targets for the treatment of bone and metabolic diseases, respectively.[178,232] These structures started a revolution in GPCR structural biology, providing a template for structure determination of active, transducer-coupled structures by cryo-EM. Indeed, cryo-EM has become the most common approach to active state GPCR structure determination, with over 200 GPCR transducer complexes determined by cryo-EM deposited into the PDB to date.[180] There are now examples of high resolution structures from many of the different major classes of GPCRs in complex with different classes of transducers, including different G protein subtypes (Gs, Gq/11, and Gi/o) that promote distinct cascades of cellular signaling. Example structures from classes A−D are highlighted in Figure 9 that illustrate the varying structural features between the classes.

Class A is the most populous class of receptors and has yielded numerous examples of high resolution GPCR structures, with 92 entries into the PDB.[180] The structures solved are varied, including structures of receptors bound by (i) nonpeptide orthosteric agonists, such as for the adenosine A_{2A} receptor,[179] rhodopsin,[233] and the muscarinic acetylcholine receptor,[234] (ii) peptide agonists, such as CCK,[148] and (iii) receptors cobound with orthosteric and allosteric ligands, such as the adenosine A_1

https://doi.org/10.1021/acs.chemrev.1c00837
Chem. Rev. 2022, 122, 13989−14017

receptor,[235] providing insights into binding and modulation of receptors by different types of ligands. These structures also include receptors bound to three of the major classes of G proteins, ~30 structures with G_s, ~35 with $G_{i/o}$, and 4 bound to $G_{q/11}$; albeit, there is only one example of a class A GPCR where there are structures complexed with two different G proteins, that of the CCK1R coupled with Gq and Gs. In addition to G protein bound complexes, for four GPCRs, there are also structures of receptors coupled to β arrestins, which regulate G protein signaling and induce G protein independent signaling cascades.[236,237] One such example is a 3.3 Å structure of the β1-adrenoeptor in lipid nanodiscs.[238] The structural information gained from GPCR structures bound to different transducers could lead to the design of novel agonists that act as biased signaling modulators, which can be beneficial in the development of more desirable therapeutic agents through targeting signaling states that are therapeutically beneficial, while avoiding those that lead to on-target side effects.[239,240] Within the class A GPCR subfamily there are also structures of orphan receptors, such as GPR52, which was determined in the absence of a bound ligand but coupled to heterotrimeric Gs protein, providing insights into constitutive G protein coupling and also providing templates for future structure-based drug discovery efforts to target orphan receptors.[241]

Structures for the majority of class B1 GPCRs have now been determined, in complex with peptide hormones and primary G protein transducer Gs. In addition, there are also structures emerging of these receptors coupled to clinically used peptide agonists, nonpeptide agonists, and allosteric modulators, providing unprecedented structural insights into drug action. While the class B1 GPCRs predominantly couple to Gs, they promiscuously couple to different transducers, although, to date, only one structure of this subfamily has been determined coupled to a non-Gs transducer; the human glucagon receptor bound to G_i,[242] which provided novel insights into promiscuous G protein coupling to this receptor subfamily. Receptor function can also be modified by association of receptor-activity modifying proteins (RAMPs),[243] and cryo-EM structures of GPCRs together with RAMPs have been solved both in complex with and in the absence of G proteins, to understand the activity of important receptor families such as the calcitonin or calcitonin-like family of class B1 GPCRs. A recent example by Cao et al. determined 10 cryo-EM structures of calcitonin-like and amylin-like peptides bound to the calcitonin receptor with and without RAMPs showing different peptide conformations and receptor/RAMP dynamics that can explain downstream processes.[244]

Another key breakthrough achieved for this target class was the application of cryo-EM to determine key intermediate states in the activation process of this receptor subfamily, using minimally modified receptor constructs. The exemplar receptor for this work was the calcitonin gene-related peptide (CGRP) receptor, a class B1 GPCR involved in control of vascular tone and a contributor to the pathology of migraines.[196] For the first time, cryo-EM was used to solve the structures of a CGRP receptor in the apo state, as well as the peptide-bound state without G proteins or any other additional stabilizing "superbodies" or mutations.[196] The study further emphasized the importance of understanding the conformational dynamics of membrane proteins for interpretation of function. Similarly, for some GPCR examples, it is only through study of conformational variance through 3DVA that insight into the distinct pharmacology of individual peptide ligands has been revealed, differences that were not apparent from the static consensus structures.[245,194,195] Collectively, these examples also highlight how the ongoing evolution of cryo-EM is starting to facilitate pivotal structural insights into small, conformationally dynamic, <100 kDa membrane protein systems.

There are also examples from class C (CaSR),[246] class D (Ste2),[247] and class F (frizzled),[160] which act as obligate dimers and highlight the unique structural architectures of the receptors from different GPCR classes. Unlike the other GPCR classes, the majority of the cryo-EM structures of class C GPCRs are not bound by transducers; albeit, recent work has also resolved G protein bound structures of members of this subfamily.[248,249] Class C GPCRs form homo- or heterodimers and also have large extracellular domains that facilitate particle alignments in the determination of high resolution structures. Multiple class C receptors have been studied using cryo-EM; γ-aminobutyric acid receptors ($GABA_B$),[250−252] multiple metabotropic glutamate receptors (mGlu),[253−256] and the calcium sensing receptor (CaS).[246] The structures of these receptors were solved in the presence of a variety of ligands, including agonists, inverse agonists, and antagonists, facilitating the understanding of the structural changes that occur upon ligand binding and G protein binding, and for understanding how to target these receptors by different ligand classes.

For the class D GPCR Ste2, there are five structures determined of the receptor in different conformational states: ligand-free inactive, antagonist-bound inactive, agonist-bound inactive-like, agonist-bound active-like, and agonist-bound G protein-coupled active.[257] These structures show how the transmembrane helices in the receptor rearrange upon activation to facilitate G protein binding, highlighting again how immensely powerful cryo-EM is at resolving the different functional states of a protein.

These examples highlight the diversity of the GPCR superfamily and how the advances in cryo-EM have yielded particular benefit to the understanding of these membrane proteins.

4.4. Transporters

Transporters are another highly important, and diverse, class of membrane proteins that facilitate the selective transport of a variety of substrates such as ions, nutrients, or drugs across biological membranes. Once again, cryo-EM has provided exciting insights for this class of proteins. One system studied is the Type III bacterial secretion system that transports its substrates across the bacterial membrane using an injection mechanism. Miletic et al. were able to solve cryo-EM structures in the apo and substrate-bound forms, which provided insight into the conformation changes involved in substrate transport and allowed for a mechanism of action for the translocation of substrates to be proposed.[258] Cryo-EM has also successfully been used to solve high resolution structures of the Type VII secretion system in *Mycobacterium tuberculosis*, which showed that the 2.32 MDa complex existed in a hexameric arrangement and provided a novel mechanism of protein transport.[259]

There are many other examples of smaller transporters being solved by cryo-EM, including LAT1, the large amino acid transporter that is an anticancer therapeutic target,[260] the ABC transporters that use ATP powered hydrolysis to drive substrate transport,[261−263] and the glutamine SLC1A5 transporters,[264] that provide novel insights into how glutamate can be transported across membranes. ABC transporters are a large superfamily of membrane proteins that are responsible for

https://doi.org/10.1021/acs.chemrev.1c00837
Chem. Rev. 2022, 122, 13989−14017

extruding a large variety of substances across cell membranes.[265] As such, they can be highly dynamic and can exist in different catalytic conformations. By using cryo-EM to determine eight structures of TmrAB in different catalytic conformations, Hofmann et al. were able to resolve key catalytic states of the ABC transporter, thus providing a mechanism for how this important class of enzymes carry out their function.[266]

4.5. Membrane-Associated Proteins and Pore-Forming Proteins

While not a focus of this review, a large class of proteins associated with membranes are the pore-forming proteins and toxins, which alter the membrane properties of target cells through punching holes into membranes and/or delivering toxins through these holes into target cells. Many of these proteins exist in conformations that range from soluble prepore states to membrane-spanning pore-forming states, and they can have a variety of functions in cells and organisms. These include, for example, membrane attack complex proteins such as MPEG1,[121] which plays a role in the human immune response; however, these proteins can also be harnessed as weapons of bacterial pathogens such as anthrax[267,268] and Tc toxins.[269−271]

4.6. Application of Cryo-EM to the Understanding of Drug Binding

Approximately 60% of all FDA approved drugs target membrane proteins; therefore, the gains in technology supporting cryo-EM structure determination that have been made over the past few years have also enabled cryo-EM to become a key tool in drug discovery programs. The high resolutions attained have led to determination of the cryo-EM structures of membrane proteins with well resolved density for small molecule ligands, including, in some cases, interactions mediated via stable water molecules. These drug−target complexes provide invaluable structural information that can be utilized in structure-based drug design and development programs. Examples of ligand-bound cryo-EM structures are shown in Figure 10.

There are now cryo-EM structure examples of clinically relevant small molecule drugs bound to proteins for each of the four major classes of membrane proteins discussed above. For instance, structures of the bedaquiline-bound mycobacterial ATP synthase[272] and bafilomycin-bound vacuolar-ATPase[273] were resolved to 3.7 and 3.6 Å, respectively. Moreover, there are examples of small molecule ligands present in multiple TRP channel structures, including TRPC5[274] and TRPA1,[190] and the ABC transporters. One example of the latter is the ABCB1 transporter, where the protein was reconstituted into nanodiscs and a stabilizing Fab was used to enable high resolution structural determination. In total, five structures were solved;[161] one in the apo state and four with different inhibitory small molecules bound. The cryo-EM structures revealed that the compounds bound in pairs, providing important insight into why the molecules could act as substrates at low concentrations but interfere with protein function at higher concentrations. This unique insight can now be used to develop more potent inhibitors for this important anticancer drug target.

For the GLP-1 receptor, there are published structures available with three different small molecule chemotypes that have each progressed into clinical trials: TT-OAD2,[275] OWL-833 (LY3502970),[276] and PF 06882961.[277] The cryo-EM structures revealed that these compounds bind in three distinct positions within the transmembrane core, providing insight into their differing pharmacology. In the higher resolution PF 06882961 bound structure (in addition to structures bound by structural analogues of OWL-833), water networks were also resolved in the binding pockets that were important both for ligand binding and in determining different signaling profiles, thus revealing different modes of GLP-1 receptor activation by small molecule ligands.[277] The GLP-1 receptor is a highly validated target for the treatment of metabolic diseases, including type 2 diabetes and obesity, with multiple clinically approved peptide agonists.[278,279] The wealth of new structural information on potential modes of small molecule activation of the GLP-1 receptor provides enormous opportunity for exploitation for the next generation of orally active therapeutics.

In this section, we have provided a small selection of recent highlights arising from cryo-EM structure determination and the potential application to drug discovery and development. In reality, there are hundreds of membrane protein cryo-EM structures that have now been deposited into the EMDB, and although each of these is impressive in their own way, we could not, unfortunately, list them all.

5. FUTURE PROSPECTS

Our review provides an overview of the important steps involved in determining membrane protein structures using cryo-EM as well as highlighting historically important cryo-EM membrane protein structures. The most recent biochemical and technical advances in the field enable us to foresee the future prospects of the cryo-EM field in membrane protein structure determination.

Most certainly, we must mention the most recent public release of AlphaFold2, a large step toward *in silico* predictions of surprisingly accurate protein structures by artificial intelligence.[84,85] Membrane proteins that have been most difficult to determine experimentally can now benefit from AlphaFold2 prediction, to at least have a "picture" of their folded protein in mind that might be exploited in protein design for structure determination or to facilitate model building for new protein structures, in addition to the direct use of predicted structures for computationally assisted drug discovery. Nonetheless, the accuracy of structure predictions is debatable, as is whether AlphaFold can be used for drug discovery, especially in regard to the prediction of ligand−protein interactions within binding sites.[280] While many structural biologists have openly discussed the broad agreement of AlphaFold2 predictions with their unpublished work, others have noted problems with membrane protein predictions of states that are overpopulated in the databases, such as active structures (particularly of class B1 GPCRs) in comparison to inactive or apo GPCR structures (low population). AlphaFold2 is also not able to predict flexible regions of GPCRs, such as extracellular loops, which are important for ligand interactions, and does not account for the ligand-specific adaptations that are observed in drug−target complexes. Nevertheless, the enormous and continuously evolving AlphaFold2 structure prediction database provides an unprecedented tool for structural and computational biologists, by improving decision making in project design, e.g. on purification tags or homology models. While some commentators have heralded Alphafold2 as the beginning of the end for experimental structural biology, the majority of structural biologists are looking forward to working with AlphaFold2 predictions, as a welcome addition to the tools for interpretation of experimental data.

While cryo-EM was viewed as the "blob-ology" technique for decades, the current application of the technique to determination of high resolution structures has most definitely overwritten the term. Membrane proteins and drug discovery

https://doi.org/10.1021/acs.chemrev.1c00837
Chem. Rev. 2022, 122, 13989−14017

have already benefited tremendously from the advances in cryo-EM, allowing for the accurate visualization of small molecule ligand binding to their target proteins. This will become even more relevant with increasing numbers of higher resolution structures, with the possibility of regularly solving sub-2 Å structures of bound drugs and potential application of this knowledge to development of new medicines that evolve from understanding of their bonding/interaction environment with important drug targets (as illustrated in section 4 and Figure 10). High throughput screening methods such as fragment-based drug discovery (FBDD)[281] will increasingly benefit from both improved resolution and higher throughput cryo-EM pipelines, with the latter incorporating the latest technological developments, such as freezing of multiple samples on one grid (feasible using, for example, spray/write vitrification robots), collection of smaller data sets at faster rates due to advances in hardware and software correction methods, and rapid on-the-fly data processing.[282,283]

Optimizing expression, solubilization, and purification protocols, most certainly, will remain the slowest step and bottleneck in high throughput cryo-EM on membrane proteins. Therefore, scientists will increasingly look at the feasibility of solving structures from heterogeneous mixes of proteins in lysates. Cell lysates of *E. coli* have been used to establish new structure determination methods termed "Build and Retrieve"[284] that might overcome expression and solubilization limitations for some protein classes. For example, endogenous structures from heterogeneous, impure mixtures of bacterial membrane proteins have been determined to high resolution in a combination of enrichment of samples and "*in silico* purification" (through 2D and 3D classification steps) as well as mass spectrometry.[284] The feasibility of this technique for mammalian cells still needs to be established. Moreover, developments in cell-free expression systems have resulted in membrane proteins, such as GPCRs, being produced outside of the cell, and interested readers can follow up on recent developments in published reviews and papers.[285−287] Although this approach has not yet yielded high resolution cryo-EM structures, proteins produced in this way have the potential to impact the cryo-EM field in the future.

As mentioned above, membrane protein solubilization remains a tricky balancing act between efficiency, stability, and speed of protein purification. Scientists struggling with this crucial step can be referred to high throughput methods to optimize solubilization and stabilization conditions using a variety of detergents.[288] Moreover, the fast-paced improvements within the cryo-ET field will almost certainly lead to the technique becoming a key tool for elucidating structural insights into how membrane proteins behave within the cell, allowing for invaluable *in situ* insights to be made.

6. CONCLUSIONS

This review has provided an overview of the diverse world of membrane protein structure determination by cryo-EM, from protein biochemistry to vitrification, imaging, and data processing. While we could not cover all aspects of membrane protein cryo-EM structures, we hope that we have provided the reader insight into some of the recent technical and biological highlights that have arisen, as well as the intriguing potential that will come with future innovations. We anticipate that the spectrum of membrane protein structures will continue to grow rapidly, with an exponential growth of novel proteins, protein complexes, and drug targeted structures that is enabled by the ever-advancing cryo-EM field.

AUTHOR INFORMATION

Corresponding Authors

Sarah J. Piper − *Drug Discovery Biology theme, Monash Institute of Pharmaceutical Sciences, Monash University, Parkville 3052 Victoria, Australia; ARC Centre for Cryo-electron Microscopy of Membrane Proteins, Monash Institute of Pharmaceutical Sciences, Monash University, Parkville 3052 Victoria, Australia;* orcid.org/0000-0001-5337-5197; Email: sarah.piper@monash.edu

Rachel M. Johnson − *Drug Discovery Biology theme, Monash Institute of Pharmaceutical Sciences, Monash University, Parkville 3052 Victoria, Australia; ARC Centre for Cryo-electron Microscopy of Membrane Proteins, Monash Institute of Pharmaceutical Sciences, Monash University, Parkville 3052 Victoria, Australia*; Email: rachel.johnson@monash.edu

Denise Wootten − *Drug Discovery Biology theme, Monash Institute of Pharmaceutical Sciences, Monash University, Parkville 3052 Victoria, Australia; ARC Centre for Cryo-electron Microscopy of Membrane Proteins, Monash Institute of Pharmaceutical Sciences, Monash University, Parkville 3052 Victoria, Australia;* orcid.org/0000-0003-4563-1642; Email: denise.wootten@monash.edu

Patrick M. Sexton − *Drug Discovery Biology theme, Monash Institute of Pharmaceutical Sciences, Monash University, Parkville 3052 Victoria, Australia; ARC Centre for Cryo-electron Microscopy of Membrane Proteins, Monash Institute of Pharmaceutical Sciences, Monash University, Parkville 3052 Victoria, Australia;* orcid.org/0000-0001-8902-2473; Email: patrick.sexton@monash.edu

Complete contact information is available at: https://pubs.acs.org/10.1021/acs.chemrev.1c00837

Author Contributions

S.J.P. and R.M.J. contributed equally to this paper. R.M.J. and S.J.P. drafted the manuscript and prepared the figures. All authors contributed to the writing and editing of the final manuscript and figures.

Funding

D.W. is a Senior Research Fellow (grant no: 1155302) and P.M.S. a Senior Principal Research Fellow (grant no: 1154434) of the National Health and Medical Research Council of Australia. P.M.S. is Director of the Australian Research Council Industrial Transformation Training Centre for Cryo-EM of Membrane Proteins (grant no: IC200100052).

Notes

The authors declare the following competing financial interest(s): P.M.S. is a Founder and shareholder in Septerna Inc. D.W. is a shareholder in Septerna Inc. P.M.S. and D.W. receive in-kind support from Thermo Fisher Scientific.

Biographies

Sarah J. Piper was awarded a B.Sc. degree in Biology and a M.Sc. degree in Systems Biology from the University of Bielefeld, Germany. In 2015, she was awarded a UQ International Scholarship to pursue her Ph.D. research at The University of Queensland, Australia, in the groups of Prof. Glenn King and Assoc. Prof. Michael Landsberg. During her Ph.D. studies she focused on determining the structures of pore-forming bacterial toxin complexes using cryo-electron microscopy. She was

https://doi.org/10.1021/acs.chemrev.1c00837
Chem. Rev. 2022, 122, 13989−14017

recruited to the Monash Institute of Pharmaceutical Sciences (MIPS) in Melbourne, Australia, in 2019 as a Postdoctoral Research Fellow to specialize in biochemistry and cryo-electron microscopy of G protein-coupled receptors (GPCRs) in the laboratories of Patrick Sexton and Denise Wootten. Sarah has particular interests in protein biochemistry, cryo-EM, and data processing as well as science visualization and communication.

Rachel M. Johnson completed her B.Sc., MChem, and Ph.D. degrees at the University of Leeds within the Astbury Biostructure Laboratory. Her Ph.D. project focused on determining whether cryo-EM could be used as a tool in structure-based drug design programs. In November 2019, she moved to the Monash Institute of Pharmaceutical Sciences to undertake a postdoctoral position in the laboratories of Christopher Langmead, Patrick Sexton, and Denise Wootten, where she continues to use cryo-EM to aid GPCR drug discovery.

Denise Wootten is an NHMRC Senior Research Fellow at the Monash Institute of Pharmaceutical Sciences and Monash University Node Leader of the ARC Centre for Cryo-electron Microscopy of Membrane Proteins (www.ccemmp.org). Denise is an international leader in the study of the biochemistry, molecular pharmacology and structure of GPCRs. Her laboratory, co-led by Patrick Sexton, is at the forefront of the application of cryo-EM for the elucidation of the structure and dynamics of GPCRs.

Patrick M. Sexton is a NHMRC Senior Principal Research Fellow at the Monash Institute of Pharmaceutical Sciences and Director of the ARC Centre for Cryo-electron Microscopy of Membrane Proteins (www.ccemmp.org). Patrick is a leader in the study of GPCRs, biased agonism, and also allosteric interactions between GPCRs and other proteins and small molecule ligands. More recently, his laboratory, co-led by Denise Wootten, is at the forefront of the application of cryo-EM for the elucidation of the structure and dynamics of GPCRs.

ACKNOWLEDGMENTS

Figures were created with UCSF ChimeraX, developed by the Resource for Biocomputing, Visualization, and Informatics at the University of California, San Francisco, with support from National Institutes of Health R01-GM129325 and the Office of Cyber Infrastructure and Computational Biology, National Institute of Allergy and Infectious Diseases. Figures were also rendered using Blender 2.92. Blender is the free and open source 3D creation suite. https://www.blender.org/. A PDB file of LMNG (Figure 1) was created by Dr Brian Cary. Atomic coordinates and cryo-EM maps, as well as graphs and tables were obtained from public databases RSCB PDB https://www.rcsb.org/ and EMDB https://www.ebi.ac.uk/emdb/. GPCRdb (https://gpcrdb.org/) was used to analyse the number of GPCR structures that were determined using cryo-EM.

REFERENCES

(1) Lodish, H.; Baltimore, D.; Berk, A.; Zipursky, S.; Matsudaira, P.; Darnell, J. *Molecular Cell Biology*, 3rd ed.; Scientific American Books Inc.: New York and Oxford, 1995; pp 604−612.
(2) Luckey, M. Introduction to the Structural Biology of Membrane Proteins. In *Computational Biophysics of Membrane Protein*; Domene, C., Ed.; Royal Society of Chemistry: 2016, pp 1−18.
(3) Porta-Pardo, E.; Ruiz-Serra, V.; Valentini, S.; Valencia, A. The Structural Coverage of the Human Proteome before and after Alphafold. *PLoS Comp. Biol.* **2022**, *18*, No. e1009818.
(4) Amporndanai, K.; Johnson, R. M.; O'Neill, P. M.; Fishwick, C. W. G.; Jamson, A. H.; Rawson, S.; Muench, S. P.; Hasnain, S. S.; Antonyuk, S. V. X-Ray and Cryo-Em Structures of Inhibitor-Bound Cytochrome Bc(1) Complexes for Structure-Based Drug Discovery. *IUCrJ.* **2018**, *5*, 200−210.
(5) Krebs, A.; Edwards, P. C.; Villa, C.; Li, J.; Schertler, G. F. The Three-Dimensional Structure of Bovine Rhodopsin Determined by Electron Cryomicroscopy. *J. Biol. Chem.* **2003**, *278*, 50217−50225.
(6) Vasseur, L.; Cens, T.; Wagner, R.; Saint, N.; Kugler, V.; Chavanieu, A.; Ouvry, C.; Dupré, C.; Ferry, G.; Boutin, J. A. Importance of the Choice of a Recombinant System to Produce Large Amounts of Functional Membrane Protein Herg. *Int. J. Mol. Sci.* **2019**, *20*, 3181.
(7) Goth, C. K.; Petäjä-Repo, U. E.; Rosenkilde, M. M. G Protein-Coupled Receptors in the Sweet Spot: Glycosylation and Other Post-Translational Modifications. *ACS Pharmacol. Trans. Sci.* **2020**, *3*, 237−245.
(8) Magnani, F.; Serrano-Vega, M. J.; Shibata, Y.; Abdul-Hussein, S.; Lebon, G.; Miller-Gallacher, J.; Singhal, A.; Strege, A.; Thomas, J. A.; Tate, C. G. A Mutagenesis and Screening Strategy to Generate Optimally Thermostabilized Membrane Proteins for Structural Studies. *Nat. Protoc.* **2016**, *11*, 1554−1571.
(9) Desuzinges Mandon, E.; Agez, M.; Pellegrin, R.; Igonet, S.; Jawhari, A. Novel Systematic Detergent Screening Method for Membrane Proteins Solubilization. *Anal. Biochem.* **2017**, *517*, 40−49.
(10) Lee, S.; Mao, A.; Bhattacharya, S.; Robertson, N.; Grisshammer, R.; Tate, C. G.; Vaidehi, N. How Do Short Chain Nonionic Detergents Destabilize G-Protein-Coupled Receptors? *J. Am. Chem. Soc.* **2016**, *138*, 15425−15433.
(11) Gewering, T.; Januliene, D.; Ries, A. B.; Moeller, A. Know Your Detergents: A Case Study on Detergent Background in Negative Stain Electron Microscopy. *J. Struct. Biol.* **2018**, *203*, 242−246.
(12) Peisley, A.; Skiniotis, G. 2D Projection Analysis of GPCR Complexes by Negative Stain Electron Microscopy. In *G Protein-Coupled Receptors in Drug Discovery: Methods and Protocols*; Filizola, M., Ed.; Springer New York: New York, NY, 2015; pp 29−38.
(13) Raynal, B.; Lenormand, P.; Baron, B.; Hoos, S.; England, P. Quality Assessment and Optimization of Purified Protein Samples: Why and How? *Microb. Cell Fact.* **2014**, *13*, 180.
(14) Some, D.; Amartely, H.; Tsadok, A.; Lebendiker, M. Characterization of Proteins by Size-Exclusion Chromatography Coupled to Multi-Angle Light Scattering (SEC-MALS). *J. Visualized Exp.* **2019**, *148*, e59615 DOI: 10.3791/59615.
(15) Stetefeld, J.; McKenna, S. A.; Patel, T. R. Dynamic Light Scattering: A Practical Guide and Applications in Biomedical Sciences. *Biophys. Rev.* **2016**, *8*, 409−427.
(16) Greenfield, N. J. Using Circular Dichroism Spectra to Estimate Protein Secondary Structure. *Nat. Protoc.* **2006**, *1*, 2876−2890.
(17) Domon, B.; Aebersold, R. Mass Spectrometry and Protein Analysis. *Science* **2006**, *312*, 212−217.
(18) Kühlbrandt, W. The Resolution Revolution. *Science* **2014**, *343*, 1443.
(19) Sirohi, D.; Chen, Z.; Sun, L.; Klose, T.; Pierson, T. C.; Rossmann, M. G.; Kuhn, R. J. The 3.8 Å Resolution Cryo-Em Structure of Zika Virus. *Science* **2016**, *352*, 467.
(20) Conley, M. J.; McElwee, M.; Azmi, L.; Gabrielsen, M.; Byron, O.; Goodfellow, I. G.; Bhella, D. Calicivirus Vp2 Forms a Portal-Like Assembly Following Receptor Engagement. *Nature* **2019**, *565*, 377−381.
(21) Yuan, S.; Wang, J.; Zhu, D.; Wang, N.; Gao, Q.; Chen, W.; Tang, H.; Wang, J.; Zhang, X.; Liu, H.; et al. Cryo-EM Structure of a Herpesvirus Capsid at 3.1 Å. *Science* **2018**, *360*, No. eaao7283.
(22) Hashem, Y.; des Georges, A.; Fu, J.; Buss, S. N.; Jossinet, F.; Jobe, A.; Zhang, Q.; Liao, H. Y.; Grassucci, R. A.; Bajaj, C.; et al. High-Resolution Cryo-Electron Microscopy Structure of the Trypanosoma Brucei Ribosome. *Nature* **2013**, *494*, 385−389.
(23) Dong, Y.; Zhang, S.; Wu, Z.; Li, X.; Wang, W. L.; Zhu, Y.; Stoilova-McPhie, S.; Lu, Y.; Finley, D.; Mao, Y. Cryo-Em Structures and Dynamics of Substrate-Engaged Human 26s Proteasome. *Nature* **2019**, *565*, 49−55.
(24) Schweitzer, A.; Aufderheide, A.; Rudack, T.; Beck, F.; Pfeifer, G.; Plitzko, J. M.; Sakata, E.; Schulten, K.; Förster, F.; Baumeister, W.

https://doi.org/10.1021/acs.chemrev.1c00837
Chem. Rev. 2022, 122, 13989−14017

Structure of the Human 26s Proteasome at a Resolution of 3.9 Å. *Proc. Natl. Acad. Sci. U. S. A.* **2016**, *113*, 7816−7821.
(25) Fitzpatrick, A. W. P.; Falcon, B.; He, S.; Murzin, A. G.; Murshudov, G.; Garringer, H. J.; Crowther, R. A.; Ghetti, B.; Goedert, M.; Scheres, S. H. W. Cryo-Em Structures of Tau Filaments from Alzheimer's Disease. *Nature* **2017**, *547*, 185−190.
(26) Scheres, S. H. W.; Zhang, W.; Falcon, B.; Goedert, M. Cryo-Em Structures of Tau Filaments. *Curr. Opin. Struct. Biol.* **2020**, *64*, 17−25.
(27) Nakane, T.; Kotecha, A.; Sente, A.; McMullan, G.; Masiulis, S.; Brown, P. M. G. E.; Grigoras, I. T.; Malinauskaite, L.; Malinauskas, T.; Miehling, J.; et al. Single-Particle Cryo-EM at Atomic Resolution. *Nature* **2020**, *587*, 152−156.
(28) Yip, K. M.; Fischer, N.; Paknia, E.; Chari, A.; Stark, H. Atomic-Resolution Protein Structure Determination by Cryo-Em. *Nature* **2020**, *587*, 157−161.
(29) Choy, B. C.; Cater, R. J.; Mancia, F.; Pryor, E. E. A 10-Year Meta-Analysis of Membrane Protein Structural Biology: Detergents, Membrane Mimetics, and Structure Determination Techniques. *Biochim. Biophys. Acta* **2021**, *1863*, 183533.
(30) Cheng, Y.; Grigorieff, N.; Penczek, P. A.; Walz, T. A Primer to Single-Particle Cryo-Electron Microscopy. *Cell* **2015**, *161*, 438−449.
(31) Frank, J. Advances in the Field of Single-Particle Cryo-Electron Microscopy over the Last Decade. *Nat. Protoc.* **2017**, *12*, 209−212.
(32) Tan, Y. Z.; Carragher, B. Seeing Atoms: Single-Particle Cryo-Em Breaks the Atomic Barrier. *Mol. Cell* **2020**, *80*, 938−939.
(33) Turk, M.; Baumeister, W. The Promise and the Challenges of Cryo-Electron Tomography. *FEBS Lett.* **2020**, *594*, 3243−3261.
(34) Wan, W.; Briggs, J. A. G. Cryo-Electron Tomography and Subtomogram Averaging. In *Methods in Enzymology*; Crowther, R. A., Ed.; Academic Press, 2016; Vol. *579*, Chapter 13, pp 329−367.
(35) Wagner, F. R.; Watanabe, R.; Schampers, R.; Singh, D.; Persoon, H.; Schaffer, M.; Fruhstorfer, P.; Plitzko, J.; Villa, E. Preparing Samples from Whole Cells Using Focused-Ion-Beam Milling for Cryo-Electron Tomography. *Nat. Protoc.* **2020**, *15*, 2041−2070.
(36) Schaffer, M.; Pfeffer, S.; Mahamid, J.; Kleindiek, S.; Laugks, T.; Albert, S.; Engel, B. D.; Rummel, A.; Smith, A. J.; Baumeister, W.; et al. A Cryo-Fib Lift-out Technique Enables Molecular-Resolution Cryo-Et within Native Caenorhabditis Elegans Tissue. *Nat. Methods* **2019**, *16*, 757−762.
(37) Tuijtel, M. W.; Koster, A. J.; Jakobs, S.; Faas, F. G. A.; Sharp, T. H. Correlative Cryo Super-Resolution Light and Electron Microscopy on Mammalian Cells Using Fluorescent Proteins. *Sci. Rep.* **2019**, *9*, 1369.
(38) Schur, F. K. M.; Obr, M.; Hagen, W. J. H.; Wan, W.; Jakobi, A. J.; Kirkpatrick, J. M.; Sachse, C.; Kräusslich, H.-G.; Briggs, J. A. G. An Atomic Model of Hiv-1 Capsid-Sp1 Reveals Structures Regulating Assembly and Maturation. *Science* **2016**, *353*, 506−508.
(39) Tegunov, D.; Xue, L.; Dienemann, C.; Cramer, P.; Mahamid, J. Multi-Particle Cryo-Em Refinement with M Visualizes Ribosome-Antibiotic Complex at 3.5 Å in Cells. *Nat. Methods* **2021**, *18*, 186−193.
(40) Passmore, L. A.; Russo, C. J. Specimen Preparation for High-Resolution Cryo-EM. In *Methods in Enzymology*; Crowther, R. A., Ed.; Academic Press, 2016; Chapter 3, Vol. *579*, pp 51−86.
(41) Thompson, R. F.; Walker, M.; Siebert, C. A.; Muench, S. P.; Ranson, N. A. An Introduction to Sample Preparation and Imaging by Cryo-Electron Microscopy for Structural Biology. *Methods* **2016**, *100*, 3−15.
(42) Drulyte, I.; Johnson, R. M.; Hesketh, E. L.; Hurdiss, D. L.; Scarff, C. A.; Porav, S. A.; Ranson, N. A.; Muench, S. P.; Thompson, R. F. Approaches to Altering Particle Distributions in Cryo-Electron Microscopy Sample Preparation. *Acta Crystallogr. Sect. D. Biol. Crystallogr.* **2018**, *74*, 560−571.
(43) Kampjut, D.; Steiner, J.; Sazanov, L. A. Cryo-Em Grid Optimization for Membrane Proteins. *iScience* **2021**, *24*, 102139.
(44) Noble, A. J.; Dandey, V. P.; Wei, H.; Brasch, J.; Chase, J.; Acharya, P.; Tan, Y. Z.; Zhang, Z.; Kim, L. Y.; Scapin, G.; et al. Routine Single Particle Cryoem Sample and Grid Characterization by Tomography. *eLife* **2018**, *7*, No. e34257.
(45) Adrian, M.; Dubochet, J.; Lepault, J.; McDowall, A. W. Cryo-Electron Microscopy of Viruses. *Nature* **1984**, *308*, 32−36.
(46) Cressey, D.; Callaway, E. Cryo-Electron Microscopy Wins Chemistry Nobel. *Nature* **2017**, *550*, 167−167.
(47) Glaeser, R. M.; Han, B.-G. Opinion: Hazards Faced by Macromolecules When Confined to Thin Aqueous Films. *Biophysics Reports* **2017**, *3*, 1−7.
(48) Jain, T.; Sheehan, P.; Crum, J.; Carragher, B.; Potter, C. S. Spotiton: A Prototype for an Integrated Inkjet Dispense and Vitrification System for Cryo-Tem. *J. Struct. Biol.* **2012**, *179*, 68−75.
(49) Dandey, V. P.; Wei, H.; Zhang, Z.; Tan, Y. Z.; Acharya, P.; Eng, E. T.; Rice, W. J.; Kahn, P. A.; Potter, C. S.; Carragher, B. Spotiton: New Features and Applications. *J. Struct. Biol.* **2018**, *202*, 161−169.
(50) Ravelli, R. B. G.; Nijpels, F. J. T.; Henderikx, R. J. M.; Weissenberger, G.; Thewessem, S.; Gijsbers, A.; Beulen, B. W. A. M. M.; López-Iglesias, C.; Peters, P. J. Cryo-EM Structures from Sub-nl Volumes Using Pin-Printing and Jet Vitrification. *Nat. Commun.* **2020**, *11*, 2563.
(51) Arnold, S. A.; Albiez, S.; Bieri, A.; Syntychaki, A.; Adaixo, R.; McLeod, R. A.; Goldie, K. N.; Stahlberg, H.; Braun, T. Blotting-Free and Lossless Cryo-Electron Microscopy Grid Preparation from Nanoliter-Sized Protein Samples and Single-Cell Extracts. *J. Struct. Biol.* **2017**, *197*, 220−226.
(52) Wei, H.; Dandey, V. P.; Zhang, Z.; Raczkowski, A.; Rice, W. J.; Carragher, B.; Potter, C. S. Optimizing "Self-Wicking" Nanowire Grids. *J. Struct. Biol.* **2018**, *202*, 170−174.
(53) Schmidli, C.; Albiez, S.; Rima, L.; Righetto, R.; Mohammed, I.; Oliva, P.; Kovacik, L.; Stahlberg, H.; Braun, T. Microfluidic Protein Isolation and Sample Preparation for High-Resolution Cryo-Em. *Proc. Natl. Acad. Sci. U. S. A.* **2019**, *116*, 15007.
(54) Kontziampasis, D.; Klebl, D. P.; Iadanza, M. G.; Scarff, C. A.; Kopf, F.; Sobott, F.; Monteiro, D. C. F.; Trebbin, M.; Muench, S. P.; White, H. D. A Cryo-Em Grid Preparation Device for Time-Resolved Structural Studies. *IUCrJ.* **2019**, *6*, 1024−1031.
(55) Klebl, D. P.; Gravett, M. S. C.; Kontziampasis, D.; Wright, D. J.; Bon, R. S.; Monteiro, D. C. F.; Trebbin, M.; Sobott, F.; White, H. D.; Darrow, M. C.; et al. Need for Speed: Examining Protein Behavior During Cryoem Grid Preparation at Different Timescales. *Structure* **2020**, *28*, 1238−1248.e4.
(56) Rubinstein, J. L.; Guo, H.; Ripstein, Z. A.; Haydaroglu, A.; Au, A.; Yip, C. M.; Di Trani, J. M.; Benlekbir, S.; Kwok, T. Shake-It-Off: A Simple Ultrasonic Cryo-Em Specimen-Preparation Device. *Acta Crystallogr. D Struct Biol.* **2019**, *75*, 1063−1070.
(57) Bammes, B. E.; Rochat, R. H.; Jakana, J.; Chen, D.-H.; Chiu, W. Direct Electron Detection Yields Cryo-Em Reconstructions at Resolutions Beyond 3/4 Nyquist Frequency. *J. Struct. Biol.* **2012**, *177*, 589−601.
(58) McMullan, G.; Faruqi, A. R.; Henderson, R. Direct Electron Detectors. In *Methods in Enzymology*; Crowther, R. A., Ed.; Academic Press, 2016; Vol. *579*, Chapter 1, pp 1−17.
(59) Li, X.; Mooney, P.; Zheng, S.; Booth, C. R.; Braunfeld, M. B.; Gubbens, S.; Agard, D. A.; Cheng, Y. Electron Counting and Beam-Induced Motion Correction Enable near-Atomic-Resolution Single-Particle Cryo-Em. *Nat. Methods* **2013**, *10*, 584−590.
(60) Zheng, S. Q.; Palovcak, E.; Armache, J.-P.; Verba, K. A.; Cheng, Y.; Agard, D. A. Motioncor2: Anisotropic Correction of Beam-Induced Motion for Improved Cryo-Electron Microscopy. *Nat. Methods* **2017**, *14*, 331−332.
(61) Baker, L. A.; Rubinstein, J. L. Radiation Damage in Electron Cryomicroscopy. *Methods Enzymol.* **2010**, *481*, 371−388.
(62) Glaeser, R. M.; Taylor, K. A. Radiation Damage Relative to Transmission Electron Microscopy of Biological Specimens at Low Temperature: A Review. *J. Microsc* **1978**, *112*, 127−138.
(63) Guo, H.; Franken, E.; Deng, Y.; Benlekbir, S.; Lezcano, G. S.; Janssen, B.; Yu, L.; Ripstein, Z. A.; Tan, Y. Z.; Rubinstein, J. L. Electron-Event Representation Data Enable Efficient Cryoem File Storage with Full Preservation of Spatial and Temporal Resolution. *IUCrJ.* **2020**, *7*, 860−869.

https://doi.org/10.1021/acs.chemrev.1c00837
Chem. Rev. 2022, 122, 13989−14017

(64) Schröder, R. R. Zero-Loss Energy-Filtered Imaging of Frozen-Hydrated Proteins: Model Calculations and Implications for Future Developments. *J. Microsc* **1992**, *166*, 389−400.
(65) Langmore, J. P.; Smith, M. F. Quantitative Energy-Filtered Electron Microscopy of Biological Molecules in Ice. *Ultramicroscopy* **1992**, *46*, 349−373.
(66) Danev, R.; Baumeister, W. Cryo-EM Single Particle Analysis with the Volta Phase Plate. *eLife* **2016**, *5*, No. e13046.
(67) Danev, R.; Buijsse, B.; Khoshouei, M.; Plitzko, J. M.; Baumeister, W. Volta Potential Phase Plate for in-Focus Phase Contrast Transmission Electron Microscopy. *Proc. Natl. Acad. Sci. U. S. A.* **2014**, *111*, 15635−15640.
(68) Schwartz, O.; Axelrod, J. J.; Campbell, S. L.; Turnbaugh, C.; Glaeser, R. M.; Müller, H. Laser Phase Plate for Transmission Electron Microscopy. *Nat. Methods* **2019**, *16*, 1016−1020.
(69) Nogales, E.; Scheres, S. H. W. Cryo-EM: A Unique Tool for the Visualization of Macromolecular Complexity. *Mol. Cell* **2015**, *58*, 677−689.
(70) Zivanov, J.; Nakane, T.; Scheres, S. H. W. A Bayesian Approach to Beam-Induced Motion Correction in Cryo-Em Single-Particle Analysis. *IUCrJ.* **2019**, *6*, 5−17.
(71) von Loeffelholz, O.; Natchiar, S. K.; Djabeur, N.; Myasnikov, A. G.; Kratzat, H.; Ménétret, J.-F.; Hazemann, I.; Klaholz, B. P. Focused Classification and Refinement in High-Resolution Cryo-Em Structural Analysis of Ribosome Complexes. *Curr. Opin. Struct. Biol.* **2017**, *46*, 140−148.
(72) Zivanov, J.; Nakane, T.; Forsberg, B. O.; Kimanius, D.; Hagen, W. J. H.; Lindahl, E.; Scheres, S. H. W. New Tools for Automated High-Resolution Cryo-EM Structure Determination in RELION-3. *eLife* **2018**, *7*, No. e42166.
(73) Fernández, J. J.; Luque, D.; Castón, J. R.; Carrascosa, J. L. Sharpening High Resolution Information in Single Particle Electron Cryomicroscopy. *J. Struct. Biol.* **2008**, *164*, 170−175.
(74) Henderson, R.; McMullan, G. Problems in Obtaining Perfect Images by Single-Particle Electron Cryomicroscopy of Biological Structures in Amorphous Ice. *Microscopy* **2013**, *62*, 43−50.
(75) Sigworth, F. J. Principles of Cryo-Em Single-Particle Image Processing. *Microscopy* **2016**, *65*, 57−67.
(76) Orlova, E. V.; Saibil, H. R. Structural Analysis of Macromolecular Assemblies by Electron Microscopy. *Chem. Rev.* **2011**, *111*, 7710−7748.
(77) Scheres, S. H. W. Relion: Implementation of a Bayesian Approach to Cryo-Em Structure Determination. *J. Struct. Biol.* **2012**, *180*, 519−530.
(78) Punjani, A.; Rubinstein, J. L.; Fleet, D. J.; Brubaker, M. A. Cryosparc: Algorithms for Rapid Unsupervised Cryo-Em Structure Determination. *Nat. Methods* **2017**, *14*, 290−296.
(79) Tang, G.; Peng, L.; Baldwin, P. R.; Mann, D. S.; Jiang, W.; Rees, I.; Ludtke, S. J. Eman2: An Extensible Image Processing Suite for Electron Microscopy. *J. Struct. Biol.* **2007**, *157*, 38−46.
(80) Grant, T.; Rohou, A.; Grigorieff, N. cisTEM, User-Friendly Software for Single-Particle Image Processing. *eLife* **2018**, *7*, No. e35383.
(81) Caesar, J.; Reboul, C. F.; Machello, C.; Kiesewetter, S.; Tang, M. L.; Deme, J. C.; Johnson, S.; Elmlund, D.; Lea, S. M.; Elmlund, H. SIMPLE 3.0. Stream Single-Particle cryo-EM Analysis in Real Time. *J. Struct. Biol.: X* **2020**, *4*, 100040.
(82) Wagner, T.; Merino, F.; Stabrin, M.; Moriya, T.; Antoni, C.; Apelbaum, A.; Hagel, P.; Sitsel, O.; Raisch, T.; Prumbaum, D.; et al. SPHIRE-crYOLO Is a Fast and Accurate Fully Automated Particle Picker for cryo-EM. *Commun. Biol.* **2019**, *2*, 218.
(83) Bepler, T.; Morin, A.; Rapp, M.; Brasch, J.; Shapiro, L.; Noble, A. J.; Berger, B. Positive-Unlabeled Convolutional Neural Networks for Particle Picking in Cryo-Electron Micrographs. *Nat. Methods* **2019**, *16*, 1153−1160.
(84) Jumper, J.; Evans, R.; Pritzel, A.; Green, T.; Figurnov, M.; Ronneberger, O.; Tunyasuvunakool, K.; Bates, R.; Žídek, A.; Potapenko, A.; et al. Highly Accurate Protein Structure Prediction with Alphafold. *Nature* **2021**, *596*, 583−589.
(85) Porta-Pardo, E.; Ruiz-Serra, V.; Valencia, A. The Structural Coverage of the Human Proteome before and after AlphaFold. *PLoS Comput. Biol.* **2022**, *18*, e1009818.
(86) Emsley, P.; Lohkamp, B.; Scott, W. G.; Cowtan, K. Features and Development of Coot. *Acta Crystallogr. D Biol. Crystallogr.* **2010**, *66*, 486−501.
(87) Afonine, P. V.; Poon, B. K.; Read, R. J.; Sobolev, O. V.; Terwilliger, T. C.; Urzhumtsev, A.; Adams, P. D. Real-Space Refinement in Phenix for Cryo-Em and Crystallography. *Acta Crystallogr. D Struct Biol.* **2018**, *74*, 531−544.
(88) Murshudov, G. N.; Skubák, P.; Lebedev, A. A.; Pannu, N. S.; Steiner, R. A.; Nicholls, R. A.; Winn, M. D.; Long, F.; Vagin, A. A. Refmac5 for the Refinement of Macromolecular Crystal Structures. *Acta Crystallogr. D Biol. Crystallogr.* **2011**, *67*, 355−367.
(89) Croll, T. I. Isolde: A Physically Realistic Environment for Model Building into Low-Resolution Electron-Density Maps. *Acta Crystallogr. D Struct Biol.* **2018**, *74*, 519−530.
(90) Trabuco, L. G.; Villa, E.; Schreiner, E.; Harrison, C. B.; Schulten, K. Molecular Dynamics Flexible Fitting: A Practical Guide to Combine Cryo-Electron Microscopy and X-Ray Crystallography. *Methods* **2009**, *49*, 174−180.
(91) Pettersen, E. F.; Goddard, T. D.; Huang, C. C.; Couch, G. S.; Greenblatt, D. M.; Meng, E. C.; Ferrin, T. E. Ucsf Chimera-a Visualization System for Exploratory Research and Analysis. *J. Comput. Chem.* **2004**, *25*, 1605−1612.
(92) Goddard, T. D.; Huang, C. C.; Meng, E. C.; Pettersen, E. F.; Couch, G. S.; Morris, J. H.; Ferrin, T. E. Ucsf Chimerax: Meeting Modern Challenges in Visualization and Analysis. *Protein Sci.* **2018**, *27*, 14−25.
(93) Pettersen, E. F.; Goddard, T. D.; Huang, C. C.; Meng, E. C.; Couch, G. S.; Croll, T. I.; Morris, J. H.; Ferrin, T. E. Ucsf Chimerax: Structure Visualization for Researchers, Educators, and Developers. *Protein Sci.* **2021**, *30*, 70−82.
(94) Schrödinger, L.; DeLano, W. *Pymol*; 2020. http://www.pymol.org/pymol (accessed 2022-07-04).
(95) Rosenthal, P. B.; Henderson, R. Optimal Determination of Particle Orientation, Absolute Hand, and Contrast Loss in Single-Particle Electron Cryomicroscopy. *J. Mol. Biol.* **2003**, *333*, 721−745.
(96) van Heel, M.; Schatz, M. Fourier Shell Correlation Threshold Criteria. *J. Struct. Biol.* **2005**, *151*, 250−262.
(97) Afonine, P. V.; Klaholz, B. P.; Moriarty, N. W.; Poon, B. K.; Sobolev, O. V.; Terwilliger, T. C.; Adams, P. D.; Urzhumtsev, A. New Tools for the Analysis and Validation of Cryo-Em Maps and Atomic Models. *Acta Crystallogr. D Struct Biol.* **2018**, *74*, 814−840.
(98) Young, J. Y.; Westbrook, J. D.; Feng, Z.; Sala, R.; Peisach, E.; Oldfield, T. J.; Sen, S.; Gutmanas, A.; Armstrong, D. R.; Berrisford, J. M.; et al. Onedep: Unified Wwpdb System for Deposition, Biocuration, and Validation of Macromolecular Structures in the Pdb Archive. *Structure* **2017**, *25*, 536−545.
(99) Henderson, R. Avoiding the Pitfalls of Single Particle Cryo-Electron Microscopy: Einstein from Noise. *Proc. Natl. Acad. Sci. U. S. A.* **2013**, *110*, 18037−18041.
(100) van Heel, M. Finding Trimeric HIV-1 Envelope Glycoproteins in Random Noise. *Proc. Natl. Acad. Sci. U. S. A.* **2013**, *110*, E4175−E4177.
(101) Scheres, S. H. W.; Chen, S. Prevention of Overfitting in Cryo-Em Structure Determination. *Nat. Methods* **2012**, *9*, 853−854.
(102) Nickels, J. D.; Chatterjee, S.; Stanley, C. B.; Qian, S.; Cheng, X.; Myles, D. A. A.; Standaert, R. F.; Elkins, J. G.; Katsaras, J. The in Vivo Structure of Biological Membranes and Evidence for Lipid Domains. *PLoS Biol.* **2017**, *15*, No. e2002214.
(103) Fu, X.; Ning, J.; Zhong, Z.; Ambrose, Z.; Charles Watkins, S.; Zhang, P. AutoCLEM: An Automated Workflow for Correlative Live-Cell Fluorescence Microscopy and Cryo-Electron Tomography. *Sci. Rep.* **2019**, *9*, 19207.
(104) Mageswaran, S. K.; Yang, W. Y.; Chakrabarty, Y.; Oikonomou, C. M.; Jensen, G. J. A Cryo-Electron Tomography Workflow Reveals Protrusion-Mediated Shedding on Injured Plasma Membrane. *Sci. Adv.* **2021**, *7*, No. eabc6345.

https://doi.org/10.1021/acs.chemrev.1c00837
Chem. Rev. 2022, 122, 13989−14017

(105) Rapisarda, C.; Cherrak, Y.; Kooger, R.; Schmidt, V.; Pellarin, R.; Logger, L.; Cascales, E.; Pilhofer, M.; Durand, E.; Fronzes, R. In Situ and High-Resolution Cryo-EM Structure of a Bacterial Type VI Secretion System Membrane Complex. *EMBO J.* **2019**, *38*, No. e100886.
(106) Bayburt, T. H.; Grinkova, Y. V.; Sligar, S. G. Self-Assembly of Discoidal Phospholipid Bilayer Nanoparticles with Membrane Scaffold Proteins. *Nano Lett.* **2002**, *2*, 853−856.
(107) Brouillette, C. G.; Jones, J. L.; Ng, T. C.; Kercret, H.; Chung, B. H.; Segrest, J. P. Structural Studies of Apolipoprotein a-I/Phosphatidylcholine Recombinants by High-Field Proton Nmr, Nondenaturing Gradient Gel Electrophoresis, and Electron Microscopy. *Biochemistry* **1984**, *23*, 359−367.
(108) Bayburt, T. H.; Sligar, S. G. Membrane Protein Assembly into Nanodiscs. *FEBS Lett.* **2010**, *584*, 1721−1727.
(109) Denisov, I. G.; Grinkova, Y. V.; Lazarides, A. A.; Sligar, S. G. Directed Self-Assembly of Monodisperse Phospholipid Bilayer Nanodiscs with Controlled Size. *J. Am. Chem. Soc.* **2004**, *126*, 3477−3487.
(110) Postis, V.; Rawson, S.; Mitchell, J. K.; Lee, S. C.; Parslow, R. A.; Dafforn, T. R.; Baldwin, S. A.; Muench, S. P. The Use of Smalps as a Novel Membrane Protein Scaffold for Structure Study by Negative Stain Electron Microscopy. *Biochim. Biophys. Acta* **2015**, *1848*, 496−501.
(111) Lee, S. C.; Knowles, T. J.; Postis, V. L. G.; Jamshad, M.; Parslow, R. A.; Lin, Y.-p.; Goldman, A.; Sridhar, P.; Overduin, M.; Muench, S. P.; et al. A Method for Detergent-Free Isolation of Membrane Proteins in Their Local Lipid Environment. *Nat. Protoc.* **2016**, *11*, 1149−1162.
(112) Angiulli, G.; Dhupar, H. S.; Suzuki, H.; Wason, I. S.; Duong Van Hoa, F.; Walz, T. New Approach for Membrane Protein Reconstitution into Peptidiscs and Basis for Their Adaptability to Different Proteins. *eLife* **2020**, *9*, No. e53530.
(113) Knowles, T. J.; Finka, R.; Smith, C.; Lin, Y.-P.; Dafforn, T.; Overduin, M. Membrane Proteins Solubilized Intact in Lipid Containing Nanoparticles Bounded by Styrene Maleic Acid Copolymer. *J. Am. Chem. Soc.* **2009**, *131*, 7484−7485.
(114) Brown, C. J.; Trieber, C.; Overduin, M. Structural Biology of Endogenous Membrane Protein Assemblies in Native Nanodiscs. *Curr. Opin. Struct. Biol.* **2021**, *69*, 70−77.
(115) Guo, Y. Detergent-Free Systems for Structural Studies of Membrane Proteins. *Biochem. Soc. Trans.* **2021**, *49*, 1361−1374.
(116) Sligar, S. G.; Denisov, I. G. Nanodiscs: A Toolkit for Membrane Protein Science. *Protein Sci.* **2021**, *30*, 297−315.
(117) Nadezhdin, K. D.; Neuberger, A.; Trofimov, Y. A.; Krylov, N. A.; Sinica, V.; Kupko, N.; Vlachova, V.; Zakharian, E.; Efremov, R. G.; Sobolevsky, A. I. Structural Mechanism of Heat-Induced Opening of a Temperature-Sensitive Trp Channel. *Nat. Struct. Mol. Biol.* **2021**, *28*, 564−572.
(118) Flores, J. A.; Haddad, B. G.; Dolan, K. A.; Myers, J. B.; Yoshioka, C. C.; Copperman, J.; Zuckerman, D. M.; Reichow, S. L. Connexin-46/50 in a Dynamic Lipid Environment Resolved by CryoEM at 1.9 Å. *Nat. Commun.* **2020**, *11*, 4331.
(119) Sun, C.; Benlekbir, S.; Venkatakrishnan, P.; Wang, Y.; Hong, S.; Hosler, J.; Tajkhorshid, E.; Rubinstein, J. L.; Gennis, R. B. Structure of the Alternative Complex Iii in a Supercomplex with Cytochrome Oxidase. *Nature* **2018**, *557*, 123−126.
(120) Yao, X.; Fan, X.; Yan, N. Cryo-Em Analysis of a Membrane Protein Embedded in the Liposome. *Proc. Natl. Acad. Sci. U. S. A.* **2020**, *117*, 18497−18503.
(121) Pang, S. S.; Bayly-Jones, C.; Radjainia, M.; Spicer, B. A.; Law, R. H. P.; Hodel, A. W.; Parsons, E. S.; Ekkel, S. M.; Conroy, P. J.; Ramm, G.; et al. The Cryo-EM Structure of the Acid Activatable Pore-Forming Immune Effector Macrophage-Expressed Gene 1. *Nat. Comms.* **2019**, *10*, 4288.
(122) Pollock, N. L.; Lee, S. C.; Patel, J. H.; Gulamhussein, A. A.; Rothnie, A. J. Structure and Function of Membrane Proteins Encapsulated in a Polymer-Bound Lipid Bilayer. *Biochim. Biophys. Acta* **2018**, *1860*, 809−817.
(123) Gulati, S.; Jamshad, M.; Knowles, T. J.; Morrison, K. A.; Downing, R.; Cant, N.; Collins, R.; Koenderink, J. B.; Ford, R. C.; Overduin, M.; et al. Detergent-Free Purification of Abc (Atp-Binding-Cassette) Transporters. *Biochem. J.* **2014**, *461*, 269−278.
(124) Qiu, W.; Fu, Z.; Xu, G. G.; Grassucci, R. A.; Zhang, Y.; Frank, J.; Hendrickson, W. A.; Guo, Y. Structure and Activity of Lipid Bilayer within a Membrane-Protein Transporter. *Proc. Natl. Acad. Sci. U. S. A.* **2018**, *115*, 12985−12990.
(125) Hesketh, S. J.; Klebl, D. P.; Higgins, A. J.; Thomsen, M.; Pickles, I. B.; Sobott, F.; Sivaprasadarao, A.; Postis, V. L. G.; Muench, S. P. Styrene Maleic-Acid Lipid Particles (Smalps) into Detergent or Amphipols: An Exchange Protocol for Membrane Protein Characterisation. *Biochim. Biophys. Acta* **2020**, *1862*, 183192.
(126) Yoder, N.; Gouaux, E. The His-Gly Motif of Acid-Sensing Ion Channels Resides in a Reentrant 'Loop' Implicated in Gating and Ion Selectivity. *eLife* **2020**, *9*, No. e56527.
(127) Kumar, A.; Basak, S.; Rao, S.; Gicheru, Y.; Mayer, M. L.; Sansom, M. S. P.; Chakrapani, S. Mechanisms of Activation and Desensitization of Full-Length Glycine Receptor in Lipid Nanodiscs. *Nat. Comms.* **2020**, *11*, 3752.
(128) Bada Juarez, J. F.; Munoz-Garcia, J. C.; Inacio Dos Reis, R.; Henry, A.; McMillan, D.; Kriek, M.; Wood, M.; Vandenplas, C.; Sands, Z.; Castro, L.; et al. Detergent-Free Extraction of a Functional Low-Expressing Gpcr from a Human Cell Line. *Biochim. Biophys. Acta. Biomembr.* **2020**, *1862*, 183152.
(129) Routledge, S. J.; Jamshad, M.; Little, H. A.; Lin, Y.-P.; Simms, J.; Thakker, A.; Spickett, C. M.; Bill, R. M.; Dafforn, T. R.; Poyner, D. R.; et al. Ligand-Induced Conformational Changes in a Smalp-Encapsulated Gpcr. *Biochim. Biophys. Acta* **2020**, *1862*, 183235.
(130) Sarkar, K.; Joedicke, L.; Westwood, M.; Burnley, R.; Wright, M.; McMillan, D.; Byrne, B. Modulation of PTH1R Signaling by an ECD Binding Antibody Results in Inhibition of β-Arrestin 2 Coupling. *Sci. Rep.* **2019**, *9*, 14432.
(131) Gulamhussein, A. A.; Uddin, R.; Tighe, B. J.; Poyner, D. R.; Rothnie, A. J. A Comparison of Sma (Styrene Maleic Acid) and Dibma (Di-Isobutylene Maleic Acid) for Membrane Protein Purification. *Biochim. Biophys. Acta* **2020**, *1862*, 183281.
(132) Kolata, P.; Efremov, R. G. Structure of Escherichia coli Respiratory Complex I Reconstituted into Lipid Nanodiscs Reveals an Uncoupled Conformation. *eLife* **2021**, *10*, No. e68710.
(133) Li, B.; Rietmeijer, R. A.; Brohawn, S. G. Structural Basis for Ph Gating of the Two-Pore Domain K+ Channel Task2. *Nature* **2020**, *586*, 457−462.
(134) Takeda, H.; Tsutsumi, A.; Nishizawa, T.; Lindau, C.; Busto, J. V.; Wenz, L.-S.; Ellenrieder, L.; Imai, K.; Straub, S. P.; Mossmann, W.; et al. Mitochondrial Sorting and Assembly Machinery Operates by B-Barrel Switching. *Nature* **2021**, *590*, 163−169.
(135) Reid, M. S.; Kern, D. M.; Brohawn, S. G. Cryo-EM Structure of the Potassium-Chloride Cotransporter KCC4 in Lipid Nanodiscs. *eLife* **2020**, *9*, No. e52505.
(136) Kern, D. M.; Sorum, B.; Mali, S. S.; Hoel, C. M.; Sridharan, S.; Remis, J. P.; Toso, D. B.; Kotecha, A.; Bautista, D. M.; Brohawn, S. G. Cryo-Em Structure of Sars-Cov-2 Orf3a in Lipid Nanodiscs. *Nat. Struct. Mol. Biol.* **2021**, *28*, 573−582.
(137) Zhang, M.; Gui, M.; Wang, Z.-F.; Gorgulla, C.; Yu, J. J.; Wu, H.; Sun, Z.-y. J.; Klenk, C.; Merklinger, L.; Morstein, L.; et al. Cryo-Em Structure of an Activated Gpcr-G Protein Complex in Lipid Nanodiscs. *Nat. Struct. Mol. Biol.* **2021**, *28*, 258−267.
(138) Staus, D. P.; Hu, H.; Robertson, M. J.; Kleinhenz, A. L. W.; Wingler, L. M.; Capel, W. D.; Latorraca, N. R.; Lefkowitz, R. J.; Skiniotis, G. Structure of the M2Muscarinic Receptor-B-Arrestin Complex in a Lipid Nanodisc. *Nature* **2020**, *579*, 297−302.
(139) Zhao, D. Y.; Pöge, M.; Morizumi, T.; Gulati, S.; Van Eps, N.; Zhang, J.; Miszta, P.; Filipek, S.; Mahamid, J.; Plitzko, J. M.; et al. Cryo-Em Structure of the Native Rhodopsin Dimer in Nanodiscs. *J. Biol. Chem.* **2019**, *294*, 14215−14230.
(140) Carlson, M. L.; Young, J. W.; Zhao, Z.; Fabre, L.; Jun, D.; Li, J.; Li, J.; Dhupar, H. S.; Wason, I.; Mills, A. T.; et al. The Peptidisc, a Simple Method for Stabilizing Membrane Proteins in Detergent-Free Solution. *eLife* **2018**, *7*, No. e34085.

https://doi.org/10.1021/acs.chemrev.1c00837
Chem. Rev. 2022, 122, 13989−14017

(141) Frauenfeld, J.; Löving, R.; Armache, J.-P.; Sonnen, A. F. P.; Guettou, F.; Moberg, P.; Zhu, L.; Jegerschöld, C.; Flayhan, A.; Briggs, J. A. G.; et al. A Saposin-Lipoprotein Nanoparticle System for Membrane Proteins. *Nat. Methods* **2016**, *13*, 345−351.
(142) Du, D.; Neuberger, A.; Orr, M. W.; Newman, C. E.; Hsu, P.-C.; Samsudin, F.; Szewczak-Harris, A.; Ramos, L. M.; Debela, M.; Khalid, S.; et al. Interactions of a Bacterial Rnd Transporter with a Transmembrane Small Protein in a Lipid Environment. *Structure* **2020**, *28*, 625−634.
(143) Zhang, Y.; Dijkman, P. M.; Zou, R.; Zandl-Lang, M.; Sanchez, R. M.; Eckhardt-Strelau, L.; Köfeler, H.; Vogel, H.; Yuan, S.; Kudryashev, M. Asymmetric Opening of the Homopentameric 5-HT3aASerotonin Receptor in Lipid Bilayers. *Nat. Comms.* **2021**, *12*, 1074.
(144) Le Bon, C.; Marconnet, A.; Masscheleyn, S.; Popot, J.-L.; Zoonens, M. Folding and Stabilizing Membrane Proteins in Amphipol A8−35. *Methods* **2018**, *147*, 95−105.
(145) Liao, M.; Cao, E.; Julius, D.; Cheng, Y. Structure of the Trpv1 Ion Channel Determined by Electron Cryo-Microscopy. *Nature* **2013**, *504*, 107−112.
(146) Saponaro, A.; Bauer, D.; Giese, M. H.; Swuec, P.; Porro, A.; Gasparri, F.; Sharifzadeh, A. S.; Chaves-Sanjuan, A.; Alberio, L.; Parisi, G.; et al. Gating Movements and Ion Permeation in Hcn4 Pacemaker Channels. *Mol. Cell* **2021**, *81*, 2929−2943.
(147) Chen, Y.; Clarke, O. B.; Kim, J.; Stowe, S.; Kim, Y.-K.; Assur, Z.; Cavalier, M.; Godoy-Ruiz, R.; von Alpen, D. C.; Manzini, C. Structure of the STRA6 Receptor for Retinol Uptake. *Science (New York, N.Y.)* **2016**, *353*, 887.
(148) Mobbs, J. I.; Belousoff, M. J.; Harikumar, K. G.; Piper, S. J.; Xu, X.; Furness, S. G. B.; Venugopal, H.; Christopoulos, A.; Danev, R.; Wootten, D.; et al. Structures of the Human Cholecystokinin 1 (Cck1) Receptor Bound to Gs and Gq Mimetic Proteins Provide Insight into Mechanisms of G Protein Selectivity. *PLoS Biol.* **2021**, *19*, No. e3001295.
(149) Zampieri, V.; Gobet, A.; Robert, X.; Falson, P.; Chaptal, V. Cryoem Reconstructions of Membrane Proteins Solved in Several Amphipathic Solvents, Nanodisc, Amphipol and Detergents, Yield Amphipathic Belts of Similar Sizes Corresponding to a Common Ordered Solvent Layer. *Biochim. Biophys. Acta - Biomembr.* **2021**, *1863*, 183693.
(150) Ehsan, M.; Katsube, S.; Cecchetti, C.; Du, Y.; Mortensen, J. S.; Wang, H.; Nygaard, A.; Ghani, L.; Loland, C. J.; Kobilka, B. K.; et al. New Malonate-Derived Tetraglucoside Detergents for Membrane Protein Stability. *ACS Chem. Biol.* **2020**, *15*, 1697−1707.
(151) Hauer, F.; Gerle, C.; Fischer, N.; Oshima, A.; Shinzawa-Itoh, K.; Shimada, S.; Yokoyama, K.; Fujiyoshi, Y.; Stark, H. Grader: Membrane Protein Complex Preparation for Single-Particle Cryo-Em. *Structure* **2015**, *23*, 1769−1775.
(152) Wu, S.; Avila-Sakar, A.; Kim, J.; Booth, D. S.; Greenberg, C. H.; Rossi, A.; Liao, M.; Li, X.; Alian, A.; Griner, S. L.; et al. Fabs Enable Single Particle CryoEM Studies of Small Proteins. *Structure* **2012**, *20*, 582−592.
(153) Rasmussen, S. G.; DeVree, B. T.; Zou, Y.; Kruse, A. C.; Chung, K. Y.; Kobilka, T. S.; Thian, F. S.; Chae, P. S.; Pardon, E.; Calinski, D.; et al. Crystal Structure of the B2 Adrenergic Receptor-Gs Protein Complex. *Nature* **2011**, *477*, 549−555.
(154) Koehl, A.; Hu, H.; Maeda, S.; Zhang, Y.; Qu, Q.; Paggi, J. M.; Latorraca, N. R.; Hilger, D.; Dawson, R.; Matile, H.; et al. Structure of the M-Opioid Receptor-Gi Protein Complex. *Nature* **2018**, *558*, 547−552.
(155) Uchański, T.; Masiulis, S.; Fischer, B.; Kalichuk, V.; López-Sánchez, U.; Zarkadas, E.; Weckener, M.; Sente, A.; Ward, P.; Wohlkönig, A.; et al. Megabodies Expand the Nanobody Toolkit for Protein Structure Determination by Single-Particle Cryo-Em. *Nat. Methods* **2021**, *18*, 60−68.
(156) Wu, X.; Rapoport, T. A. Cryo-EM Structure Determination of Small Proteins by Nanobody-Binding Scaffolds (Legobodies). *Proc. Natl. Acad. Sci. U. S. A.* **2021**, *118*, No. e2115001118.
(157) Bloch, J. S.; Mukherjee, S.; Kowal, J.; Filippova, E. V.; Niederer, M.; Pardon, E.; Steyaert, J.; Kossiakoff, A. A.; Locher, K. P. Development of a Universal Nanobody-Binding Fab Module for Fiducial-Assisted Cryo-EM Studies of Membrane Proteins. *Proc. Natl. Acad. Sci. U. S. A.* **2021**, *118*, No. e2115435118.
(158) Plenge, P.; Yang, D.; Salomon, K.; Laursen, L.; Kalenderoglou, I. E.; Newman, A. H.; Gouaux, E.; Coleman, J. A.; Loland, C. J. The Antidepressant Drug Vilazodone Is an Allosteric Inhibitor of the Serotonin Transporter. *Nat. Comms.* **2021**, *12*, 5063.
(159) Marino, J.; Schertler, G. F. X. A Set of Common Movements within Gpcr-G-Protein Complexes from Variability Analysis of Cryo-Em Datasets. *J. Struct. Biol.* **2021**, *213*, 107699.
(160) Tsutsumi, N.; Mukherjee, S.; Waghray, D.; Janda, C. Y.; Jude, K. M.; Miao, Y.; Burg, J. S.; Aduri, N. G.; Kossiakoff, A. A.; Gati, C.; et al. Structure of Human Frizzled5 by Fiducial-Assisted Cryo-EM Supports a Heterodimeric Mechanism of Canonical Wnt Signaling. *eLife* **2020**, *9*, No. e58464.
(161) Nosol, K.; Romane, K.; Irobalieva, R. N.; Alam, A.; Kowal, J.; Fujita, N.; Locher, K. P. Cryo-Em Structures Reveal Distinct Mechanisms of Inhibition of the Human Multidrug Transporter Abcb1. *Proc. Natl. Acad. Sci. U. S. A.* **2020**, *117*, 26245−26253.
(162) Kim, J.; Tan, Y. Z.; Wicht, K. J.; Erramilli, S. K.; Dhingra, S. K.; Okombo, J.; Vendome, J.; Hagenah, L. M.; Giacometti, S. I.; Warren, A. L.; et al. Structure and Drug Resistance of the Plasmodium Falciparum Transporter Pfcrt. *Nature* **2019**, *576*, 315−320.
(163) Zhang, H.; Huang, C.-S.; Yu, X.; Lee, J.; Vaish, A.; Chen, Q.; Zhou, M.; Wang, Z.; Min, X. Cryo-EM Structure of ABCG5/G8 in Complex with Modulating Antibodies. *Commun. Biol.* **2021**, *4*, 526.
(164) Lee, Y.; Wiriyasermkul, P.; Jin, C.; Quan, L.; Ohgaki, R.; Okuda, S.; Kusakizako, T.; Nishizawa, T.; Oda, K.; Ishitani, R.; et al. Cryo-Em Structure of the Human L-Type Amino Acid Transporter 1 in Complex with Glycoprotein Cd98hc. *Nat. Struct. Mol. Biol.* **2019**, *26*, 510−517.
(165) Oosterheert, W.; Gros, P. Cryo-Electron Microscopy Structure and Potential Enzymatic Function of Human Six-Transmembrane Epithelial Antigen of the Prostate 1 (Steap1). *J. Bio. Chem.* **2020**, *295*, 9502−9512.
(166) Danev, R.; Belousoff, M.; Liang, Y.-L.; Zhang, X.; Eisenstein, F.; Wootten, D.; Sexton, P. M. Routine Sub-2.5 Å Cryo-EM Structure Determination of GPCRs. *Nat. Commun.* **2021**, *12*, 4333.
(167) Tan, Y. Z.; Zhang, L.; Rodrigues, J.; Zheng, R. B.; Giacometti, S. I.; Rosário, A. L.; Kloss, B.; Dandey, V. P.; Wei, H.; Brunton, R.; et al. Cryo-Em Structures and Regulation of Arabinofuranosyltransferase Aftd from Mycobacteria. *Mol. Cell* **2020**, *78*, 683−699.
(168) Han, Y.; Fan, X.; Wang, H.; Zhao, F.; Tully, C. G.; Kong, J.; Yao, N.; Yan, N. High-Yield Monolayer Graphene Grids for near-Atomic Resolution Cryoelectron Microscopy. *Proc. Natl. Acad. Sci. U. S. A.* **2020**, *117*, 1009.
(169) Palovcak, E.; Wang, F.; Zheng, S. Q.; Yu, Z.; Li, S.; Betegon, M.; Bulkley, D.; Agard, D. A.; Cheng, Y. A Simple and Robust Procedure for Preparing Graphene-Oxide Cryo-Em Grids. *J. Struct. Biol.* **2018**, *204*, 80−84.
(170) Woll, K. A.; Haji-Ghassemi, O.; Van Petegem, F. Pathological Conformations of Disease Mutant Ryanodine Receptors Revealed by Cryo-EM. *Nat. Comms.* **2021**, *12*, 807.
(171) Bokori-Brown, M.; Martin, T. G.; Naylor, C. E.; Basak, A. K.; Titball, R. W.; Savva, C. G. Cryo-EM Structure of Lysenin Pore Elucidates Membrane Insertion by an Aerolysin Family Protein. *Nat. Commun.* **2016**, *7*, 11293.
(172) Meyerson, J. R.; Rao, P.; Kumar, J.; Chittori, S.; Banerjee, S.; Pierson, J.; Mayer, M. L.; Subramaniam, S. Self-Assembled Monolayers Improve Protein Distribution on Holey Carbon Cryo-EM Supports. *Sci. Rep.* **2015**, *4*, 7084.
(173) Blaza, J. N.; Vinothkumar, K. R.; Hirst, J. Structure of the Deactive State of Mammalian Respiratory Complex I. *Structure* **2018**, *26*, 312−319.
(174) Herzik, M. A.; Wu, M.; Lander, G. C. High-Resolution Structure Determination of Sub-100 kDa Complexes Using Conventional Cryo-EM. *Nat. Comms.* **2019**, *10*, 1032.
(175) Wu, M.; Lander, G. C.; Herzik, M. A. Sub-2 Angstrom Resolution Structure Determination Using Single-Particle Cryo-EM at 200 keV. *J. Struct. Biol.: X* **2020**, *4*, 100020.

https://doi.org/10.1021/acs.chemrev.1c00837
Chem. Rev. 2022, 122, 13989−14017

(176) Zhang, X.; Johnson, R. M.; Drulyte, I.; Yu, L.; Kotecha, A.; Danev, R.; Wootten, D.; Sexton, P. M.; Belousoff, M. J. Evolving Cryo-EM Structural Approaches for GPCR Drug Discovery. *Structure* **2021**, *29*, 963−974.
(177) Isaikina, P.; Tsai, C.-J.; Dietz, N.; Pamula, F.; Grahl, A.; Goldie, K. N.; Guixà-González, R.; Branco, C.; Paolini-Bertrand, M.; Calo, N.; et al. Structural Basis of the Activation of the CC Chemokine Receptor 5 by a Chemokine Agonist. *Sci. Adv.* **2021**, *7*, No. eabg8685.
(178) Liang, Y.-L.; Khoshouei, M.; Radjainia, M.; Zhang, Y.; Glukhova, A.; Tarrasch, J.; Thal, D. M.; Furness, S. G. B.; Christopoulos, G.; Coudrat, T.; et al. Phase-Plate Cryo-Em Structure of a Class B Gpcr-G-Protein Complex. *Nature* **2017**, *546*, 118−123.
(179) García-Nafría, J.; Lee, Y.; Bai, X.; Carpenter, B.; Tate, C. G. Cryo-EM Structure of the Adenosine A2A Receptor Coupled to an Engineered Heterotrimeric G Protein. *eLife* **2018**, *7*, No. e35946.
(180) Pándy-Szekeres, G.; Munk, C.; Tsonkov, T. M.; Mordalski, S.; Harpsøe, K.; Hauser, A. S.; Bojarski, A. J.; Gloriam, D. E. GPCRdb in 2018: Adding Gpcr Structure Models and Ligands. *Nucleic Acids Res.* **2018**, *46*, D440−d446.
(181) Wood, C. A. P.; Zhang, J.; Aydin, D.; Xu, Y.; Andreone, B. J.; Langen, U. H.; Dror, R. O.; Gu, C.; Feng, L. Structure and Mechanism of Blood-Brain-Barrier Lipid Transporter Mfsd2a. *Nature* **2021**, *596*, 444−448.
(182) Wang, N.; Jiang, X.; Zhang, S.; Zhu, A.; Yuan, Y.; Xu, H.; Lei, J.; Yan, C. Structural Basis of Human Monocarboxylate Transporter 1 Inhibition by Anti-Cancer Drug Candidates. *Cell* **2021**, *184*, 370−383.
(183) Sauer, D. B.; Trebesch, N.; Marden, J. J.; Cocco, N.; Song, J.; Koide, A.; Koide, S.; Tajkhorshid, E.; Wang, D.-N. Structural Basis for the Reaction Cycle of DASS Dicarboxylate Transporters. *eLife* **2020**, *9*, No. e61350.
(184) Bai, X. C.; Yan, C.; Yang, G.; Lu, P.; Ma, D.; Sun, L.; Zhou, R.; Scheres, S. H. W.; Shi, Y. An Atomic Structure of Human Γ-Secretase. *Nature* **2015**, *525*, 212−217.
(185) Ma, J.; You, X.; Sun, S.; Wang, X.; Qin, S.; Sui, S.-F. Structural Basis of Energy Transfer in Porphyridium Purpureum Phycobilisome. *Nature* **2020**, *579*, 146−151.
(186) Gray, D. A.; White, J. B. R.; Oluwole, A. O.; Rath, P.; Glenwright, A. J.; Mazur, A.; Zahn, M.; Baslé, A.; Morland, C.; Evans, S. L.; et al. Insights into SusCD-Mediated Glycan Import by a Prominent Gut Symbiont. *Nat. Comms.* **2021**, *12*, 44.
(187) Madej, M.; White, J. B. R.; Nowakowska, Z.; Rawson, S.; Scavenius, C.; Enghild, J. J.; Bereta, G. P.; Pothula, K.; Kleinekathoefer, U.; Baslé, A.; et al. Structural and Functional Insights into Oligopeptide Acquisition by the Ragab Transporter from Porphyromonas Gingivalis. *Nature Microbiology* **2020**, *5*, 1016−1025.
(188) Rougé, L.; Chiang, N.; Steffek, M.; Kugel, C.; Croll, T. I.; Tam, C.; Estevez, A.; Arthur, C. P.; Koth, C. M.; Ciferri, C.; et al. Structure of Cd20 in Complex with the Therapeutic Monoclonal Antibody Rituximab. *Science* **2020**, *367*, 1224.
(189) Xu, H.; Li, T.; Rohou, A.; Arthur, C. P.; Tzakoniati, F.; Wong, E.; Estevez, A.; Kugel, C.; Franke, Y.; Chen, J.; et al. Structural Basis of Nav1.7 Inhibition by a Gating-Modifier Spider Toxin. *Cell* **2019**, *176*, 702−715.
(190) Liu, C.; Reese, R.; Vu, S.; Rougé, L.; Shields, S. D.; Kakiuchi-Kiyota, S.; Chen, H.; Johnson, K.; Shi, Y. P.; Chernov-Rogan, T.; et al. A Non-Covalent Ligand Reveals Biased Agonism of the Trpa1 Ion Channel. *Neuron* **2021**, *109*, 273−284.
(191) Punjani, A.; Zhang, H.; Fleet, D. J. Non-Uniform Refinement: Adaptive Regularization Improves Single-Particle Cryo-Em Reconstruction. *Nat. Methods* **2020**, *17*, 1214−1221.
(192) Punjani, A.; Fleet, D. J. 3d Variability Analysis: Resolving Continuous Flexibility and Discrete Heterogeneity from Single Particle Cryo-Em. *J. Struct. Biol.* **2021**, *213*, 107702.
(193) Dong, M.; Deganutti, G.; Piper, S. J.; Liang, Y.-L.; Khoshouei, M.; Belousoff, M. J.; Harikumar, K. G.; Reynolds, C. A.; Glukhova, A.; Furness, S. G. B.; et al. Structure and Dynamics of the Active Gs-Coupled Human Secretin Receptor. *Nat. Comms.* **2020**, *11*, 4137.
(194) Liang, Y.-L.; Belousoff, M. J.; Fletcher, M. M.; Zhang, X.; Khoshouei, M.; Deganutti, G.; Koole, C.; Furness, S. G. B.; Miller, L. J.; Hay, D. L.; et al. Structure and Dynamics of Adrenomedullin Receptors Am1 and Am2 Reveal Key Mechanisms in the Control of Receptor Phenotype by Receptor Activity-Modifying Proteins. *ACS Pharmacol. Trans. Sci.* **2020**, *3*, 263−284.
(195) Zhang, X.; Belousoff, M. J.; Liang, Y.-L.; Danev, R.; Sexton, P. M.; Wootten, D. Structure and Dynamics of Semaglutide- and Taspoglutide-Bound Glp-1r-Gs Complexes. *Cell Rep.* **2021**, *36*, 109374.
(196) Josephs, T. M.; Belousoff, M. J.; Liang, Y.-L.; Piper, S. J.; Cao, J.; Garama, D. J.; Leach, K.; Gregory, K. J.; Christopoulos, A.; Hay, D. L.; et al. Structure and Dynamics of the CGRP Receptor in Apo and Peptide-Bound Forms. *Science* **2021**, *372*, No. eabf7258.
(197) Su, C.-C.; Morgan, C. E.; Kambakam, S.; Rajavel, M.; Scott, H.; Huang, W.; Emerson Corey, C.; Taylor Derek, J.; Stewart Phoebe, L.; Bonomo Robert, A.; et al. Cryo-Electron Microscopy Structure of an Acinetobacter Baumannii Multidrug Efflux Pump. *mBio* **2019**, *10*, e01295−01219.
(198) Punjani, A.; Fleet, D. J. 3D Flexible Refinement: Structure and Motion of Flexible Proteins from Cryo-EM. *bioRxiv* **2021**, DOI: 10.1101/2021.04.22.440893.
(199) Murphy, B. J.; Klusch, N.; Langer, J.; Mills, D. J.; Yildiz, Ö.; Kühlbrandt, W. Rotary Substates of Mitochondrial ATP Synthase Reveal the Basis of Flexible F_1-F_0 Coupling. *Science* **2019**, *364*, No. eaaw9128.
(200) Zhang, Y.; Lu, W.-J.; Bulkley, D. P.; Liang, J.; Ralko, A.; Han, S.; Roberts, K. J.; Li, A.; Cho, W.; Cheng, Y.; et al. Hedgehog Pathway Activation through Nanobody-Mediated Conformational Blockade of the Patched Sterol Conduit. *Proc. Natl. Acad. Sci. U. S. A.* **2020**, *117*, 28838−28846.
(201) Baker, M. R.; Fan, G.; Seryshev, A. B.; Agosto, M. A.; Baker, M. L.; Serysheva, I. I. Cryo-EM Structure of Type 1 IP3R Channel in a Lipid Bilayer. *Commun. Biol.* **2021**, *4*, 625.
(202) Henderson, R.; Unwin, P. N. T. Three-Dimensional Model of Purple Membrane Obtained by Electron Microscopy. *Nature* **1975**, *257*, 28−32.
(203) Liu, S.; Gonen, T. MicroED Structure of the NaK Ion Channel Reveals a Na+ Partition Process into the Selectivity Filter. *Commun. Biol.* **2018**, *1*, 38.
(204) Martynowycz, M. W.; Khan, F.; Hattne, J.; Abramson, J.; Gonen, T. Microed Structure of Lipid-Embedded Mammalian Mitochondrial Voltage-Dependent Anion Channel. *Proc. Natl. Acad. Sci. U. S. A.* **2020**, *117*, 32380−32385.
(205) Zhu, L.; Bu, G.; Jing, L.; Shi, D.; Lee, M.-Y.; Gonen, T.; Liu, W.; Nannenga, B. L. Structure Determination from Lipidic Cubic Phase Embedded Microcrystals by Microed. *Structure* **2020**, *28*, 1149−1159.
(206) Caffrey, M. A Comprehensive Review of the Lipid Cubic Phase or in Meso Method for Crystallizing Membrane and Soluble Proteins and Complexes. *Acta. Crystallogr. F:Struct. Biol. Commun.* **2015**, *71*, 3−18.
(207) Landau, E. M.; Rosenbusch, J. P. Lipidic Cubic Phases: A Novel Concept for the Crystallization of Membrane Proteins. *Proc. Natl. Acad. Sci. U. S. A.* **1996**, *93*, 14532−14535.
(208) Agip, A.-N. A.; Blaza, J. N.; Bridges, H. R.; Viscomi, C.; Rawson, S.; Muench, S. P.; Hirst, J. Cryo-Em Structures of Complex I from Mouse Heart Mitochondria in Two Biochemically Defined States. *Nat. Struct. Mol. Biol.* **2018**, *25*, 548−556.
(209) Parey, K.; Brandt, U.; Xie, H.; Mills, D. J.; Siegmund, K.; Vonck, J.; Kühlbrandt, W.; Zickermann, V. Cryo-EM Structure of Respiratory Complex I at Work. *eLife* **2018**, *7*, No. e39213.
(210) McPhillie, M. J.; Zhou, Y.; Hickman, M. R.; Gordon, J. A.; Weber, C. R.; Li, Q.; Lee, P. J.; Amporndanai, K.; Johnson, R. M.; Darby, H.; et al., Potent Tetrahydroquinolone Eliminates Apicomplexan Parasites. *Front. Cell. Infect. Microbiol.* **2020**, *10*, DOI: 10.3389/fcimb.2020.00203.
(211) Gu, J.; Wu, M.; Guo, R.; Yan, K.; Lei, J.; Gao, N.; Yang, M. The Architecture of the Mammalian Respirasome. *Nature* **2016**, *537*, 639−643.
(212) Wu, M.; Gu, J.; Guo, R.; Huang, Y.; Yang, M. Structure of Mammalian Respiratory Supercomplex I1 Iii2 Iv1. *Cell* **2016**, *167*, 1598−1609.

(213) Blum, T. B.; Hahn, A.; Meier, T.; Davies, K. M.; Kühlbrandt, W. Dimers of Mitochondrial Atp Synthase Induce Membrane Curvature and Self-Assemble into Rows. *Proc. Natl. Acad. Sci. U. S. A.* **2019**, *116*, 4250−4255.
(214) Spikes, T. E.; Montgomery, M. G.; Walker, J. E. Structure of the Dimeric Atp Synthase from Bovine Mitochondria. *Proc. Natl. Acad. Sci. U. S. A.* **2020**, *117*, 23519−23526.
(215) Mühleip, A.; Kock Flygaard, R.; Ovciarikova, J.; Lacombe, A.; Fernandes, P.; Sheiner, L.; Amunts, A. ATP Synthase Hexamer Assemblies Shape Cristae of Toxoplasma Mitochondria. *Nat. Commun.* **2021**, *12*, 120.
(216) Kolbe, F.; Safarian, S.; Piórek, Ż.; Welsch, S.; Müller, H.; Michel, H. Cryo-EM Structures of Intermediates Suggest an Alternative Catalytic Reaction Cycle for Cytochrome c Oxidase. *Nat. Commun.* **2021**, *12*, 6903.
(217) Sobti, M.; Ueno, H.; Noji, H.; Stewart, A. G. The Six Steps of the Complete F1-ATPase Rotary Catalytic Cycle. *Nat. Commun.* **2021**, *12*, 4690.
(218) Suga, M.; Ozawa, S.-I.; Yoshida-Motomura, K.; Akita, F.; Miyazaki, N.; Takahashi, Y. Structure of the Green Algal Photosystem I Supercomplex with a Decameric Light-Harvesting Complex I. *Nat. Plants.* **2019**, *5*, 626−636.
(219) Gardiner, A. T.; Naydenova, K.; Castro-Hartmann, P.; Nguyen-Phan, T. C.; Russo, C. J.; Sader, K.; Hunter, C. N.; Cogdell, R. J.; Qian, P. The 2.4 Å Cryo-EM Structure of a Heptameric Light-Harvesting 2 Complex Reveals Two Carotenoid Energy Transfer Pathways. *Sci. Adv.* **2021**, *7*, No. eabe4650.
(220) Akita, F.; Nagao, R.; Kato, K.; Nakajima, Y.; Yokono, M.; Ueno, Y.; Suzuki, T.; Dohmae, N.; Shen, J.-R.; Akimoto, S.; et al. Structure of a Cyanobacterial Photosystem I Surrounded by Octadecameric Isia Antenna Proteins. *Commun. Biol.* **2020**, *3*, 232.
(221) Goretzki, B.; Guhl, C.; Tebbe, F.; Harder, J.-M.; Hellmich, U. A. Unstructural Biology of Trp Ion Channels: The Role of Intrinsically Disordered Regions in Channel Function and Regulation. *J. Mol. Biol.* **2021**, *433*, 166931.
(222) Paulsen, C. E.; Armache, J.-P.; Gao, Y.; Cheng, Y.; Julius, D. Structure of the Trpa1 Ion Channel Suggests Regulatory Mechanisms. *Nature* **2015**, *520*, 511−517.
(223) Huynh, K. W.; Cohen, M. R.; Jiang, J.; Samanta, A.; Lodowski, D. T.; Zhou, Z. H.; Moiseenkova-Bell, V. Y. Structure of the Full-Length RPV2 Channel by Cryo-EM. *Nat. Commun.* **2016**, *7*, 11130.
(224) Duan, J.; Li, J.; Chen, G.-L.; Ge, Y.; Liu, J.; Xie, K.; Peng, X.; Zhou, W.; Zhong, J.; Zhang, Y.; et al. Cryo-EM Structure of TRPC5 at 2.8-Å Resolution Reveals Unique and Conserved Structural Elements Essential for Channel Function. *Sci. Adv.* **2019**, *5*, No. eaaw7935.
(225) Yin, Y.; Wu, M.; Zubcevic, L.; Borschel, W. F.; Lander, G. C.; Lee, S.-Y. Structure of the Cold- and Menthol-Sensing Ion Channel Trpm8. *Science* **2018**, *359*, 237.
(226) Hirschi, M.; Herzik Jr, M. A.; Wie, J.; Suo, Y.; Borschel, W. F.; Ren, D.; Lander, G. C.; Lee, S.-Y. Cryo-Electron Microscopy Structure of the Lysosomal Calcium-Permeable Channel Trpml3. *Nature* **2017**, *550*, 411−414.
(227) Wang, Q.; Corey, R. A.; Hedger, G.; Aryal, P.; Grieben, M.; Nasrallah, C.; Baronina, A.; Pike, A. C. W.; Shi, J.; Carpenter, E. P.; et al. Lipid Interactions of a Ciliary Membrane Trp Channel: Simulation and Structural Studies of Polycystin-2. *Structure* **2020**, *28*, 169−184.
(228) Wang, W.; MacKinnon, R. Cryo-Em Structure of the Open Human Ether-À-Go-Go-Related K(+) Channel Herg. *Cell* **2017**, *169*, 422−430.
(229) Asai, T.; Adachi, N.; Moriya, T.; Oki, H.; Maru, T.; Kawasaki, M.; Suzuki, K.; Chen, S.; Ishii, R.; Yonemori, K.; et al. Cryo-Em Structure of K+-Bound Herg Channel Complexed with the Blocker Astemizole. *Structure (London, England: 1993)* **2021**, *29*, 203−212.
(230) Shen, H.; Li, Z.; Jiang, Y.; Pan, X.; Wu, J.; Cristofori-Armstrong, B.; Smith, J. J.; Chin, Y. K. Y.; Lei, J.; Zhou, Q.; et al. Structural Basis for the Modulation of Voltage-Gated Sodium Channels by Animal Toxins. *Science* **2018**, *362*, No. eaau2596.
(231) Shen, H.; Liu, D.; Wu, K.; Lei, J.; Yan, N. Structures of Human Na(V)1.7 Channel in Complex with Auxiliary Subunits and Animal Toxins. *Science* **2019**, *363*, 1303−1308.
(232) Zhang, Y.; Sun, B.; Feng, D.; Hu, H.; Chu, M.; Qu, Q.; Tarrasch, J. T.; Li, S.; Sun Kobilka, T.; Kobilka, B. K.; et al. Cryo-Em Structure of the Activated Glp-1 Receptor in Complex with a G Protein. *Nature* **2017**, *546*, 248−253.
(233) Kang, Y.; Kuybeda, O.; de Waal, P. W.; Mukherjee, S.; Van Eps, N.; Dutka, P.; Zhou, X. E.; Bartesaghi, A.; Erramilli, S.; Morizumi, T.; et al. Cryo-Em Structure of Human Rhodopsin Bound to an Inhibitory G Protein. *Nature* **2018**, *558*, 553−558.
(234) Maeda, S.; Qu, Q.; Robertson, M. J.; Skiniotis, G.; Kobilka, B. K. Structures of the M1 and M2Muscarinic Acetylcholine Receptor/G-Protein Complexes. *Science* **2019**, *364*, 552.
(235) Draper-Joyce, C. J.; Bhola, R.; Wang, J.; Bhattarai, A.; Nguyen, A. T. N.; Cowie-Kent, I.; O'Sullivan, K.; Chia, L. Y.; Venugopal, H.; Valant, C.; et al. Positive Allosteric Mechanisms of Adenosine A1 Receptor-Mediated Analgesia. *Nature* **2021**, *597*, 571−576.
(236) Huang, W.; Masureel, M.; Qu, Q.; Janetzko, J.; Inoue, A.; Kato, H. E.; Robertson, M. J.; Nguyen, K. C.; Glenn, J. S.; Skiniotis, G.; et al. Structure of the Neurotensin Receptor 1 in Complex with B-Arrestin 1. *Nature* **2020**, *579*, 303−308.
(237) Staus, D. P.; Hu, H.; Robertson, M. J.; Kleinhenz, A. L. W.; Wingler, L. M.; Capel, W. D.; Latorraca, N. R.; Lefkowitz, R. J.; Skiniotis, G. Structure of the M2Muscarinic Receptor-B-Arrestin Complex in a Lipid Nanodisc. *Nature* **2020**, *579*, 297−302.
(238) Lee, Y.; Warne, T.; Nehmé, R.; Pandey, S.; Dwivedi-Agnihotri, H.; Chaturvedi, M.; Edwards, P. C.; García-Nafría, J.; Leslie, A. G. W.; Shukla, A. K.; et al. Molecular Basis of B-Arrestin Coupling to Formoterol-Bound B(1)-Adrenoceptor. *Nature* **2020**, *583*, 862−866.
(239) Gundry, J.; Glenn, R.; Alagesan, P.; Rajagopal, S. A Practical Guide to Approaching Biased Agonism at G Protein Coupled Receptors. *Front. Neurosci.* **2017**, *11*, DOI: 10.3389/fnins.2017.00017.
(240) Wootten, D.; Christopoulos, A.; Marti-Solano, M.; Babu, M. M.; Sexton, P. M. Mechanisms of Signalling and Biased Agonism in G Protein-Coupled Receptors. *Nat. Rev. Mol. Cell Biol.* **2018**, *19*, 638−653.
(241) Lin, X.; Li, M.; Wang, N.; Wu, Y.; Luo, Z.; Guo, S.; Han, G.-W.; Li, S.; Yue, Y.; Wei, X.; et al. Structural Basis of Ligand Recognition and Self-Activation of Orphan Gpr52. *Nature* **2020**, *579*, 152−157.
(242) Qiao, A.; Han, S.; Li, X.; Li, Z.; Zhao, P.; Dai, A.; Chang, R.; Tai, L.; Tan, Q.; Chu, X.; et al. Structural Basis of Gs and Gi Recognition by the Human Glucagon Receptor. *Science* **2020**, *367*, 1346−1352.
(243) Sexton, P. M.; Albiston, A.; Morfis, M.; Tilakaratne, N. Receptor Activity Modifying Proteins. *Cell. Signal.* **2001**, *13*, 73−83.
(244) Cao, J.; Belousoff, M. J.; Liang, Y.-L.; Johnson, R. M.; Josephs, T. M.; Fletcher, M. M.; Christopoulos, A.; Hay, D. L.; Danev, R.; Wootten, D.; Sexton, P. M.; et al. A Structural Basis for Amylin Receptor Phenotype. *Science* **2022**, *375*, No. eabm9609.
(245) Johnson, R. M.; Zhang, X.; Piper, S. J.; Nettleton, T. J.; Vandekolk, T. H.; Langmead, C. J.; Danev, R.; Sexton, P. M.; Wootten, D. Cryo-Em Structure of the Dual Incretin Receptor Agonist, Peptide-19, in Complex with the Glucagon-Like Peptide-1 Receptor. *Biochem. Biophys. Res. Commun.* **2021**, *578*, 84−90.
(246) Ling, S.; Shi, P.; Liu, S.; Meng, X.; Zhou, Y.; Sun, W.; Chang, S.; Zhang, X.; Zhang, L.; Shi, C.; et al. Structural Mechanism of Cooperative Activation of the Human Calcium-Sensing Receptor by Ca2+ Ions and L-Tryptophan. *Cell Res.* **2021**, *31*, 383−394.
(247) Velazhahan, V.; Ma, N.; Pándy-Szekeres, G.; Kooistra, A. J.; Lee, Y.; Gloriam, D. E.; Vaidehi, N.; Tate, C. G. Structure of the Class D Gpcr Ste2 Dimer Coupled to Two G Proteins. *Nature* **2021**, *589*, 148−153.
(248) Shen, C.; Mao, C.; Xu, C.; Jin, N.; Zhang, H.; Shen, D. D.; Shen, Q.; Wang, X.; Hou, T.; Chen, Z.; et al. Structural Basis of Gaba(B) Receptor-G(I) Protein Coupling. *Nature* **2021**, *594*, 594−598.
(249) Lin, S.; Han, S.; Cai, X.; Tan, Q.; Zhou, K.; Wang, D.; Wang, X.; Du, J.; Yi, C.; Chu, X.; et al. Structures of G(I)-Bound Metabotropic Glutamate Receptors Mglu2 and Mglu4. *Nature* **2021**, *594*, 583−588.

(250) Kim, Y.; Jeong, E.; Jeong, J.-H.; Kim, Y.; Cho, Y. Structural Basis for Activation of the Heterodimeric Gabab Receptor. *J. Mol. Biol.* **2020**, *432*, 5966−5984.
(251) Park, J.; Fu, Z.; Frangaj, A.; Liu, J.; Mosyak, L.; Shen, T.; Slavkovich, V. N.; Ray, K. M.; Taura, J.; Cao, B.; et al. Structure of Human Gabab Receptor in an Inactive State. *Nature* **2020**, *584*, 304−309.
(252) Mao, C.; Shen, C.; Li, C.; Shen, D.-D.; Xu, C.; Zhang, S.; Zhou, R.; Shen, Q.; Chen, L.-N.; Jiang, Z.; et al. Cryo-Em Structures of Inactive and Active Gabab Receptor. *Cell Res.* **2020**, *30*, 564−573.
(253) Koehl, A.; Hu, H.; Feng, D.; Sun, B.; Zhang, Y.; Robertson, M. J.; Chu, M.; Kobilka, T. S.; Laeremans, T.; Steyaert, J.; et al. Structural Insights into the Activation of Metabotropic Glutamate Receptors. *Nature* **2019**, *566*, 79−84.
(254) Du, J.; Wang, D.; Fan, H.; Xu, C.; Tai, L.; Lin, S.; Han, S.; Tan, Q.; Wang, X.; Xu, T.; et al. Structures of Human Mglu2 and Mglu7 Homo- and Heterodimers. *Nature* **2021**, *594*, 589−593.
(255) Seven, A. B.; Barros-Álvarez, X.; de Lapeyrière, M.; Papasergi-Scott, M. M.; Robertson, M. J.; Zhang, C.; Nwokonko, R. M.; Gao, Y.; Meyerowitz, J. G.; Rocher, J.-P.; et al. G-Protein Activation by a Metabotropic Glutamate Receptor. *Nature* **2021**, *595*, 450−454.
(256) Nasrallah, C.; Cannone, G.; Briot, J.; Rottier, K.; Berizzi, A. E.; Huang, C.-Y.; Quast, R. B.; Hoh, F.; Banères, J.-L.; Malhaire, F.; et al. Agonists and Allosteric Modulators Promote Signaling from Different Metabotropic Glutamate Receptor 5 Conformations. *Cell Rep.* **2021**, *36*, 109648.
(257) Velazhahan, V.; Ma, N.; Vaidehi, N.; Tate, C. G. Activation Mechanism of the Class D Fungal Gpcr Dimer Ste2. *Nature* **2022**, *603*, 743−748.
(258) Miletic, S.; Fahrenkamp, D.; Goessweiner-Mohr, N.; Wald, J.; Pantel, M.; Vesper, O.; Kotov, V.; Marlovits, T. C. Substrate-Engaged Type III Secretion System Structures Reveal Gating Mechanism for Unfolded Protein Translocation. *Nat. Commun.* **2021**, *12*, 1546.
(259) Bunduc, C. M.; Fahrenkamp, D.; Wald, J.; Ummels, R.; Bitter, W.; Houben, E. N. G.; Marlovits, T. C. Structure and Dynamics of a Mycobacterial Type vii Secretion System. *Nature* **2021**, *593*, 445−448.
(260) Yan, R.; Zhao, X.; Lei, J.; Zhou, Q. Structure of the Human Lat1−4f2hc Heteromeric Amino Acid Transporter Complex. *Nature* **2019**, *568*, 127−130.
(261) Fitzpatrick, A. W. P.; Llabrés, S.; Neuberger, A.; Blaza, J. N.; Bai, X.-C.; Okada, U.; Murakami, S.; van Veen, H. W.; Zachariae, U.; Scheres, S. H. W.; et al. Structure of the MacAB-TolC ABC-Type Tripartite Multidrug Efflux Pump. *Nature Microbiology* **2017**, *2*, 17070.
(262) Nosol, K.; Bang-Sørensen, R.; Irobalieva, R. N.; Erramilli, S. K.; Stieger, B.; Kossiakoff, A. A.; Locher, K. P. Structures of ABCB4 Provide Insight into Phosphatidylcholine Translocation. *Proc. Natl. Acad. Sci. U. S. A.* **2021**, *118*, No. e2106702118.
(263) Taylor, N. M. I.; Manolaridis, I.; Jackson, S. M.; Kowal, J.; Stahlberg, H.; Locher, K. P. Structure of the Human Multidrug Transporter Abcg2. *Nature* **2017**, *546*, 504−509.
(264) Yu, X.; Plotnikova, O.; Bonin, P. D.; Subashi, T. A.; McLellan, T. J.; Dumlao, D.; Che, Y.; Dong, Y. Y.; Carpenter, E. P.; West, G. M.; et al. Cryo-EM Structures of the Human Glutamine Transporter SLC1A5 (ASCT2) in the Outward-Facing Conformation. *eLife* **2019**, *8*, No. e48120.
(265) Fath, M. J.; Kolter, R. Abc Transporters: Bacterial Exporters. *Microbiol. Rev.* **1993**, *57*, 995−1017.
(266) Hofmann, S.; Januliene, D.; Mehdipour, A. R.; Thomas, C.; Stefan, E.; Brüchert, S.; Kuhn, B. T.; Geertsma, E. R.; Hummer, G.; Tampé, R.; et al. Conformation Space of a Heterodimeric Abc Exporter under Turnover Conditions. *Nature* **2019**, *571*, 580−583.
(267) Jiang, J.; Pentelute, B. L.; Collier, R. J.; Zhou, Z. H. Atomic Structure of Anthrax Protective Antigen Pore Elucidates Toxin Translocation. *Nature* **2015**, *521*, 545−549.
(268) Antoni, C.; Quentin, D.; Lang, A. E.; Aktories, K.; Gatsogiannis, C.; Raunser, S. Cryo-Em Structure of the Fully-Loaded Asymmetric Anthrax Lethal Toxin in Its Heptameric Pre-Pore State. *PLOS Pathogens* **2020**, *16*, No. e1008530.
(269) Leidreiter, F.; Roderer, D.; Meusch, D.; Gatsogiannis, C.; Benz, R.; Raunser, S. Common Architecture of Tc Toxins from Human and Insect Pathogenic Bacteria. *Sci. Adv.* **2019**, *5*, No. eaax6497.
(270) Roderer, D.; Hofnagel, O.; Benz, R.; Raunser, S. Structure of a Tc Holotoxin Pore Provides Insights into the Translocation Mechanism. *Proc. Natl. Acad. Sci. U. S. A.* **2019**, *116*, 23083−23090.
(271) Piper, S. J.; Brillault, L.; Rothnagel, R.; Croll, T. I.; Box, J. K.; Chassagnon, I.; Scherer, S.; Goldie, K. N.; Jones, S. A.; Schepers, F.; et al. Cryo-EM Structures of the Pore-Forming a Subunit from the Yersinia Entomophaga ABC Toxin. *Nat. Commun.* **2019**, *10*, 1952.
(272) Guo, H.; Courbon, G. M.; Bueler, S. A.; Mai, J.; Liu, J.; Rubinstein, J. L. Structure of Mycobacterial Atp Synthase Bound to the Tuberculosis Drug Bedaquiline. *Nature* **2021**, *589*, 143−147.
(273) Wang, R.; Wang, J.; Hassan, A.; Lee, C.-H.; Xie, X.-S.; Li, X. Molecular Basis of V-ATPase Inhibition by Bafilomycin A1. *Nat. Comms.* **2021**, *12*, 1782.
(274) Wright, D. J.; Simmons, K. J.; Johnson, R. M.; Beech, D. J.; Muench, S. P.; Bon, R. S. Human TRPC5 Structures Reveal Interaction of a Xanthine-Based TRPC1/4/5 Inhibitor with a Conserved Lipid Binding Site. *Commun. Biol.* **2020**, *3*, 704.
(275) Zhao, P.; Liang, Y.-L.; Belousoff, M. J.; Deganutti, G.; Fletcher, M. M.; Willard, F. S.; Bell, M. G.; Christe, M. E.; Sloop, K. W.; Inoue, A.; et al. Activation of the Glp-1 Receptor by a Non-Peptidic Agonist. *Nature* **2020**, *577*, 432−436.
(276) Kawai, T.; Sun, B.; Yoshino, H.; Feng, D.; Suzuki, Y.; Fukazawa, M.; Nagao, S.; Wainscott, D. B.; Showalter, A. D.; Droz, B. A.; et al. Structural Basis for Glp-1 Receptor Activation by Ly3502970, an Orally Active Nonpeptide Agonist. *Proc. Natl. Acad. Sci. U. S. A.* **2020**, *117*, 29959−29967.
(277) Zhang, X.; Belousoff, M. J.; Zhao, P.; Kooistra, A. J.; Truong, T. T.; Ang, S. Y.; Underwood, C. R.; Egebjerg, T.; Šenel, P.; Stewart, G. D.; et al. Differential Glp-1r Binding and Activation by Peptide and Non-Peptide Agonists. *Mol. Cell* **2020**, *80*, 485−500.
(278) Brown, E.; Cuthbertson, D. J.; Wilding, J. P. Newer Glp-1 Receptor Agonists and Obesity-Diabetes. *Peptides* **2018**, *100*, 61−67.
(279) Nauck, M. A.; Meier, J. J. Management of Endocrine Disease: Are All Glp-1 Agonists Equal in the Treatment of Type 2 Diabetes? *Eur. J. Endocrinol.* **2019**, *181*, R211−R234.
(280) Mullard, A. What Does Alphafold Mean for Drug Discovery? *Nat. Rev. Drug Discovery* **2021**, *20*, 725−727.
(281) Saur, M.; Hartshorn, M. J.; Dong, J.; Reeks, J.; Bunkoczi, G.; Jhoti, H.; Williams, P. A. Fragment-Based Drug Discovery Using Cryo-Em. *Drug Discovery Today* **2020**, *25*, 485−490.
(282) Tegunov, D.; Cramer, P. Real-Time Cryo-Electron Microscopy Data Preprocessing with Warp. *Nat. Methods* **2019**, *16*, 1146−1152.
(283) Stabrin, M.; Schoenfeld, F.; Wagner, T.; Pospich, S.; Gatsogiannis, C.; Raunser, S. TranSPHIRE: Automated and Feedback-Optimized on-the-Fly Processing for Cryo-EM. *Nat. Commun.* **2020**, *11*, 5716.
(284) Su, C.-C.; Lyu, M.; Morgan, C. E.; Bolla, J. R.; Robinson, C. V.; Yu, E. W. A 'Build and Retrieve' Methodology to Simultaneously Solve Cryo-Em Structures of Membrane Proteins. *Nat. Methods* **2021**, *18*, 69−75.
(285) Segers, K.; Masure, S. Cell-Free Expression of G Protein-Coupled Receptors. *Curr. Protoc Protein Sci.* **2015**, *81*, 29.14.21−29.14.29.
(286) Kögler, L. M.; Stichel, J.; Kaiser, A.; Beck-Sickinger, A. G. Cell-Free Expression and Photo-Crosslinking of the Human Neuropeptide Y2 Receptor. *Front. Pharmacol.* **2019**, *10*, DOI: 10.3389/fphar.2019.00176.
(287) Silverman, A. D.; Karim, A. S.; Jewett, M. C. Cell-Free Gene Expression: An Expanded Repertoire of Applications. *Nat. Rev. Genet.* **2020**, *21*, 151−170.
(288) Kotov, V.; Bartels, K.; Veith, K.; Josts, I.; Subhramanyam, U. K. T.; Günther, C.; Labahn, J.; Marlovits, T. C.; Moraes, I.; Tidow, H.; et al. High-Throughput Stability Screening for Detergent-Solubilized Membrane Proteins. *Sci. Rep.* **2019**, *9*, 10379.